Molecular regulation of P-selectin ligand in T_H1 and T_H2 cells *in vitro*, crucial for the homing of $CD4^+$ T cells into inflamed tissue.

Inaugural-Dissertation
to obtain the academic degree
Doctor rerum naturalium (Dr. rer. nat.)

submitted to the Department of Biology, Chemistry, and Pharmacy
of Freie Universität Berlin

by

Maibritt Mardahl

from Nairobi, Kenya

March, 2016

This work was carried out from January 1, 2013 until December 31, 2015
under the supervision of Prof. Dr. Alf Hamann and PD Uta Syrbe
at the Deutsche Rheuma-Forschungszentrum, Chariteplatz 1, 10117 Berlin

1. Reviewer: Prof. Dr. Alf Hamann
2. Reviewer: Prof. Dr. Heribert Hofer

Date of defense: 15.09.2016

Acknowledgments

First of all, I would like to thank my supervisors, Prof. Dr. Alf Hamann and Dr. Uta Syrbe, for giving me the opportunity to work with them on this project. I am sincerely grateful for their continued encouragement, energy, and fruitful discussions that fuelled my motivation throughout this project. Particular thank yous goes also to everyone in the Hamann group for their extensive scientific knowledge and good spirits in the lab. In particular, I would like to thank Ute Hoffmann for critical reading of this thesis. Second, I sincerely thank Prof. Dr. Heribert Hofer for taking the time to review this dissertation. Third, a thank you to the DRFZ institute and its members for making the experiments easier to run smoothly - in particular Yuriy Shebzukov and Martin Karl for assisting me in experimental troubleshooting. Last, but not least, my husband and family deserve a warm thank you for their patience and support when I was in the lab long hours or was occupied by the project always in the back of my head. Thanks to my mom for critical reading of my dissertation.
Tak Ricki, fordi du altid er der for mig.

Contents

List of Figures

List of Tables

Abbreviations

α4	integrin alpha 4
APC	antigen presenting cell
C2-GlcNAcT-I	Core2-β1,6 glucosaminyltransferase-I
CD	cluster of differentiation
CCL	Chemokine C-C motif ligand
CCR	CC chemokine receptor
ChIP	chromatin immunoprecipitation
CNS	conserved non-coding sequence
CREB	cAMP response element binding protein
CsA	Cyclosporine A
CXCR	CXC chemokine receptor
CYP	Cytochrome P450
DNA	deoxyribonucleic acid
DNMT	DNA methyltransferase
FCS	fetal calf serum
FucT-VII	Fucosyltransferase-VII
fut7	gene encoding FucT-VII
EC	endothelial cell
E-lig	E-selectin ligand
gcnt1	gene encoding C2-GlcNAcT-I
H3K4me2	dimethylation of Lysine 4 of histone 4
H3K27me3	trimethylation of Lysine 27 of histone 4
HAT	histone acetyltransferase
HDAC	histone deacetylase
HEV	high endothelial venule
IFN	Interferon
IL	Interleukin
itga4	gene encoding α4

LN	lymph node
mLN	mesenteric lymph node
NFAT	Nuclear Factor of Activated T cells
P-lig	P-selectin ligand
pLN	peripheral lymph node
PSGL-1	P-selectin glycoprotein ligand-1
RA	retinoid acid
RAR	retinoic acid receptor
RARE	retinoic acid response element
RNA	ribonucleic acid
RXR	retinoid X receptor
sLe^x	sialylated Lewis X antigen
SLO	secondary lymphoid organ
STAT	signal and transducer of activation and transcription
T-bet	T-box transcription factor TBX21
TCR	T cell receptor
T_{eff} cell	effector T cell
TF	transcription factor
TGF	Tumor growth factor
T_H	T helper
TNF	Tumor Necrosis Factor
TsA	Trichostatin A
TSS	transcriptional start site

1. Summary

The proper localization of immune cells within the body is a prerequisite to effectively mount an immune response. P-selectin ligands (P-ligs) are oligosaccharide epitopes that support recruitment of T cells to the skin and inflamed tissue. P-ligs are synthesized by several glycosyltransferases, of which Core2-β 1,6 glucosaminyltransferase-I (C2-GlcNAcT-I) and Fucosyltransferase-VII (FucT-VII) are crucial because T cells from mice deficient in the genes that encode them, *gcnt1* and *fut7*, respectively, do not migrate to the site of immunization in classic delayed type hypersensitivity models. Initial and long-term molecular regulation of these genes and subsequently upregulation and maintenance of P-lig expression is not fully understood. Although P-lig has been observed on murine T_H1 and T_H2 cells *in vivo* [1] during inflammation, this has not been recapitulated *in vitro* for T_H2 cells. In this thesis, the regulation of both *gcnt1* and *fut7* is characterized in T_H1 and T_H2 cells generated *in vitro*.

In T_H1 cells, we have shown that *gcnt1* expression is induced and maintained by the transcription factors STAT4 and T-bet, respectively. Furthermore, using available ChIP-seq data, we observed that these transcription factors are implicated in the opening of the *gcnt1* locus by promoting changes in histone methylation that affect its transcription. This is the first direct evidence of epigenetic regulation of P-lig that we have postulated in earlier studies [2]. This promotes long-term P-lig expression to give T cells a topographical migratory memory, which enables them to recirculate between blood and the tissue of first antigen encounter. For *fut7*, we have shown that initial activation in T_H1 cells is induced by the transcription factors CREB and STAT5, the actions of which are inhibited by DNA methylation and the presence of RA, respectively. Unlike *gcnt1*, long-term expression of *fut7* is therefore regulated by DNA methylation. In T_H2 cells, we have shown that RA suppresses expression of both *gcnt1* and *fut7* through the nuclear receptor RARα. Minute amounts of RA are present in FCS-containing media, which prevents upregulation of P-lig in T_H2 cells *in vitro* (in contrast to *in vivo*). Moreover, we have shown a reciprocal relationship between Il4 and Gcnt1 mRNA availability in mesenteric and peripheral lymph nodes (mLNs and pLNs) that might promote tight regulation of P-lig in mLNs. Finally, we have shown that the enhancer for *gcnt1* in T_H1 cells acts as a silencer in T_H2 cells.

This suggests that a complex interplay between epigenetic modifications, cytokine signaling, and microenvironmental factors control the molecular regulation/induction of *gcnt1* and *fut7*, and subsequently P-lig on developing effector cells that are distinct in T_H1 and T_H2 *in vitro* generated cells.

2. Zusammenfassung

Die Lokalisierung von Immunzellen im Körper ist eine wichtige Voraussetzung für eine effektive Immunantwort. P-Selektin-Liganden (P-lig) sind Oligosaccharid-Epitope, die die Einwanderung von T-Zellen in die Haut und in andere entzündete Gewebe unterstützen. P-lig werden von verschiedenen Glycosyltransferasen synthetisiert. Vor allem die Core2-β 1,6 Glucosaminyltransferase-I (C2-GlcNAcT-I) und die Fucosyltransferase-VII (FucT-VII) sind essentiell. So hat sich im Modell der Hypersensitivität vom verzögerten Typ gezeigt, dass T-Zellen aus Mäusen, die diese Enzyme nicht exprimieren, nicht in der Lage sind, an den Ort der Entzündung zu migrieren. Es ist jedoch unklar, wie die Initiation der Expression beider Gene bzw deren Langzeitexpression und der daraus resultierenden Hochregulation der P-lig-Expression auf molekularer Ebene reguliert wird. Obwohl P-lig *in vivo* sowohl in T_H1- und T_H2-Zellen [1] exprimiert wird, konnte dies *in vitro* nur für T_H1-Zellen gezeigt werden. In der vorliegenden Arbeit wurde die Regulation beider Gene, *gcnt1* und *fut7*, sowohl für T_H1 als auch für T_H2-Zellen *in vitro* untersucht.

In T_H1-Zellen wird die *gcnt1* Expression von STAT4 und T-bet induziert und aufrechterhalten. ChIP-seq Daten haben ergeben, dass diese Transkriptionsfaktoren in die öffnung des *gcnt1* Locus involviert sind, indem sie änderungen der Histon-Methylierung hervorrufen und damit die Transkription beeinflussen. Das ist der erste direkte Beweis für epigenetische Regulation von P-lig, die wir in früheren Studien bisher nur postulieren konnten (78). Diese epigenetische Modifikation begünstigt Langzeit-P-lig-Expression, wodurch die T-Zellen ein topografisches Gedächtnis erhalten. Das ermöglicht ihnen, zwischen Blut und dem Gewebe zu rezirkulieren, in dem sie das erste Mal Antigen-Kontakt hatten. In T_H1-Zellen wird die initiale Aktivierung des *fut7*-Gens durch die Transkriptionsfaktoren CREB und STAT5 induziert, was durch DNA-Methylierung und durch Anwesenheit von Retinolsäure (RA) inhibiert wird. Im Gegensatz zu *gcnt1* wird daher die Langzeitexpression von *fut7* durch DNA-Methylierung reguliert. In T_H2 Zellen wurde gezeigt, dass RA die Expression beider Gene, *gcnt1* und *fut7*, durch Bindung an den nukleären Rezeptor RARa unterdrückt. Es reichen bereits minimale Mengen an RA aus, um die P-lig Expression in T_H2-Zellen zu verhindern. Das erklärt auch das Fehlen von P-lig auf T_H2-Zellen *in vitro*, denn das FCS, was herkömmlichen Zellkulturmedien zugesetzt wird, enthält ebenfalls

geringe Konzentrationen an RA. Außerdem haben wir *in vivo* eine reziproke Korrelation zwischen Il4 und Gcnt1 mRNA Verfügbarkeit in mesenterialen und peripheren Lymphknoten (mLN und pLN) nachgewiesen. Das könnte Ursache für die restriktive Regulation der P-lig Expression in mLN sein. Letztendlich haben wir gezeigt, dass der Enhancer für *gcnt1* in T_H1-Zellen als ein Silencer für T_H2-Zellen fungiert.

Das alles legt ein komplexes Zusammenspiel zwischen epigenetischen Modifikationen, Zytokinsignalen und Faktoren der Mikroumgebung nahe, die die molekulare Regulation/ Induktion von *gcnt1* und *fut7* kontrollieren. Dadurch wir die Expression von P-lig auf sich entwickelnden Effektorzellen gesteuert, die sich von *in vitro* generierten T_H1- und T_H2-Zellen unterscheiden.

3. Introduction

The immune system is a double-edged sword that needs to be tightly regulated to avoid excessive immune responses. The primary task of the immune system is not only to detect danger signals from pathogens and abnormal cells in the host, but also to be accepting of self-antigens as well as food antigens. If a pathogen successfully enters the host by crossing epithelial barriers, an immune response is initiated. The initial tissue damage incurred promotes a local immune response (inflammation) to recruit cellular players to the site of infection. Local immune responses involve soluble and cellular components of the immune system. So-called cytokines and chemokines are important soluble mediators, while leukocytes such as granulocytes, monocytes, and lymphocytes comprise the cellular component of the immune system. The cellular component of the immune system is classically subdivided into innate and adaptive compartments, with cells of each compartment being activated in parallel during an immune response. The cells of the immune system circulate in the body in a dynamic fashion facilitated by the cooperative functions of adhesion molecules, chemokines, and integrin molecules, that promote correct positioning (homing) of cells with effector functions required to resolve inflammation and clear up the infection. At a crucial point this immune response must be suppressed by regulating local immune cells to prevent overt damage to host tissues.

While the innate immune cells respond to inflammation immediately and non-specifically, the adaptive immune response is antigen-specific and requires prior processing of a given pathogen's antigen by mature specialized antigen presenting cells (APCs) of the innate immune compartment. The effector functions of innate immune cells include releasing their toxic granulocytic content to kill pathogens and engulfing the resulting pathogen debris. This occurs in an immediate and non-specific manner, in parallel with release of cytokines that promote recruitment of adaptive immune cells such as T and B lymphocytes. The adaptive immune response takes longer than the innate response, but has several advantages for the host, of which antigen specificity is particularly important. While B cells have the ability to modulate their antigenic response by recombining antibody genes to perfect the antibody against a given antigenic epitope on a pathogen, T cells, after exiting the thymus, are predetermined to be specific to one antigen. This means the antigen

repertoire of T cells is incredibly diverse. Notably, a small subset of effector T cells retain memory of an infection and continue to circulate in the tissue of first antigen encounter as memory T cells. T cells are extremely versatile in their effector functions, with different subsets combating intra- and extracellular pathogens, virus, funghi, or parasites. Immune responses by T cells require 1) prior pathogen detection, 2) T cell activation and differentiation, and 3) proper positioning/homing of the cells within the inflamed tissue. The distribution/homing of immune cells is controlled by adhesion molecules, chemokines, and integrin molecules (collectively referred to as homing receptors). This work aims to uncover the regulation of homing receptors during $CD4^+$ T cell activation and differentiation that subsequently modulates T cell trafficking. Therefore, the biology of $CD4^+$ T cell activation and differentiation is explained in more detail in the next section.

3.1 T cells

Each T cell espresses a unique T cell receptor (TCR) recognizing only a single (cognate) antigenic peptide presented by mature antigen presenting cells (APCs) such as macrophages, dendritic cells, and B cells. The APCs process antigens and present antigen-derived peptides on their surface within major histocompatibility complexes (MHCs). Because each T cell expresses a unique TCR, the T cell repertoire can respond to a vast number of antigens. $CD4^+$ T cells are designated T helper (T_H) cells because their effector functions involve the recruiting and enabling of suitable cells (granulocytes and $CD8^+$ T cells) to resolve infection, as well as assisting B cells in immunoglobulin isotype class switching to promote appropriate antibody production against a given infection. In this way, T cells orchestrate the immune response at the site of infection/inflammation. Before a T cell can mount an immune response, it must mature in the thymus. After maturation, $CD4^+$ T lymphocytes leave the thymus as naive $CD4^+$ T cells and home to the lymph nodes (LN) where they become primed/activated by their cognate antigen.

Activation of the naive T cell requires initiation of the TCR signaling pathway by two signals derived from the APC. The first signal is provided by the antigenic peptide:MHC on the APC, which ligates with the TCR and co-receptor CD4 on the T cell. The second signal is delivered by a costimulatory molecule such as B7 on the APC that interacts with CD28 expressed by the T cell. The co-stimulatory signal controls T cell activation by reinforcing that the antigen is a bonafide foreign antigen and strengthens TCR:peptide:MHC ligation. An additional third signal is necessary to instruct the T cell into which T_H lineage it should differentiate. This signal comes from cytokines present in the lymph node during activation. Cytokines promote differentiation of the naive T cell into a particular $CD4^+$ T helper lineage/subset, by stimulating the T cell JAK/STAT pathway that is introduced later. Altogether, these three signals trigger different intracellular signaling

cascades leading to nuclear translocation of selective transcription factors that culminate in the transcription of lineage-appropriate genes required for the T cell to gain effector functions. The epigenetic imprinting of these genes ensures continued accessibility and expression during the lifetime of the T cell as an effector or memory T cell.

TCR signaling leads to activation of protein kinases through initiation of the Ras-Raf-MAPK pathway and transient intracellular mobilization of Ca^{2+} stores [3]. Ca^{2+} is an important mineral that initiates Ca^{2+}-dependent signaling to promote nuclear translocation of important transcription factors (TFs) such as Nuclear Factor of Activated T cells (NFAT) [4, 5]. Once in the nucleus, NFAT and many other TFs promote or repress gene transcription at promoters and enhancers/silencers, depending on their binding partners, which in turn determine which genes and, of particular interest here, which cytokines are expressed. In addition, TFs recruit chromatin modifiers and therefore play a role in the epigenetic regulation of their target genes. Epigenetics is defined as heritable changes in gene expression that do not involve changing the DNA genetic code, but involve the accessibility of the DNA to the transcriptional machinery. Epigenetic mechanisms (introduced in section 3.4.2) as such can imprint the activation or silencing of genes to T cell clones upon differentiation into one of the T cell lineages.

Once a naive T cell is activated by its cognate antigen, it differentiates into a T cell with effector functions and clonally expands within the LN for a few days, before exiting the LN to home to the infected/inflamed tissue [6]. During activation, cytokines and microenvironmental factors present in the lymph node (LN) promote lineage-specific (signature) cytokine expression crucial to resolve the given inflammation/infection. As such this determines which $CD4^+$ helper T cell subtype the naive T cell differentiates into. Importantly, this process also leads to upregulation of adhesion molecules, chemokine receptors, and integrin molecules (homing receptors) that will enable the effector T cell to migrate from the blood circulation into the inflamed tissue in a process known as extravasation. The effector T cell is initially activated to combat infection or resolve inflammation, and if it is continuously primed by the same lineage-defining cytokines during its differentiation, it will become committed to that helper T cell lineage fate and potentially proceed to become a memory T cell. Memory T cells efficiently respond to the same pathogen with the same effector functions due to a permissive chromatin state at signature cytokine genes.

3.1.1 $CD4^+$ T helper subsets

Thymic-derived $CD4^+$ T cells migrate to lymph nodes where they await meeting their cognate antigen. When properly activated, and depending on the polarizing cytokines present during activation, naive T cells differentiate into one of several effector T cell lineages/subsets. To date, several $CD4^+$ T_H lineages have been discovered, of which the

following T_H cells have been well described: T_H1, T_H2, T_H17, T follicular helper (T_{FH}), and regulatory T cells (T_{Reg}) (Figure 3.1). As this work entails experiments on T_H1 and T_H2 cells, these lineages are described in more detail than the other subsets.

Naive T cells commit to the $\mathbf{T_H1}$ cell fate/lineage when they are activated/primed in the presence of the cytokines Interferon (IFN) γ and Interleukin (IL)-12. Gene regulation is marked by an upregulation of the master transcriptional regulator for T_H1 cells, T-box transcription factor TBX21 (T-bet), encoded by the gene *tbx21*. Subsequently, T_H1 cells produce the signature cytokines IFNγ and Tumor Necrosis Factor (TNF)α [7, 8]. The T_H1 signature cytokines are pivotal for their effector functions, which is to aid in the combat of intracellular pathogens such as *Toxoplasma gondii* [9], *Mycobacterium tuberculosis* [10], and Influenza A virus [1]. At the site of infection, production of INFγ recruits cytotoxic $CD4^+$ T cells, B cells, and macrophages to induce apoptosis, opsonization, and engulfment of infected cells, respectively (Reviewed in [11]). IFNγ signaling activates the JAK/STAT pathway, in particular STAT1. STAT1 induces expression of T-bet, which in turn enters into a positive feedback loop to generate more IFNγ. Moreover, T-bet ensures the upregulating of IL-12Rβ2 to enable IL-12 responsiveness, while concomitantly downregulating GATA3 expression to prevent T_H2 differentiation. Once TCR stimulation ceases, IFNγ signaling stops, and IL-12 signaling activates STAT4, which induces transcription of T-bet. Together, STAT4 and T-bet induce robust proliferation and imprinting of the T_H1 lineage by promoting opening of the chromatin at signature cytokines such as *ifng* [7, 12, 13, 14, 15].

The cytokines IL-4 and IL-2 induce commitment to the $\mathbf{T_H2}$ cell fate. Upregulation of the master transcriptional regulator for the T_H2 cell fate, GATA Binding Protein 3 (GATA3), promotes production of the T_H2 signature cytokines IL-4, IL-5, and IL-13 [7, 12]. An essential T_H2 effector function is mediating immunity against extracellular pathogens and parasites such as helminths like *Nippostrongylus brasiliensis* [16, 1]. In doing so, T_H2 cells promote isotype class switching to IgG1 and IgE in B cells. If, however, the T_H2 response to a self-antigen or an allergen continues unregulated (e.g. by lack of suppression by T_{Regs}), continued exposure to that antigen can turn into an allergic type I hypersensitivity reaction (Reviewed in [11]). In T_H2 cells, IL-4 and IL-2 signaling leads to activation of STAT6 and STAT5, respectively. STAT6 induces expression of GATA3, and GATA3 and STAT5 both bind to the *il4/il13* locus to drive expression of IL-4. Importantly, STAT5 promotes upregulation of the IL-4Rα to enhance IL-4 responsiveness. IL-4 as such enters in a positive feedback loop to maintain IL-4 production in committed T_H2 cells. Concomitantly, to prevent differentiation into the T_H1 cell fate, STAT5 and GATA3 downregulate expression of T-bet and STAT4, respectively [12, 17, 18].

Tumor growth factor (TGF) β and IL-6 induce differentiation into the **T_H17** lineage. Fully committed T_H17 cells express the master transcriptional regulator for T_H17 cells, retinoic acid receptor-related orphan receptor gamma (RORγt), and produce IL-17A, IL-17F, and IL-22 [7, 19]. T_H17 cells assist in clearance of intracellular pathogens such as *Mycobacterium tuberculosis* [20] as well as extracellular bacterial and fungal infections, e.g., *Candida albicans*, by promoting recruitment of neutrophils [21].

T_{FH} cells develop in a response to activation of naive T cells in the presence of IL-6 and IL-21. This results in the upregulation of the master transcriptional regulator for T_{FH} cells, B-Cell Lymphoma 6 (BCL-6), that promotes production of IL-4 and IL-21. T_{FH} cells home to the B cell follicles of LNs, by virtue of CXC chemokine receptor (CXCR) 5 expression. They promote isotype class switching in B cells and the subsequent formation of germinal centres (Reviewed in [11]).

Unlike T_H1, T_H2, T_H17, and T_{FH} cells, **T_{Reg}** are not conventional $CD4^+$ effector T (T_{eff}) cells, but regulate/suppress the conventional $CD4^+$ T_{eff} activity described for the T_H lineages earlier, while also playing a role in modulating APCs to become tolerogenic before an overtly inflamed state is created. T_{Regs} thus serve to return the organism to a homeostatic balance where the infection is cleared and the integrity of the host tissue is not lost. Unlike conventional T_H cells that differentiate from recirculating naive $CD4^+$ T cells, T_{Reg} derive directly from the thymus (thymic-derived T_{Regs}), but can also be induced in secondary lymphoid organs (SLOs) in the presence of TGFβ. They are characterized by constitutive expression of the master transcriptional regulator for T_{Regs}, Forkhead box P3 (FoxP3), and production of TGFβ. Naive $CD4^+$ T cells can also be induced to express a T_{Reg} phenotype for a short time *in vitro*, in the presence of IL-2 and TGFβ. These cells are called "induced T_{Regs}" (iT_{Regs}), and produce TGFβ [22, 7] and IL-10 [19] (Figure 3.1).

The commitment of naive T cells into one of the T_H or T_{Reg} lineages/populations, described previously, is achieved in a highly controlled manner through TCR activation and subsequent polarization/differentiation. The cytokines and environmental cues (polarizing milieu) picked up by the APCs, or present in the LN to which the APC drained, are pivotal in shaping the differentation and resulting effector functions that the T cell will acquire [7, 23]. As described previously for T_H1 and T_H2 cells, the cytokines serve to promote the differentiation of a given T_H lineage while actively silencing the alternative T_H lineage. This is observed at the epigenetic level with the classic examples of opening and silencing of the *ifng* promoter in T_H1 and T_H2 cells, respectively, and silencing and opening of the *il4* promoter in T_H1 and T_H2 cells, respectively [7]. Cytokine-mediated chromatin changes thus become fixed/imprinted at signature cytokines such as *ifng* and *il4* during differentiation. This serves to maintain the expression of the lineage-appropriate

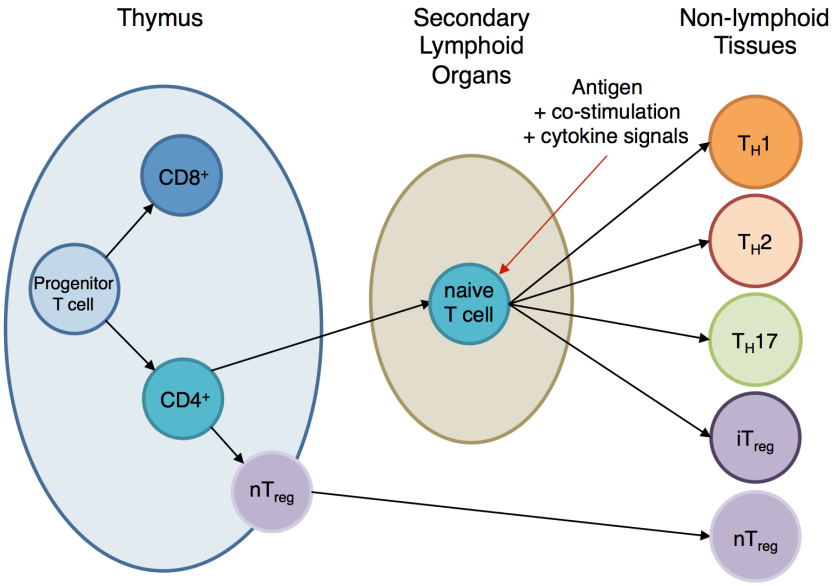

Figure 3.1: Differentiation of CD4$^+$ T cells. CD4$^+$ derive from progenitor T cells that differentiate in the thymus. Thymic-derived CD4$^+$ T cells migrate to the LNs where they await meeting their cognate antigen. Upon meeting their antigen and receiving correct TCR stimulation and cytokine signaling, they differentiate into one of the lineages of effector CD4$^+$ T cells. This depends on the presence of polarizing cytokines present during activation.

cytokines in effector T cells and memory T cells. In other words, the cells acquire an epigenetically imprinted cytokine memory, which is pivotal for efficient recall and response during future encounters with the same pathogen. In addition to acquiring a cytokine memory, T cells also change their homing receptor phenotype during activation, allowing them to alter their migration pattern in a dynamic fashion so they can reach the site of infection and mount an immune response. For memory T cells the acquisition of homing receptors is maintained so the cell can remember the tissue of first antigen encounter.

3.2 T cell trafficking/homing

While primary immune responses are initiated within LNs during activation of naive T cells, secondary immune responses are mounted at non-lymphoid sites of infection or upon pathogen encounter. This means that apart from a highly controlled functional differentiation of T cells, immune responses also require correct positioning of effector T cell populations in the body. Lymph surrounds all cells in the body. Innate and adaptive immune cells alike drain from the lymph into nearby LNs, after which migration of T cells proceeds through secondary lymphoid organs, except the spleen, only to drain into the blood via the main lymphatic vessel, the thoracic duct. The thoracic duct drains into the circulation via the heart. From the circulation, T cells can enter all non-lymphoid tissues of the body or re-enter LNs. To exit the circulation, the T cell must transmigrate across

the endothelial wall of post-capillary blood vessels by expressing appropriate combinations of adhesion molecules, chemokine receptors, and integrins (collectively referred to as homing receptors), which promote attachment of the T cell to the endothelial wall against the velocity of the blood flow experienced in the circulation. This is a highly regulated mechanism and is explained in more detail in the next section.

3.2.1 The multistep model of extravasation

Although naive and effector $CD4^+$ T cells express different combinations of homing receptors, and as such display different migration patterns as described later, both populations leave the circulation via the well-described multistep adhesion cascade. The lower blood pressure in small capillary venules of the LNs and non-lymphoid tissues allows T cells to extravasate through the endothelial cells lining the blood vessel in a multi-step adhesion cascade of capturing, rolling, arrest, and finally transmigration across the endothelial cell (EC) layer. These steps are mediated by distinct homing receptors expressed on ECs and their counter receptors expressed by the T cell – outlined in Figure 3.2.

In the first step, adhesion molecules on circulating T cells such as selectin ligands tether to their counter selectin receptor, expressed on ECs. The reversible selectin ligand:selectin interaction induces a catch-release action that can be seen as a rolling motion along the endothelium [24]. In the second step, the rolling motion causes G-protein coupled C-C chemokine receptors (CCRs) on the T cell to interact with tissue-derived chemokines displayed by the ECs [24]. This induces an inside-out signaling that leads to activation of integrins on the T cell. In the third step, firm arrest of the T cell on the ECs results from engagement between the activated integrins and their ligands expressed by the ECs. In the fourth step, in a process known as diapedesis, the T cell crawls along the endothelium to find an appropriate place to move through the endothelium. Diapedesis proceeds primarily between adjacent endothelial cells, but can also proceed through the EC body. The multistep adhesion cascade is a highly regulated mechanism that occurs under homeostatic conditions in LNs as well as in non-lymphoid tissues aggravated by inflammatory signals [25, 26, 27, 28, 29]. Access to different organs or tissues is further controlled by distinct combinations of adhesion molecules, chemokines, and integrin ligands on ECs that can be viewed as address codes and differential expression of T cell homing receptors corresponding to those address codes. Changes in homing receptor expression on the T cell is the main principle of the different homing patterns of naive vs. effector T cells.

3.2.2 Recirculation of naive $CD4^+$ T cells

Thymic-derived naive T cells recirculate through the secondary lymphoid organs (SLOs). SLOs include Mucosa-associated lymphoid tissue (MALT), such as Peyer's Patches (PP),

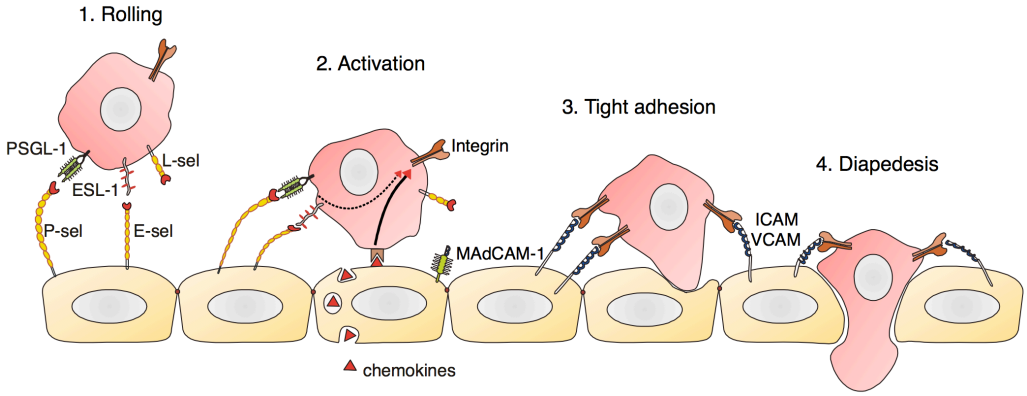

Figure 3.2: Multistep model of extravasation showing rolling, activation, firm adhesion, and transmigration/diapedesis of lymphocytes into the tissue. P-sel: P-selectin, E-sel: E-selectin, L-sel: L-selectin. Modifed from [25].

mesenteric lymph nodes (mLNs), and nasal lymph nodes, as well as peripheral lymph nodes (pLNs) and the spleen. Fluid and immune cells such as APCs, bring soluble and processed antigen, respectively, from non-lymphoid tissue when they drain into a lymph node (LN) through the afferent lymphatic vessel. The restriction of naive T cells to the LNs therefore allows maximum exposure to antigen with minimum recirculation to promote an efficient immune response.

Initially, naive T cells travel through the circulation to reach a LN via high endothelial venules (HEVs) by expressing CD62L (L-selectin) and CCR7. HEVs are post-capillary blood vesssels with specialized ECs. During homeostatic recirculation of naive T cells, the ECs of HEVs express sialylated Lewis X antigen (sLe^x)-like sugars called peripheral-node addressins (PNAds) to attract L-selectin (CD62L) expressing naive T cells, which tethers the naive T cell to the EC. Next, by virtue of CCR7 expression, the naive T cell comes into contact with the CCR7 Chemokine C-C motif ligand (CCL)19 and CCL21, both displayed by the ECs. This interaction causes activation of the integrin ligand IntraCellular Adhesion Molecule 1 (ICAM-1) in ECs, and promotes firm attachment of the naive T cell expressing the ICAM-1 ligand Lymphocyte Function-associated Antigen 1 (LFA-1). Subsequently, the naive T cell leaves the blood by transmigrating across the HEV into the LN parenchyma [30, 31]. The expression of L-selectin (CD62L) and CCR7 ensures recirculation of non-activated naive T cells back into the lymph nodes via HEVs.

3.2.3 Recirculation/homing of effector $CD4^+$ T cells

As mentioned earlier, homing receptor expression changes upon activation of naive T cells. In particular, the LN homing receptors CCR7 and CD62L are downregulated, while organ/tissue-specific homing receptors required to enter non-lymphoid tissues are upregulated to ensure an efficient secondary immune response.

ECs of different non-lymphoid organs/tissues express distinct combinations of adhesion molecules, chemokines, and integrin molecules. The combinations seem to be tissue-specific and as such can be regarded as address codes. These address codes ensure that only effector T cells with the corresponding homing receptor phenotype are flagged down and allowed to enter the tissue. LNs thus activate the upregulation of organ-specific homing receptors in effector T cells to efficiently target effector T cells to the tissue of infection/inflammation, in a manner that seems to be controlled by polarizing cytokines and microenvironmental factors present during activation.

While P-lig is induced by IL-12, it seems to be suppressed by IL-4, as discussed later. Other homing receptors such as CXCR3 and CXCR5 are mainly upregulated on T_H1 cells, whereas CCR3 is mainly upregulated on T_H2 cells. On the other hand, expression of selectin ligands and integrin alpha 4 ($\alpha4$ – encoded by the gene *itga4*) are also influenced by microenvironmental factors such as the vitamin A metabolite retinoic acid (RA). This work analyzed cytokine and microenvironmental factors' influence, in particular IL-12, IL-4, IL-2, and RA, on tissue homing instruction; therefore, tissue-specific homing is explained in more detail in the next section.

3.2.3.1 Organ/tissue-specific homing

Different homing receptor phenotypes for effector $CD4^+$ T cells have been discovered for the gut, skin, liver, lungs, the central nervous system, and bone marrow, of which the gut and skin homing receptor phenotypes have been particularly well described. The homing receptors involved mediate either tethering, chemokine-induced activation of integrins, or firm arrest, as described earlier. Because this work deals mainly with gut and skin, homing to these organs are described in more detail.

Gut homing refers to the preferential recirculation of effector T cells to the intestines. The gut homing phenotype is acquired upon priming/activation in the gut-associated lymphoid tissue (GALT). It is mediated by T cell upregulation of $\alpha4\beta7$, LFA-1, and CCR9 that interact with EC-induced Mucosal vascular addressin Cell Adhesion Molecule 1 (MadCAM-1), ICAM-1, and CCL25, respectively [32]. It should be mentioned that CCL25 can also activate $\alpha4\beta7$ [33]. While $\alpha4$ in a heterodimer with the integrin $\beta7$ directs T cells to the gut, CCR9 specifically targets T cells to the small intestine. This is consistent with the strict RA-mediated upregulation of CCR9 expression, that derives principally from cells of the small intestine [32]. This is discussed in more detail later.

Skin homing describes the preferential recirculation of effector T cells to the skin. T cells acquire the skin homing phenotype after being primed in the pLNs. It is characterized by

the expression of E-selectin ligands (E-ligs), as well as the CCR4 and CCR10 that interact with the chemokines CCL17 and CCL27 expressed in the dermis and keratinocytes of the epidermis, respectively. E-ligs mediate tethering to E-selectin on ECs. P-selectin can also recruit P-selectin ligand (P-lig) expressing T cells to the skin, but this homing receptor is preferentially upregulated during inflammation. It is unclear whether CCR4 and CCR10 induce LFA-1 integrin activation and subsequent entry by interacting with ICAM-1, but once in the dermis CCL17 and CCL27 direct migration of $CCR4^+$ or $CCR10^+$ T cells into the dermis and epidermis, respectively [32].

Apart from microenvironmental factors, inflamed tissues also attract effector T cells. ECs near inflamed tissues express P-selectin, which attract effector T cells expressing P-ligs [34]. As such, under inflammatory conditions P-ligs have been observed to play a role in migration to the liver [1], brain [35], lungs [36], gut [37, 38, 39, 40], and skin [41]. Importantly, P-lig expression during inflammation often overlaps with the homing receptors normally targeting organ-specific homing. For example, P-lig^+ T cells have been recruited to inflamed ECs of the colon in ileitis or colitis-induced mice alone or while being co-expressed with $\alpha 4\beta 7$ [42, 43, 40]. Despite the seemingly global use of P-lig during inflammation, its expression is tightly regulated by cytokines and microenvironmental factors, as described earlier, in a manner that is not yet fully understood.

3.2.3.2 Regulators of organ/tissue specific homing

While vitamin A is primarily found in the gut, vitamin D is enriched in the skin. Their respective metabolites, retinoic acid (RA) and $1{,}25(OH)_2D3$, play a role in regulating the immune response by controlling homing receptor expression during T cell activation [45, 6, 32]. RA promotes the upregulation of $\alpha 4\beta 7$ and CCR9, while $1{,}25(OH)_2D3$ upregulates CCR10 (Figure 3.3). CCR10 is important for the migration into the epidermis but not for the extravasation of the T cell into the tissue, for which reason it is not discussed further in this work. Cytokines, such as IL-12 and IL-4, are also implicated in the regulation of homing receptors and their influence on P-lig expression is described later in this section.

Unlike dermal fibroblasts and stromal cells of pLNs within the skin, DCs, stromal cells, and small intestinal ECs of the GALT contain alcohol dehydrogenases and retinaldehyde dehydrogenases [46, 47], which enables them to convert food-derived vitamin A (retinol) into retinal and RA, respectively. The expression of retinol metabolizing enzymes is in turn regulated by dietary vitamin A [48]. RA is a small lipophilic molecule that can diffuse through the lipid bilayer of the cell membrane after which it finds its way into the nucleus. RA triggers RA signaling as a ligand for the soluble nuclear receptors retinoic acid receptor (RAR) α, RARβ, and RARγ. These receptors bind to retinoic acid response

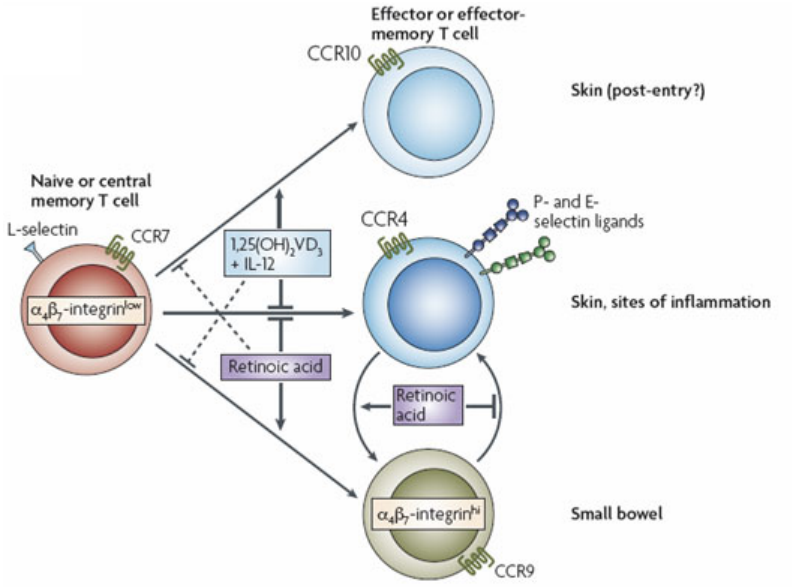

Figure 3.3: Influence of RA and 1,25(OH)$_2$D3 on the homing receptor expression. RA induces $\alpha 4\beta 7$ and CCR9 that targets effector T cells to the intestine and small intestine, respectively. RA inhibits the expression of the skin homing phenotype suppressing induction of E-lig, P-lig and CCR4 and possibly also CCR10. 1,25(OH)$_2$D3 induces the expression of CCR10, while blocking both gut homing receptors as well as E-lig, P-lig, and CCR4. Borrowed from [44].

elements (RAREs) within DNA in a heterodimer with one of the retinoid X receptors (RXRs): RXRα, RXRβ, and RXRγ. RA cannot bind as a ligand to RXRs; however, the stereoisomer of RA, cis-retinoic acid, has affinity for both RAR and RXR [49]. Experimentally, synthetic RAR antagonists, such as LE540, have been used to examine the effects of blocking RA signaling *in vitro*, but its exact antagonistic mechanism is not clear.

Due to the anatomy of the gastro-intestinal tract, the prevalence of RA is higher in mLNs than in pLNs. As described earlier, RA is an important factor driving the gut homing phenotype. While it promotes upregulation of CCR9 expression and $\alpha 4\beta 7$, it concomitantly inhibits the expression of skin homing receptors E- and P-lig as well as CCR4 and CCR10 (Figure 3.3). This could explain why there are 2-fold more P-lig$^+$ T cells in the pLNs than mLNs, which coincides with a clear preferential trafficking of T cells from pLN to the skin [1]. During inflammation, however, it was shown that the frequency of P-lig$^+$ T cells in the gut increases, indicating that P-lig can facilitate homing of T cells to the gut [40].

Cytochrome P450s (CYPs) play a significant role in regulating RA signaling by catabolizing RAR and RXR ligands (reviewed in [49]). Antigen-experienced CD44$^+$ T cells of the gut (PPs and mLNs) express only one CYP family member, Cyp26b1, but those from skin draining LNs (pLNs) or the spleen express none [50]. This means that RA is

catabolized by Cyp26b1 in the mLNs, but not in the pLNs or spleen.

For part of this work, the combined effect on P-lig expression by microenvironmental factors and cytokines was investigated. Apart from vitamin A and D metabolites, cytokines also seem to regulate the expression of homing receptors during T cell activation. Previous results in our group showed that IL-12 is a potent inducer of E- and P-ligs *in vitro* and *in vivo* [51]. However, the T_H2-associated cytokine, IL-4, was unable to induce E- and P-ligs *in vitro* [51]. Later studies in our lab showed that *ex vivo* isolated T_H2 cells from different LNs do express P-lig. Upon infection of mice with *B. Nippostrongylus*, which induces a T_H2 immune response, *ex vivo* isolated T_H2 from lung and spleen upregulated P-lig similar to *ex vivo* isolated T_H1 in response to infections that induce a T_H1 response. This indicated that an inflammatory milieu boosts the expression of P-lig [1] (Figure 3.3). Interestingly, this study found that P-lig frequencies in the pLN are 2× higher than in mLNs for both T_H1 and T_H2 cells. Along with gut-homing phenotype being induced by RA [52], our lab showed that blocking RA *in vitro* promoted IL-4-mediated induction of E- and P-ligs. Thus, the addition of LE540 as a pan-RAR antagonist facilitated expression of E- and P-ligs [53]. Also, in media lacking FCS, induction of E- and P-ligs were observed under T_H2 conditions, suggesting that RA inhibits the inducing effect of IL-4.

3.2.4 The selectins and their ligands

The selectins and their ligands belong to a family of single-chain transmembrane glycoprotein cell adhesion molecules expressed exclusively by leukocytes and ECs.

L-, E-, and P-selectins (named after the cell on which they were discovered: leukocytes, endothelial cells, and platelets, respectively) belong to a family of adhesion molecules with a highly evolutionary conserved Ca^{2+}-dependent lectin domain. The selectins vary only in the number of variable consensus repeat units – 2, 6, and 9 for L-, E-, and P-selectin, respectively. The N-terminal Ca^{2+}-dependent lectin domain binds fucosylated carbohydrate epitopes such as sLe^x moieties, which mediates the main physiological function of these molecules: adhesion of cells under blood flow.

L-selectin (also known as CD62L) is mainly expressed on myeloid cells and naive T cells, and interacts with the ligands GlyCAM-1, CD34, MadCAM-1, and P-selectin glycoprotein ligand-1 (PSGL-1), expressed on endothelial cells [54]. L-selectin facilitates entry of T cells from the circulation into both the LN, via the HEV, and into non-lymphoid tissues [30, 31, 55, 56, 26, 27, 28]. **E-selectin** (CD62E) is constitutively expressed in skin post capillary venules, but its transcription can also be induced in ECs during inflammation [57]. E-selectin binds several glycosylated **E-selectin ligands (E-ligs)** displayed on scaffold proteins such as PSGL-1, ESL-1, and CD44. **P-selectin** is stored in secretory

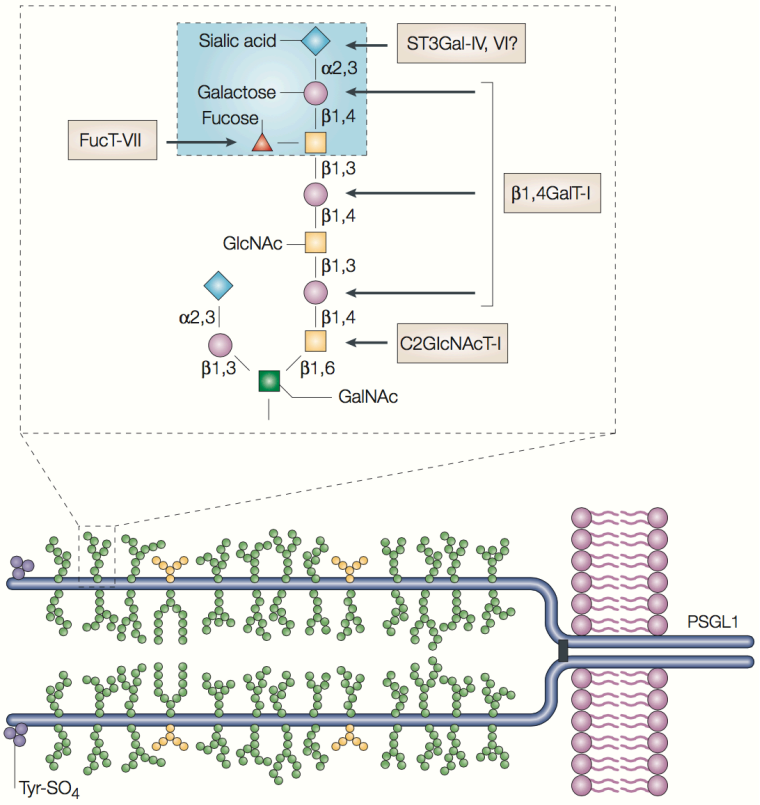

Figure 3.4: Depiction of a prototypical selectin ligand, PSGL-1, after the sequential addition of carbohydrate moieties to a scaffold protein by several glycosyltransferases as indicated. If appropriately modified, PSGL-1 can bind all three selectins. Adapted from [34].

granules such as in α-granules of platelets and in Weibel-Palade bodies in endothelial cells. P-selectin is translocated to the cell surface within minutes upon activation or its synthesis induced by inflammatory factors such as TNFα, Thrombin, and endotoxin [58, 59]. This makes P-selectin essential for recruitment of leukocytes to sites of inflammation. Most **P-selectin ligand (P-lig)** epitopes are displayed on the scaffold protein PSGL-1 [60], however, PSGL-1 also displays ligands for E-selectin [60] or L-selectin [34].

3.2.4.1 Posttranslational generation of selectin ligands

P-selectin and E-selectins bind P- and E-ligs, in a Ca^{2+}-dependent manner [61]. While E-lig binds selectively to E-selectin, P-ligs have a broader binding capacity and can bind both E- and P-selectin. The ligands are generated by a series of enzymatic reactions that posttranslationally add oligosaccharide/glycan structures to a scaffold protein [62]. The enzymes involved in the generation of selectin ligands are collectively called glycosyltransferases (glycoTs). Recent reports suggest that the glycoTs, in particular the fucosyltransferases, required for the generation of E-ligs differ between mouse and human [63, 64]. As this work is focused on the mouse system, the generation of selectin

ligands on a prototypical mouse P-lig in this system is briefly described later. Selectin ligands are mainly expressed by leukocytes, and while E-ligs are not dependent on Core 2 β1,6-glucosaminyltransferase-I (C2GlcNAcT-I or GCNT1), P-lig is. Most of the enzymes required to make P-lig are constitutively expressed in leukocytes, but C2GlcNAcT-I and α1,3-fucosyltransferase VII are upregulated during T cell activation and during differentiation into effector/memory T cells, making them the rate-limiting factors in P-lig generation.

C2GlcNAcT-I mediates the O-linked second branching of the ligand structure by addition of β1,6-GlcNAc (*N*-acetylgucosamine) to GalNAc moieties that have been deposited on Serine or Threonine residues of the scaffold protein (Figure 3.4). In a collaborative fashion, β1,4-galactosyltransferase-I (β1,4GalT-I) and C2GlcNAcT-I add galactose and GlcNAc to the structure. Finally, α1,3-fucosyltransferases, Fucosyltransferase 4 or 7 (FucT-IV or FucT-VII) mediate the fucosylation of the last GlcNAc and two sialyl transferases (in particular ST3GAL-IV) mediate the addition of sialic acid to the last galactose generating the final tetrasaccharide sLe^x epitope. The ligand epitope is complete when many such branches have been formed and at least one of the Tyrosines at the end of the scaffold protein have been sulfonated by Tyrosine sulphotransferases (TSP). This is only one variation of P-lig that has been studied on the PSGL-1 scaffold protein. E-lig and L-selectin ligands are shorter, but not well described [34, 65].

Most of these enzymes, and subsequently the ligands, are constitutively expressed in myeloid cells and neutrophils. In T cells, however, FucT-VII and C2-GlcNAcT-1 are upregulated during T cell activation to generate functional selectin ligand epitopes in effector T cells. FucT-VII is indispensible for the generation of E-ligs and P-ligs. In contrast, C2-GlcNAcT-1 is more important for P-lig synthesis and seems dispensible for E-lig synthesis [34, 66, 67]. As described earlier, the expression of P-lig and E-lig is also affected by cytokines and microenvironmental factors present during T cell activation. The molecular regulation required to upregulate the genes *gcnt1* and *fut7* that code for C2GlcNAcT-I and FucT-VII, respectively, is the main focus of this work, and what we known about their molecular regulation is described in the next section.

3.3 Molecular regulation of *gcnt1* and *fut7*

This work focused on the molecular regulation of *gcnt1* and *fut7* in $CD4^+$ T_H1 and T_H2 cells *in vitro*. These genes code for the enzymes C2-GlcNAcT-1 and FucT-VII, respectively, and are crucial for the synthesis of E- and P-ligs, as described earlier. Both of the genes are induced upon T cell activation, but through distinct regulatory mechanisms.

For instance, our previous study suggests differential involvement of the NFAT pathway in the upregulation of *gcnt1* and *fut7* after T cell activation. Reciprocal expression of P-lig was observed when culturing T_H1 and T_H2 cells with Cyclosporine A (CsA), a Calcineurin inhibitor blocking NFAT dephosphorylation and subsequent nuclear translocation downstream of TCR signaling. This resulted in a significant decrease in P-lig$^+$ T_H1 cells and an increase in P-lig$^+$ T_H2 cells [68]. This was reflected in Gcnt1 mRNA levels in these T cell cultures, but not in Fut7 mRNA levels. This indicated that *fut7* is induced by other pathways downstream of TCR activation than *gcnt1*, as suggested by studies implicating phosphoinositide 3-kinase (PI3K)-mediated H-Ras activation in the induction of *fut7* [69]. Recently, p38 Mitogen-Activated Protein Kinase (MAPK) was also shown to play an important role in inducing expression of both *gcnt1* and *fut7* [70]. Interestingly, the MAPK pathway also phosphorylates CREB (see Aim of Work), which has been shown to bind the human *fut7* locus and drive *fut7* expression in a Tax-dependent manner upon human T-lymphotropic virus type 1 (HTLV-1) infection.

In addition to TCR associated pathways, cytokine signaling is pivotal for induction of *gcnt1* and *fut7*. Lim et al. (2001) reported that IL-12-dependent upregulation of STAT4, but not IFNγ, is required to upregulate Gcnt1 mRNA, but not Fut7 mRNA. They did not observe upregulation of *gcnt1* in T_H2 or T_H0 cells (cultured in the absence of IL-12 and IFNγ), but could show upregulation of Fut7 mRNA in Th0 cells almost to the same levels as in T_H1 cells. The transcriptional levels of *gcnt1* and *fut7* correlated with E- and P-lig levels in these cell subsets as did rolling events on E- and P-selectins (a measure for the tethering capability of T cells). This means that IL-2, in Th0 cells, was sufficient to induce *fut7*, and subsequently E-selectin, and that IL-12 is not required for *fut7* induction in T_H1 cells [71]. Another study by White et al. (2001) verified the importance of STAT4 in the induction of Gcnt1 mRNA using *stat4*$^{-/-}$ T_H1 cells. These cells were unable to roll on P-selectin. Moreover, only 50% of the *stat4*$^{-/-}$ T_H1 cells could roll on E-selectin, presumably due to activity of FucT-VII in generation of E-lig[72]. Two later studies implicated T-bet in the upregulation of selectin ligands in T_H1 cells, performing *in vitro* rolling assays where *tbx21*$^{-/-}$ T_H1 cells were unable to tether to E- and P-selectin compared to WT T_H1 cells [73, 74], indicating a clear involvement of T-bet in the induction of both *gcnt1* and *fut7*. The study by Lord et al. additionally showed that homing to the peritoneal lavage in the gut upon antigen challenge was abrogated in *tbx21*$^{-/-}$ T_H1 cells polarized *in vitro* [74], further indicating a role for P-lig (and potentially E-lig) in homing to inflamed tissues even in the gut.

Apart from cytokines, microenvironmental factors, such as RA, seem to regulate homing receptor expression as described earlier. RA was shown to inhibit selectin ligand expression, mainly via suppression of *fut7*. Previous studies from our group suggest that

RA is also responsible for the lack of induction of P-lig in *in vitro* generated T_H2 cells, while P-lig is observed in T_H2 cells *in vivo*. Thus, our group has shown that culturing T_H2 cells in the absence of RA resulted in an increase in *gcnt1* and Fut7 mRNA as well as P-lig. The importance of IL-4 in the induction of *gcnt1* and P-lig was verified in *stat6*$^{-/-}$ T_H2 cells, where, even in the absence of RA, no induction of P-lig was observed. This indicates a clear involvement of IL-4 on the modulation of *gcnt1* and P-lig induction as well as partly for Fut7.

Another important phenomenon in Gcnt1, Fut7, and P-lig expression, is that it requires cell cycling – a window where chromatin modifications often occur. Previously, our lab showed that naive T cells after TCR activation must proceed through the G1/S phase to express P-lig, but that 50% of memory cells reactivated in the presence of L-mimosine, a cell cycle inhibitor targeting the G1/S phase, still upregulated P-lig [2]. This indicates that a fraction of memory cells previously primed to induce P-lig retain the ability to express it without proceeding through the cell cycle. These cells presumably have open/actively configured chromatin modifications at pivotal regulatory regions within *gcnt1* and *fut7*, enabling the memory cells to quickly recall P-lig expression upon TCR stimulation. This supports the hypothesis of highly effective memory recall and clearance of infections previously experienced by the host.

Concerning epigenetic regulation of *gcnt1* and *fut7*, DNA methylation within the *fut7* locus has been shown to correlate with repression of Fut7 mRNA in P-lig$^-$ effector/memory T cells [75]. On the other hand, *gcnt1* appears to be governed not by DNA methylation, but by histone methylation. In particular, repressive histone marks in a newly identified *gcnt1* enhancer correlate with a lack of P-lig expression [53]. Other unpublished results from our group indicate that other epigenetic mechanisms control induction of *gcnt1*, *fut7*, and thus P-lig. Polarizing T cells in the presence of Trichostatin A (TsA), a histone deacetylase (HDAC) inhibitor, leads to immediate upregulation of *gcnt1* in T_H2 cells on day 1 and day 2 of *in vitro* cultures, but does not affect expression in T_H1 cells. In contrast, TsA lowered Fut7 mRNA in T_H1 and Th0 cells, but did not affect its expression in T_H2 cells. P-lig also increased in the presence of TsA, supporting the primary involvement of *gcnt1* in the synthesis of P-lig. This also indicates that IL-4 does not repress *fut7* by GATA3-mediated recruitment of HDACs, as recently proposed by others [76].

Altogether, there is a clear difference in the induction of *gcnt1* and *fut7* during and after TCR activation that, like cytokine expression, is governed by the cytokines and other factors, such as RA, present in the LN during T cell activation.

3.4 Regulation of gene expression

Gene regulation is the result of a choreographed set of events within the cell. Coordination of transcription, RNA processing, and translation leads to stable expression or silencing of genes that are needed in a temporal fashion to ensure successful multicellular differentiation and morphogenesis. Initiation and maintenance of gene expression is no longer thought of as just decoding DNA by the transcriptional machinery: the past 20 years have uncovered several epigenetic mechanisms such as posttranslational modifications (PTMs) of amino acids of histone tails, postsynthetic DNA methylation, and noncoding RNAs that occur alongside transcriptional events to control higher order access to DNA regulatory elements such as promoters and enhancers/silencers (Reviewed in [77]).

3.4.1 Regulatory regions and transcription factor binding

A gene is composed of exons and introns between the exons; however, only exons are transcribed and spliced together by the transcriptional machinery prior to translation in the cytoplasm. To control transcription, a gene possesses regulatory regions that serve to up- or downregulate its expression. A **promoter** for a gene is located in the proximal vicinity of the transcriptional start site (TSS), and can possess a TATA box or other elements such as CpG islands to promote recruitment of the transcriptional machinery. Sometimes a gene possesses several TSSs that signify the usage of alternative transcripts. Alternative transcripts can be expressed in a tissue-specific manner [78]. **Enhancers** and **silencers** are orientation-independent regulatory regions located several genes away, distal from a gene, or within a gene. These regions bind TFs such as co-activator complexes or polycomb proteins that respectively upregulate or downregulate basal gene transcription in collaboration with events that occur at the promoter. The promoter and regulating regions are brought in the vicinity of each other by TFs that bind both regions [79].

Differentiation of T cells begins with interactions between transcription factors and regulatory regions within the DNA. Transactivating TFs such as NFATs and STATs interact with response elements (binding sites) within promoters and enhancers/silencers to initiate or silence gene transcription. The accessibility of a given enhancer and/or promoter are often discernible in DNAse hypersensitivity assays that digest accessible DNA, and is controlled by epigenetic modifications of histone tails, DNA, or the presence of regulatory long noncoding RNA. The nature of these epigenetic modifications is outlined in the next section.

3.4.2 Epigenetic mechanisms of gene regulation

Epigenetics is the study of heritable changes in gene expression that are not due to alterations in the DNA sequence. Several epigenetic mechanisms have been described to

contribute to gene regulation, such as post-translational modifications (PTMs) of histone N-terminal tails, DNA methylation of cytosines, and non-coding RNAs (ncRNAs) like miRNA, siRNA, and long noncoding RNAs (lncRNA). LncRNAs is a new and exciting field in contemporary molecular biology, and it has been shown that lncRNAs can directly recruit chromatin remodelling complexes such as Polycomb repressor complexes 1 and 2 (PRC1 and PRC2) of the Polycomb Group (PcG) protein complex to regulatory regions. PCR1 and PCR2 both possess RNA binding domains suggesting that they are guided to the DNA by lncRNAs. Additionally, PcG recruits HDACs and DNA methyltransferases 3a (DNMT3a) effectively aiding in further stable suppression of transcription. LncRNAs thereby contribute to regulation of transcription at the epigenetic level [80, 81]. ncRNAs are beyond the scope of this work and not detailed further. Histones make up the core of nucleosomes, around which the DNA coils into space-saving chromosomes. PTMs such as phosphorylation, acetylation, and methylation decorate selected amino acids, notably Lysines, on histones that influence how tight DNA folds around the nucleosomes. Heterochromatin (inactive or silenced) signifies DNA that is inaccesible to TFs due to the tight interaction to the nucleosomes. Conversely, euchromatin has DNA that is accessible to TFs due to its loose interaction with DNA. Several histone methylation marks were investigated in this work; therefore these are described in more detail in the next section.

3.4.2.1 Histone methylation

In the nucleus, 146 basepairs (bps) of eukaryotic DNA is wrapped around two sets of four histones, H2A, H2B, H3, and H4, that arrange into an octamer called a nucleosome. The N-terminal tails of histones contain positively charged Lysines and Arginines, and other amino acids that intimately interact with the negatively charged DNA. This interaction effectively coils DNA into higher order condensed chromosomal structures. This not only saves space within the nucleus, but also promotes tight control of gene expression. The polarity of histone N-terminal tails affects the attraction to DNA, and is affected by PTMs such as methylation and acetylation. Methylation of Lysine amino groups does not change its net charge and therefore this PTM does not affect the electrostatic attraction between histones and DNA. Contrary to methylation, acetylation of Lysines reduces the net charge on histones and thus contributes to a loosened histone:DNA contact with a resulting positive effect on transcriptional activity by virtue of increasing access for TFs.

Mono-, di-, and tri-methylation of Lysine 4 of histone 4 (H3K4me1, H3K4me2, and H3K4me3) are deposited by histone Lysine methyltransferases (HKMTs) such as Trithorax histone methyltransferase group of proteins (TrxG) and removed by histone demethylases such as Jumonji (JmjC) [82, 83]. These marks are associated with an open chromatin configuration, with H3K4me1 and H3K4me2 known to correlate with enhancer function of the respective genomic region. **H3K4me1** is specifically correlated with the binding of

the chromatin coactivator TF p300, and alongside high levels of H3K27ac or H3K27me3 associate with active or poised enhancer activity, respectively. Poised designates a region decorated by both active and repressive marks where most often the Polycomb Group complex (PcG) maintains the H3K27me3 mark (Figure 3.5). p300 is associated with opening of the chromatin by virtue of its inherent histone acetyltransferase (HAT) activity. High levels of **H3K4me2** are associated with TF binding regions [84] and binding of p300 and do not necessarily correlate with conserved DNA regions [82]. Unlike H3K4me1 and H3K4me2, **H3K4me3** is associated with promoters located at 5' ends of genes near the transcriptional start site (TSS) [82].

Trimethylation of Lysine 27 of histone 3 (**H3K27me3**) is deposited by the HKMT Eed-Ezh2, and maintained by the PcG, that consists of several proteins. H3K27me3 is removed by demethylases such as Jmjd3. H3K27me3 is strongly associated with repressed chromatin states and absence of transcription (Figure 3.5).

Trimethylation of Lysine 36 of histone 3 (**H3K36me3**) is associated with transcriptional elongation by RNA polymerase and, as such, marks areas where transcription is most likely occurring (Figure 3.5). Human SET2 proteins are HKMTs that bind both RNA Polymerase and H3K36, presumably to deposit methyl groups while RNA polymerase is elongating the transcript. These proteins are also involved in recruiting other histone modifiers and DNA methylases such as DNMT3A suggesting that H3K36me can regulate open or repressed chromatin states [85].

Many other marks such as **H3K27ac** have been uncovered, but are not studied in this project. For sake of completeness, Histone acetyltransferases (HATs) deposit acetyl groups to H3K27, while histone deacetylases (HDACs) removes them. H3K27ac seems to be mutually exclusive with H3K27me3 and is a histone mark marking an active or open chromatin region where transcription can occur. Together with H3K4me2 marks, this signifies an active enhancer (Figure 3.5 – upper panel).

Genome-wide histone methylation profiling of $CD4^+CD62L^{hi}CD44^-CD25^-$ naive T cells and $CD4^+CD25^+$ nTregs isolated *ex vivo*, as well as $CD4^+$ T cells polarized *in vitro* to T_H1, 2, 17, and iT_{reg} subsets, showed no significant difference in the location of active H3K4me3 and repressive H3K27me3 marks on almost 20,000 analyzed genes. The study showed that, for all subsets analyzed, the majority of H3K4me3 marks are deposited at proximal promoter regions (40-60%), intergenic regions (24-30%), and introns (14-24%), while exons possess little to none (<5%). H3K27me3 marks were observed mostly at intergenic regions (65-70%) and introns (23-28%), whereas the proximal promoter regions and exons hardly carried any marks (<6%). Interestingly, the study also showed that some

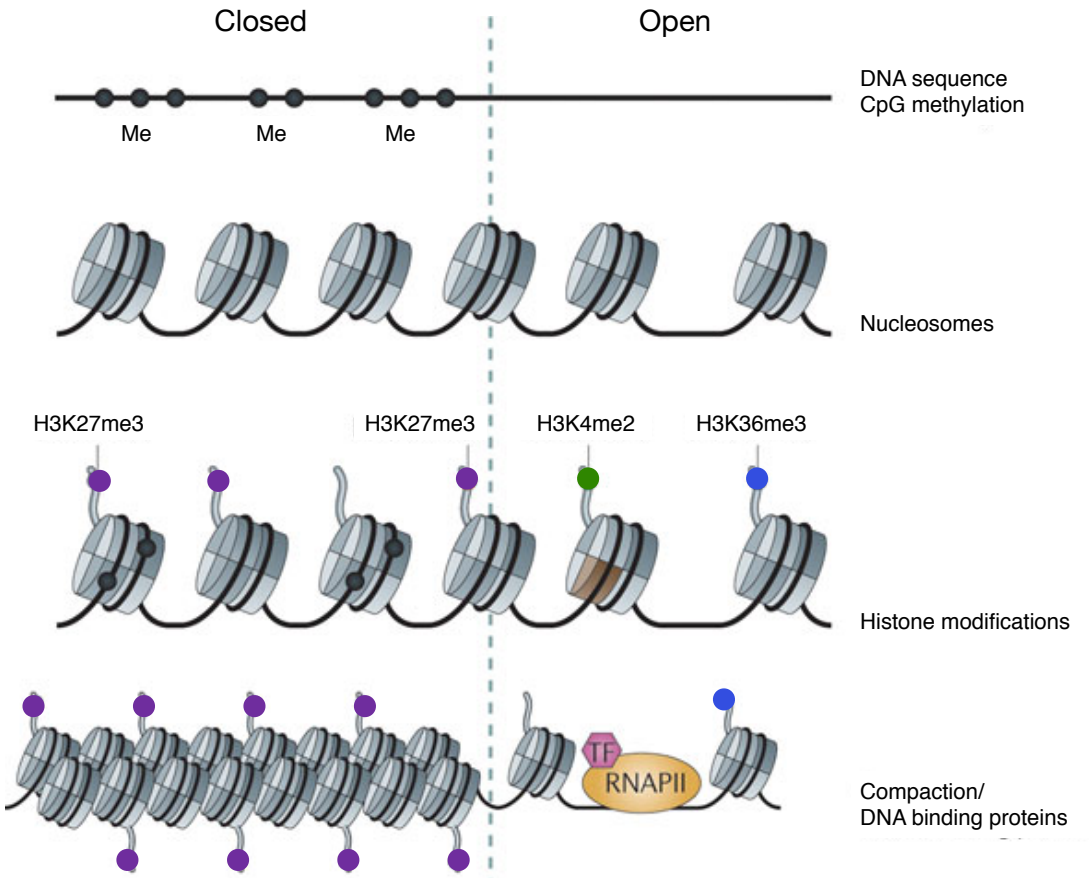

Figure 3.5: Overview of chromatin modifications. A gene can possess a closed or open chromatin configuration. Each of these states are marked by DNA methylation (or lack thereof) or histone modifications. The closed chromatin configuration prevents access to the DNA, while the open chromatin configuration allows binding by the transcriptional machinery. A closed chromatin configuration is often marked by methylated CpGs and H3K27me3 marks. DNA methylation can recruit PcG, which in turn maintains the H3K27me3 marks. The closed chromatin state is marked by nucleosomes that are positioned closely together to prevent transcription. An open chromatin configuration lacks CpG methylation and is often accompanied by H3K4me2 or H3K4me3 marks. This positions nucleosomes farther apart and thus allows RNA polymerase II to bind and initiate transcription. Adapted from [86].

genes, such as *il18r1*, that are highly expressed in T_H1 cells with almost no H3K27me3 marks, display low to varying amounts of H3K27me3 in other IL-18R1 non-expressing subsets such as T_H2, T_H17, and thymic-derived T_{regs}. This could indicate that different lineages suppress expression by various epigenetic mechanisms that might not be identical between lineages [87].

3.4.2.2 DNA methylation

DNA methylation is the only epigenetic mechanism that leads to a direct modification of the DNA, where a methyl group is transferred to the 5th carbon of the nucleotide Cytosine resulting in 5-methylcytosine (5mC) (Figure 3.5). The methyl transfer is mediated by a family of DNA methyltransferases (DNMTs) *de novo* during morphogenesis/development

by DNMT3a and DNMT3b, and maintained during cell cycling in mitosis by DNMT1 targeting hemimethylated DNA. 5mC can be removed passively by further hydroxymethylation (generating 5hmC) to prevent maintenance of the 5mC through cell division. It can also be actively removed in nondividing cells by hydroxylation and deamination by Tet enzymes and AID/APOBEC enzymes [88, 89], respectively, after which the base is recognized, excised, and replaced by DNA base excision repair glycosylases [90].

DNA methylation is intimately connected with a recruitment of chromatin modifiers and ncRNAs. The Methyl-CG-binding domain (MBD) family in mice are attracted to methyl-CGs. These recruit HDACs and proteins similar to ATP-dependent helicases that prevent RNA polymerase from binding to DNA. Similarly, it has been shown that MBD1 from mouse and methyl-CpG-binding protein 2 from rat can mediate silencing of a gene by recruiting histone methylases. Jeffrey and Nakielny (2004) reported that MBD2 proteins in mice were able to bind radioactively labeled probes of siRNA and methyl-dsDNA *in vitro*. Although the binding proceeded through two different domains, the binding was mutually exclusive: either the MBD2 bound siRNA (mimicking single-stranded ncRNA) or methyl-dsDNA (mimicking DNA), but not both. They similarly observed that DNMT3a and DNMT3b1 were able to bind the siRNA probes. This study links RNA-mediated regulation, chromatin changes through histone PTMs, and DNA methylation, and suggests that ncRNA, through complementarity with DNA, may guide DNA-methyltransferases and histone chromatin remodeling complexes to a specific gene [91, 92].

Altogether, epigenetic mechanisms are intimately connected with transcription factors in the regulation of cytokine gene expression in T cell lineages, as well as regulating homing receptor genes that are responsible for guiding T cells to the site of infection.

4. Aim of Work

The spatio-temporal regulation of correct localization of T cells during infection or inflammation is pivotal for the outcome of the immune response. Considering this as a therapeutic target, it is therefore highly interesting to understand how T cells are attracted to sites of inflammation. The past two decades have revealed organ-specific patterns of T cell immunosurveillance and, in particular, organ-non-specific involvement of P-ligs in the migration to sites of inflammation in e.g., skin and gut. Our group and others have shown that P-lig expression is retained on memory T cells, akin to cytokine memory shown for the different T_H subsets [93]. Although P-lig has been observed on murine T_H1 and T_H2 cells *in vivo* [1] during inflammation, this has not been recapitulated *in vitro*. Core2-β 1,6 glucosaminyltransferase-I (C2-GlcNAcT-I) and Fucosyltransferase-VII (FucT-VII) are expressed in T_H1 cells, but like P-ligs, are suppressed under T_H2 conditions *in vitro* [53, 75]. This suggests that IL-4 can drive expression of *Fut7* and in particular *Gcnt1 in vivo*, but is unable to do so *in vitro*. C2-GlcNAcT-I and FucT-VII are pivotal for the upregulation of P-lig and the skin homing receptor, E-lig, after T cell activation. This work aimed to understand the molecular regulation and long-term stability of *Gcnt1* and *Fut7* induction in T_H1 and T_H2 cells *in vitro* to uncover the discrepancy between P-lig expression *in vivo* and *in vitro*. Firstly, we examined the regulation of *Gcnt1* and *Fut7* in T_H1, permissive for P-lig expression. Secondly, we investigated the discrepancy between expression of *Gcnt1* and *Fut7* in T_H1 and T_H2 cells *in vitro*, in particular, under the influence of RA.

Because T_H1 cells express C2-GlcNAcT-I and FucT-VII that induce functional P-ligs *in vitro*, this work firstly aimed to understand the regulation of their genes *Gcnt1* and *Fut7* during initial and long-term T_H1 cell differentiation. For *Gcnt1*, a promoter had previously been characterized to have activity in both T_H1 and T_H2 cells. Preliminary results showed an enhancer being marked by repressive histone marks in P-lig$^-$ T_H1 cells [53], which we aimed to verify. Because STAT4 and T-bet are required for *Gcnt1* expression in T_H1 cells, we aimed to determine whether and when STAT4 and T-bet bind to the newly identified enhancer, hypothesizing that STAT4 is involved in initial induction and T-bet in long-term stable expression of Gcnt1. For *Fut7*, DNA methylation within a minimal promoter was shown to correlate with lack of Fut7 mRNA. Therefore, we aimed to

determine the methylation dependency of this region *in vitro* after initial verification of enhancer and promoter regions for the murine *Fut7*. The involvement of the methylation sensitive CREB TF was also investigated because its putative binding motif showed strong methylation in cells lacking Fut7 mRNA. Due to the implications of IL-2 in the induction of *Fut7*, its regulation by STAT5 was also investigated.

Based on the knowledge that T cells primed in the gut express virtually no P-lig but only the RA-inducible gut homing receptors, $\alpha 4\beta 7$ and CCR9, we hypothesized that RA, present in the *in vitro* media, inhibits IL-4-mediated induction of *Gcnt1* and *Fut7* as the underlying cause of P-lig suppression in these cells. Therefore, the second aim of this thesis was to understand the effect of RA on *Gcnt1* and *Fut7* induction in T_H1 and T_H2, with particular focus on the mechanism of RA suppression and its effect on the activity of the *Gcnt1* regulatory regions.

5. Materials and Methods

5.1 Materials

5.1.1 Mice

BALB/c and C57BL/6 mice were purchased from Charles River (Sulzfeld, Germany). *stat4*$^{-/-}$ and *tbx21*$^{-/-}$ mice on a C57BL/6 background were kindly provided by Dr. Andreas Thiel at the BCRT and Prof. Max Löhning at the DRFZ in Berlin, Germany. All animal experiments were performed in accordance with institutional, state and federal guidelines and with permission from the Landesamt für Gesundheit und Soziales Berlin (LaGeSo). The CpG free pCpGL plasmid was kindly provided by PD Dr. Michael Rehli (University Hospital Regensburg).

5.1.2 Consumables, instruments, kits, buffers, and reagents

Table 5.1: Consumables

Consumables	**Manufacturer**
70 µm Cell Strainer	BD Falcon
96 Well PCR Plates	Biozym Scientific
96 Well V-bottom plates	Costar
C-Chip Neubauer improved disposable cell counting chamber	Biochrom/Merck Millipore
Cell culture petri dishes (24, 12, 6-well)	Thermo Scientific
CellTrics 30 µm filters	Sysmex Partec
FACS tubes	Sarstedt
Falcon tubes (15 and 50 mL)	BD Falcon
Gloves	Kimtech
MACS LS columns	Miltenyi Biotec
MACS Multi-8 separation columns	Miltenyi Biotec
MACS pre-separation filter	Miltenyi Biotec
MicroSeal B Adhesive Seals	BioRad
PCR tubes and eppendorf tubes (0.2, 0.5, 1.5, and 2.0 mL)	Eppendorf
Pipette tips (filter)	Sarstedt
Pipette tips (no filter)	Nerbe Plus
RNAse AWAY	Life Technologies
Serological Pipets	BD Falcon
Sterile filter unit(Steritop/Steriflip)	Millipore

Table 5.2: Instruments and kits

Instruments and kits	**Manufacturer**
Agarose gel electrophoresis chamber	ComPhor L, Biozym Scientific
autoMACS separation system	Miltenyi Biotec
Bacteria incubator B6	Heraeus Instruments
Bacterial shaker TH30	Edmund Bühler
Balance Sac 51	Scaltec Instruments
Balance MXX-610	Denver Instruments
BD FACS Canto	BD Biosciences
Cell culture CO_2 incubator CB150	Binder
Centrifuge 5417R	Eppendorf
Freezer (-20°)/Refridgerator Premium no frost	Liebherr
Gel documentation	Videoprinter P90, Mitsubishi Electric
Light microscope Wilovert 30	Helmut Hund
Master Cycler Gradient	Eppendorf
Megafuge 1.0R	Heraeus
Minifuge	ROTH
MS73 sonication needle	Bandelin
MultiMacs M 96 Separator	Miltenyi Biotec
NanoDrop 2000 Spectrophotometer UV/Vis	Thermo Scientific
NEON Transfection System	Life Technologies
Orion L Microplate Luminometer	Titertek / Berthold
Pipetboy acu IBS Integra	Bioscience
Rocking table K3A	Edmund Bühler
Single channel pipettes: 2.5, 10, 100, 200, 1000 µL	Eppendorf
Sonoplus HD 2200	Bandelin
StepOnePlus II Real-Time PCR System	Life Technologies
Thermocycler comfort	Eppendorf
Vortexer	Scientif Industries
UV transilluminator: Imagemaster VDS	Pharmacia Biotech
Kits	**Manufacturer**
Dual-Luciferase Reporter Assay System	Promega
NEON Transfection System 100 µL kit	Life Technologies
NucleoSpin Gel and PCR Clean-up	Macherey-Nagel
NucleoSpin Extract II	Macherey-Nagel
NucleoBond Xtra Maxi/Midi EF	Macherey-Nagel
NucleoSpin Blood Kit	Macherey-Nagel
RNase-free DNase Set	QIAGEN
RNeasy Mini Kit	QIAGEN
QIA Shredder	QIAGEN

Table 5.3: Chemicals and reagents

Name	Manufacturer
1 kb DNA Extension Ladder	Invitrogen
2-Log DNA Ladder (0,1-10 kb)	New England BioLabs
4',6-diamidino-2-phenylindole (DAPI)	Sigma-Aldrich
All-trans retinoic acid	Sigma-Aldrich
Am 80	Sigma-Aldrich
Am 580	Sigma-Aldrich
Complete mini EDTA free protease inhibitor	Roche Diagnostics
DEPC Treated Water	Invitrogen
Deoxynucleotide (dNTP) Solution Mix	New England BioLabs
Dimethylsulfoxide (DMSO)	Sigma-Aldrich
Disuccinimidyl glutarate (DSG)	Thermo Scientific
dNTP mix (each 10mM)	New England Biolabs
Ethanol 70%	Roche
Ethylenediaminetetraacetic acid (EDTA)	Sigma-Aldrich
Fetal bovine serum (FCS)	Sigma-Aldrich
37% Formaldehyde	Merck Millipore
GelRed Nucleic Acid Gel Stain	Biotium
Gentamycin	Biochrom/Merck Millipore
Glycine	ROTH
Hank's Buffered Salt Solution	Biochrom/Merck Millipore
HEPES (1M)	Biochrom/Merck Millipore
HX630	TOCRIS
Salmon Sperm DNA Solution	Life Technologies
Isopropanol	ROTH
LE Agarose	Biozym
LE540	WAKO Chemicals
β-Mercaptoethanol	Life Technologies
Milk powder	ROTH
NaCl	Sigma-Aldrich
$NaHCO_3$	Sigma-Aldrich
NP-40	Merck Millipore
Oligo d(T) Primers	QIAGEN
Penicillin/Streptomycin	Biochrom/Merck Millipore
Phenylmethylsulfonyl fluoride (PMSF)	Fluka Analytical
Platinum SYBR Green qPCR Super-Mix-UDG	Life Technologies
Protease Inhibitor Cocktail Tablets	Roche
Random Hexamer primers	QIAGEN
RNase Away Reagent	Life Technologies
RNase OUT Recombinant Ribonuclease Inhibitor	Life Technologies
RPMI 1640 Medium	Life Technologies
Salmon sperm DNA	Life Technologies
Sodium Dodecyl Sulfate (SDS)	Merck Millipore
Sodium Pyruvate	Biochrom/Merck Millipore
STAT5 Inhibitor (Cat # 573108)	Calbiochem, Merck KGeA
Trypan blue	Life Technologies
XVIVO 10	LONZA

Table 5.4: Media and buffer compositions

Buffers, media, and solutions	**Manufacturer**
PBS/BSA (PBA)	2 g/L Bovine serum Albumin (BSA) in PBS
Phosphate buffered saline solution (PBS)	8 g/L NaCl; 0,2 g/L KH_2PO_4; 1,4 g/L Na_2PO_4·H2O
Erythrocyte Lysis Buffer	10 mM $KHCO_3$; 155 mM NH_4Cl; 0.1 mM EDTA, pH 7.5
Complete medium (cRPMI)	RPMI 1640, 25 mM HEPES; 10% FCS; 1 mM Sodium Pyruvate, 50 µM β-Mercaptoethanol; 100 U/ml Penicillin/Streptomycin; 50 µg/ml Gentamycin
Complete X-VIVO-10	As cRPMI but with X-VIVO10 instead of RPMI 1640
50 × (TAE) buffer	242 g Tris base; 57,1 mL acetic acid; 18,6 g (50 mM) Titriplex II; ddH_2O; pH 8.5
LB-low salt media (autoclaved in-house)	4 g Tryptone; 2 g NaCl; 2 g yeast extract; 400 mL ddH_2O
Buffers for ChIP	**Components**
PBS-T	PBS; 0.5% Tween
Blocking buffer	5% milk powder in 0.5% PBS-T
ChIP dilution buffer	0.01% SDS; 1.1% Triton-X-100; 1.2 mM EDTA; 167 mM NaCl; 1.2 mM Tris, pH 8.1
Low salt buffer	0.1% SDS; 1% Triton-X-100; 2 mM EDTA; 150 mM NaCl; 20 mM Tris, pH 8.1
High salt buffer	0.1% SDS; 1% Triton-X-100; 2mM EDTA; 500mM NaCl; 20mM Tris, pH 8.1
LiCl buffer	0.25M LiCl 1% IGEPAL-CA630; 1% Deoxycholic Acid; 1mM EDTA; 10mM Tris, pH 8.1
TE buffer	10mM Tris; 1mM EDTA
ChIP elution buffer	1% SDS; 0.1M $NaHCO_3$
SDS lysis buffer	1% SDS; 50mM Tris, pH 8.1; 10mM EDTA

Table 5.5: Antibodies, recombinant cytokines and magnetic beads

Antibodies (clone)	**Final concentration**	**Manufacturer**
anti-FcγReceptor (2.4G2)	20 mg/mL	DRFZ
anti-CD3 (145-2C11)	3 mg/mL	DRFZ
anti-CD28 (37.51)	4 mg/mL	DRFZ
anti-IL12 (C17.8)	5 µg/mL	DRFZ
anti-IFNγ (AN18.726)	5 µg/mL	DRFZ
anti-IL-4 (11B11)	5 µg/mL	DRFZ
anti-CD25-APC (PC61)		BD Pharmingen
anti-CD4-FITC (L3T4)		BD Biosciences
anti-CD62L-PE-(MEL-14)		BD Biosciences
anti-CD62L-PB-(MEL-14)		eBioscience
anti-CD4-APC (RM4-5)		BD Pharmingen
anti-CD43-PECy7 (1B11)		BD Biosciences
anti-CD43isotype-PECy7 (RTK2758)		BD Biosciences
P-selectin-humanIgG		BD Pharmingen
E-selectin-humanIgG		R&D Systems
human anti-IgG-PE (G18-145)		Jackson Immuno Research
Recombinant murine cytokines	**Dilution**	**Manufacturer**
Interleukin-2 (IL-2)	10 ng/mL	R&D Systems
Interleukin-12 (IL-12)	5 ng/mL	R&D Systems
Interferon γ (IFNγ)	20 ng/mL	R&D Systems
Interleukin-4 (IL-4)	30 ng/mL	R&D Systems
Micro Magnetic beads	**Dilution**	**Manufacturer**
anti-APC	1:10	Miltenyi Biotec
anti-FITC multisort kit	1:10	Miltenyi Biotec
anti-CD62L	1:10	Miltenyi Biotec
Protein A µMACS beads	50µL/2µg antibody	Miltenyi Biotec
ChIP antibodies (clone) – cat#	**Concentration/2mio cells**	**Manufacturer**
Rabbit anti-mouse STAT4 (C-20) – sc-486 X	2µg	Santa Cruz Biotech
Rabbit anti-mouse T-bet (H-210) – sc-21003 X	2µg	Santa Cruz Biotech
Rabbit anti-IgG – sc-2027 X	2µg	Santa Cruz Biotech
Rabbit anti-mouse H3K4me2 – 07-030	1:100	Millipore
Rabbit anti-mouse H3K27me3 – 07-449	5µg	Millipore
Rabbit anti-IgG 12-370	5µg	Millipore

Table 5.6: Plasmids, competent cells, and enzymes for cloning

Plasmids	**Manufacturer**
pGL3-basic	Promega
pCpGL-basic	Michael Rehli, Regensberg
pGL4.75*[hRluc/CMV]* (short: pGL4.75)	Promega
pRL-TK	Promega
Reagents and Competent cells for bacterial culture	**Manufacturer**
Agar Agar bacterilogic	Carl Roth
Ampicillin	Sigma-Aldrich
TOP 10 *E. coli*, chemically competent bacteria	DRFZ
LB-capsules (10/400 mL ddH_2O)	MP, Biomedicals
One Shot PIR1, competent bacteria	Life Technologies
S.O.C. Medium	DRFZ
Tryptone	Sigma-Aldrich
Yeast extract	Sigma-Aldrich
Zeocin	Life Technologies
Enzymes for molecular biology	**Manufacturer**
Antartic Phosphatase	New England Biolabs
AvaI	New England Biolabs
BamHI-HF	New England Biolabs
BglII	New England Biolabs
HindIII∘HF	New England Biolabs
M.SssI	New England Biolabs
Q5 DNA Polymerase	New England Biolabs
SalI-HF	New England Biolabs
SpeI	New England Biolabs
Superscript II Reverse Transcriptase	Life Technologies
T4 DNA ligase	New England Biolabs

5.2 Methods

5.2.1 Preparation of murine leukocytes from secondary lymphoid organs

Secondary lymphoid organs were harvested from mice sacrificed by cervical dislocation. Cervical, mandibular, brachial, axilial, inguinal peripheral lymph nodes (pLNs), mesenteric lymph nodes (mLNs), and spleen were isolated and pooled in PBA. The organs were homogenized with the rough end of a plunger from a 5 mL syringe, pushed through a metal sieve, and centrifuged at 1200×g for 8 minutes. To remove the red blood cells, the cell pellet was resuspended in 1 mL erylysis buffer per spleen (or 1mL per mouse) for 3 minutes, after which 20 mL PBA was added to quench the lysis. The resulting cell suspension was filtered through a 70 μM cell strainer to remove any residual fat and centrifuged as before to obtain an erythrocyte-depleted cell mixture. Subsequently, either naive $CD25^{-}$,$CD4^{+}$,$CD62L^{hi}$ T cells were isolated and cultured to differentiate to a given helper T cell subtype or RNA was isolated directly from the crude cell mixture (in which case the pLNs and mLNs were not pooled at the beginning).

If not otherwise stated, the cell washing procedure in the following protocols were performed by adding ≥20 mL PBA and then centrifuging at 1200×g for 8 minutes (naive T cell isolation) or 1200×g for 10 min (FACS staining). Staining and bead incubation was performed at 4°C for 15 minutes in the concentration or dilution indicated in Table 5.5 on page 47.

5.2.2 Isolation of $CD25^{-}CD4^{+}CD62L^{hi}$ naive T lymphocytes

Erythrocyte-depleted cells were counted and resuspended in PBS/BSA (PBA) (2×10^{8} cells/mL) and pre-incubated with anti-FcγR antibody for 5 minutes to block unspecific cell binding to the Fc-region of the subsequent antibodies, after which the cells were stained by addition of anti-CD25-APC and anti-CD4-FITC antibodies. After incubation and washing, magnetic anti-APC beads were added to 2×10^{8} cells/mL and left incubating. After washing, the cell suspension was filtered through a sterile (30μM) filter unit to ensure a single cell suspension for the resulting magnetic sorting step. The cells were magnetically sorted using either an autoMACS or manually using hand MACS LS columns. With the autoMACS, the "depleteS" program was selected to separate $CD25^{-}$ cells (in the flow through) from the $CD25^{+}$ cells that stayed on the column (positive fraction). When using hand columns the principle is the same as with the autoMACS, but the column is equilibrated with 2×3 mL PBA before addition of the single cell suspension. The magnetic hand column is placed on a magnet, and the column equilibrated before adding the sample. The negative fraction then flows through the column and the column, still on the magnet, is washed with 2×3 mL PBA, after which the positive fraction is pushed through with 2

mL PBA using the column plunger after removal of the magnetic column from the magnet.

The negative fraction with $CD25^-$ cells was washed and the cell pellet resuspended in PBA (2×10^8 cells/mL), after which multi sort FITC beads were added. After incubation and washing, the cells were filtered as before to obtain a single-cell population prior to the separation step. Using the autoMACS, the cells were taken up and sorted by the program "Posseld2" that discards $CD4^-$ fraction to the flow through and enriches $CD4^+$ cells on the column. The positive fraction was eluted and washed as before. When using a hand column the same is done as before, but the positive fraction is kept in this case and washed as before.

To release the resulting $CD25^-CD4^+$ cells from the multisort FITC beads, the positive fraction was incubated with 90µL release reagent from the FITC multi sort bead kit. Due to the light sensitivity of the release reagent, cells with release reagent are left incubating in the dark for 30 min at RT, gently manually turning the Falcon 10× every 10 min. After release, the cells were washed and resuspended in 2 mL PBA. The beads were separated from the cells with the autoMACS using the program "deplete" which binds the beads to the column and releases the cells no longer binding the beads into the flow through. With the hand column this step is performed as before, but this time keeping the negative fraction. The released cells were then washed and resuspended with CD62L beads in PBA and left incubating. After washing, the $CD62L^{hi}$ positive fraction was separated from the $CD62L^{lo}$ fraction with the autoMACS using the program "PosselD2" and the positive fraction was kept for *in vitro* cultivation. With the hand column this step was performed as described before but this time keeping the positive fraction.

To check the purity of the naive sort, a small sample from the $CD62L^{lo}$ and the $CD62L^{hi}$ fractions were incubated with CD62L-PE antibody and checked by flow cytometry against the unstained, $CD25^+$, and $CD4^-$ fractions that were used to set the gate. All naive sorts performed for this work obtained ≥90% pure $CD25^-CD4^+CD62L^{hi}$ naive T lymphocytes.

5.2.3 Polarization of naive T cells to T helper subsets

Isolated $CD25^-CD4^+CD62L^{hi}$ naive T cells were activated on plate-bound anti-CD3/anti-CD28 monoclonal antibodies (mAbs) to induce TCR activation, as well as supplemented with appropriate polarizing cytokines and alternative lineage suppressing antibodies, for 3 days. On day 3 the cells were split 1:2 with cytokines and alternative lineage suppressing antibodies added to the new media only. Hereafter, the cells expanded on uncoated plates – devoid of TCR stimulation. To promote T_H1 polarization, IL-12, IFNγ, and anti-IL-4 mAb were added. For T_H2 polarization, IL-4, anti-IL-12, and anti-IFNγ mAbs were

added. IL-2 was added to all cultures to ensure survival and proliferation and prevent cell death. The cytokines and antibodies were added according to Table 5.5 on page 47. Cells were harvested on day 1, 3, 4, or 5 depending on the experiment – this is indicated for each experiment in the results section. Cells were either cultured in RPMI, containing FCS (complete RPMI = cRPMI), or complete X-VIVO media that was prepared as the cRPMI, but without FCS. Cells were plated in 6-well, 12-well or 24-well wells at a density of 1×10^6 cells/mL culture medium.

5.2.3.1 Agonist or inhibitor cell treatment

The STAT5 inhibitor was dissolved in DMSO and supplemented to the cells on day 0 or day 3 in a final concentration of 100µM. A control sample was supplemented with DMSO alone. The STAT5 inhibitor and DMSO was diluted into the media and pre-warmed at 37°C for 30 min., after which cytokines and antibodies were added to the media. The RAR inhibitor LE540 was supplemented to cells on day 0 and day 3 of culture. LE540 was prepared in Ethanol and supplemented at a final concentration of 0.5µM. For the RA titration experiment, cells on day 0 and day 3 were either supplemented with 0, 0.1, 1, 10, or 100nM All-trans retinoic acid dissolved in Ethanol. Treatment of polarizing cells with the RAR agonists RA, Am 80, or the RXR pan-agonist, HX630, was carried out on day 0 and day 3 of culture. Each agonist was dissolved in DMSO and freshly diluted in media before use in a final concentration of 10 or 100nM. In the setting where a combination of RAR agonist and HX630 was given, each agonist was supplemented in a final concentration of 10nM only.

5.2.4 RNA isolation and reverse transcription

Prior to RNA isolation, $1\text{-}5\times 10^6$ cells were centrifuged at 400×g for 10 min and optionally stored at -80°C before homogenization with the QiaShredder and RNA purification with the RNeasy Mini Kit (Qiagen Hilden, Germany). Contaminating DNA was removed using the RNase-Free DNase Set from Qiagen. All kits were used according to the manufacturer's instructions with one modification that the RNA was eluted with $2\times$ 35µL DEPC water. The RNA was quantified using the Nanodrop 1000 or 2000, after which it was stored at -80°C until cDNA synthesis. 250 ng RNA was reverse transcribed to cDNA in two PCR cycles, the master mixes and thermal cycling conditions of which are given in Table 5.7 on page 52. The first PCR allows oligo(dT) and random hexamer primers (Qiagen) to anneal to all RNA templates in the sample. Directly after the first PCR, the master mix for the second PCR is added, which contains the reverse transcriptase Superscript II (Life Technologies). The cDNA is reverse transcribed with the thermal cycler re-set to the second PCR cycling conditions also given in the Table 5.7 on page 52. The resulting cDNA was diluted $5\times$ with DEPC water before qPCR analysis.

Table 5.7: Master mixes and RT-PCR cycling conditions

Components	**Final concentration**		**PCR temperatures**	**min:sec**
250 ng RNA	15,75 µL in H_2O			
Oligo d(T)12-16 (0.1mg/mL)	0.75 µL (2.5 µg/mL)	annealing PCR:	70°C	10:00
Random hexamers (50 µM)	0.75 µL (2.5 µM)	1 × cycle	4°C	hold
5 × FS buffer	6 µL			
H_2O	0.5 µL		25°C	10:00
dNTP-mix (10 mM each)	1.5 µL	RT-PCR:	42°C	50:00
DTT (0.1M)	3 µL	1 × cycle	94°C	05:00
RNAse out inhibitor	0.75 µL (200-400 nM)		4°C	hold
Superscript II	1 µL			

5.2.5 Chromatin immunoprecipitation (ChIP)

To study the regulation of genes, interactions between transcription factors or histones with DNA can be studied using chromatin immunoprecipitation (ChIP). ChIP involves the precipitation of protein bound to DNA. Because such complexes are not able to survive the lysis, sonication, and immunoprecipitation procedures that are part of the immunoprecipitation protocol, these can be reversibly fixed in a two-step fashion. Prior to fixation, cells were harvested, centrifuged for 10 min at 400×g and washed with PBS, after which the cells were centrifuged again before proceeding.

5.2.5.1 Two-step fixation of proteins to DNA

The first fixation step cross-links protein complexes situated on DNA that are not in direct contact with the DNA, using a *N*-hydroxysuccinimide ester, Disuccinimidyl glutarate (DSG). DSG was reconstituted at RT in DMSO to a concentration of 500 mM and diluted in PBS at RT to obtain a final concentration of 2 mM DSG, in which the cell pellet was resuspended. The two NHS ester groups in the DSG molecule react with nucleophilic primary amines on lysines or N-termini of polypeptide chains, that are positively charged at physiological pH, and form stable amide bonds with a resulting spacer arm of ∼7.7Å. The cells were left incubating in the DSG-PBS solution at RT for 45 min., after which the fixing cells were centrifuged and washed 2× with excess PBS.
The second fixation step involved resuspending the cells with another cross-linker, 1% formaldehyde diluted in PBS, at RT for 10 min – keeping the time meticulously to prevent overfixation. Lastly, a final concentration of 0.125M glycine was added to quench the fixation and the cells washed 2× with excess PBS, after which the cells were lysed with SDS-lysis buffer and stored at -80°C until further use. For transcription factor ChIPs, the results were more reproducible when proceeding with the cell lysate immediately and not storing the cells at -80°C.

5.2.5.2 Preparation of cell lysate for ChIP

Sonication was performed with 1 volume lysate and 3 volumes ChIP dilution buffer supplemented with 100µg/ml salmon sperm DNA, a complete mini protease inhibitor pill (Roche) and 1mM PMSF. Sonication was performed with a Sonopuls HD2200 equipped with a MS73 needle (on-time 5× 25 sec. at 30% power, off-time 1 min on ice). Cell debris was cleared by centrifugation at 13000×g for 10 min and the supernatant diluted 2.5× with ChIP dilution buffer to reach a final concentration of SDS $< 0.1\%$. The quality of the sonication was checked by agarose gel electrophoresis as described later. The sonication normally yielded DNA bands <500 bps.
For transcription factor ChIP, 500 µL lysate (approx. 2×10^6 cells) was left incubating O/N at +4°C rotating with 2 µg anti-STAT4, anti-T-bet, or anti-rabbit-IgG antibodies. For histone methylation mark ChIPs 5 µg anti-H3K4me2, anti-H3K27me3, or anti-rabbit-IgG antibodies were added instead (Millipore, Billerica, USA). 1/4 of the lysate amount used for ChIP was kept as input control.

5.2.5.3 Affinity purification of immune complexes

Immune complexes were affinity purified by addition of 50µL protein A beads – binding to the Fc region of the antibodies – (Miltenyi Biotec) per 2 µg antibody and left rotating for 2 hrs, after which the bound complexes were purified by MACS separation. After rotation with beads, the samples were briefly centrifuged to prevent cross-contamination during handling. Using 8 column-strips and a MACS separation device, bound bead:antibody:protein:DNA complexes were separated from unbound sample. First, each column was equilibrated with 100µL 1%NP 40 and then 100µL ChIP dilution buffer with no additives. Next, each sample was added to a separate column – unspecific binding to the columns was prevented by prior addition of two volumes of blocking buffer to the samples. To wash unbound sample and weak interacting partners off the column, a series of 1mL washes were performed in the following consecutive order: low salt buffer, high salt buffer, LiCl buffer, and TE buffer. Following the wash steps, bound bead:antibody:protein:DNA complexes were eluted from the column using 4× 50µL 95°C pre-heated ChIP elution buffer. The input samples were diluted up to 200µL with elution buffer. The buffer components can be seen in the second part of Table 5.4 on page 46.

5.2.5.4 Defixing proteins from precipitated DNA prior to qPCR

To separate the protein from the DNA, the ChIP and input samples were defixed in 0.2M NaCl O/N shaking at 500rpm at 65°C. Subsequently, the DNA was separated from proteins using the PCR and gel clean up kit from Macherey-Nagel. Prior to clean-up, 200µL isopropanol was added to each sample to prevent precipitation of SDS as well as 5 volumes of NTB (1mL). After mixing, the samples were passed through the clean-up

columns as prescribed by the manufacturer with two ensuing washing steps of 600µL and then 200µL wash buffer. Elution was performed once with 100µL DEPC water. The input samples were diluted 2.5× with DEPC water to reach 10% input (from 25%). The samples were immediately used in qPCR analysis with desired primers or stored at -20°C for a maximum of 1 month.

5.2.6 Quantitative PCR

To determine the relative amount of cDNA, or DNA precipitated by antibodies purified as described in the previous sections, quantitative PCR (qPCR) using platinum SYBR Green qPCR Super-Mix-UDG was performed on the StepOnePlus II system. Unlike conventional PCR, qPCR enables detection and quantification of cDNA or DNA after each cycle. A cycle threshold has been passed when the DNA being amplified passes the level of background detection, and is termed the C_t value of the given sample. After obtaining the raw C_t values, the relative expression levels to a housekeeping gene, or input in the case of ChIP, can be determined by implementing distinct calculations that are given in Table 5.8 on page 54. Primer sequences for mRNA expression analyses are given in Table 5.11 on page 64. Primer sequences used for quantification of the DNA target region after ChIP are given in Table 5.12 on page 65. Note, the eight primer pairs covering the *gcnt1* enhancer used for the histone, STAT4, and T-bet ChIPs produce overlapping PCR products. The following master mix and cycling conditions (for primers that were all designed to have an annealing temperature of 60°) used, were the same for mRNA and ChIP-ed DNA qPCRs:

Table 5.8: SYBR green master mix and qPCR cycling conditions

Components	**Final concentration**		**PCR temperatures**	**time min:sec**
DNA or cDNA	5 µL		50°C	02:00
SYBR green	12.5 µL		95°C	02:00
Rox dye (prediluted 1:20 in DEPC water)	1 µL	|	95°C	00:30
Fw primer (20 µM)	0.25-0.50 µL (200-400 nM)	40 × cycles |	60°C	00:30
Rv primer (20 µM)	0.25-0.50 µL (200-400 nM)	|	72°C	00:30
DEPC water	add up to 25 µL		60-95°C	melting curve

To estimate the fold difference between mRNA (reverse transcribed to cDNA) expression of a gene of interest (GOI) relative to a housekeeping gene, that should be similarly expressed across samples, comparative quantification using the ΔC_t method was employed. ΔC_t uses the raw C_t values of at least three technical replicates of both the GOI and housekeeping gene (either 18S RNA or Hprt) to reach the fold difference between the two:

$$\text{Fold difference} = 2^{\,C_{t\,\text{GOI}} - C_{t\,\text{house}}} = 2^{\Delta C_t} \tag{5.1}$$

To quantify precipitated DNA (ChIP'ed DNA) relative to the input DNA after a ChIP-qPCR experiment, two formula are applied to the raw C_t values obtained from the qPCR machine by a given primer pair. Equation 5.2 adjusts the average (avg) C_t value of three technical replicates of input DNA according to the dilution factor (=10) and the efficiency of amplification (AE) by the given primers (predetermined by the standard curve of five half-log dilutions of input DNA with the same primer concentration):

$$\mathrm{AI} = \mathrm{C_{t\ input}(avg)} - \log_{\mathrm{AE}}(10). \tag{5.2}$$

As a result, equation 5.2 gives a new C_t value for the adjusted input (AI). Subsequently, to determine the amount of antibody-precipitated DNA (from each sample), amplified by the same primer pair for which the input was adjusted using equation 5.2, the C_t value for the sample is normalized to the adjusted input using equation 5.3:

$$\%\mathrm{input} = 100 \times 2^{\,\mathrm{AI} - \mathrm{C_{t\ sample}}}. \tag{5.3}$$

5.2.7 Flow cytometry analysis of cell surface proteins

To analyze the expression of cell surface markers CD4, CD62L, 1B11, E-lig, and P-lig, cells of interest were stained with fluorochrome-conjugated antibodies and visualized by flow cytometry. All stainings were performed at 4°C in the dark, and all washing steps were carried out prior to centrifugation at 1200×g for 10 min, after which the supernatant was discarded. In each sample the cell number did not exceed $2{\times}10^8$. Firstly, PBA-washed cells were left incubating for 15 min with anti-FcγR antibodies (to prevent binding of the fluorochrome-labeled antibodies via the Fc component to the FcγR expressed on the cells) in a 30µL HBSS with 25mM HEPES. The cells were then washed and incubated with antibodies against CD4, CD62L, 1B11, E-lig, or P-lig in 30µL HBSS + 25mM HEPES according to the dilutions predetermined by titration assays. The antibodies and chimeras used are given in Table 5.5 on page 47. To label E- and P-lig, an E- or P-selectin-human IgG chimera was used in the first staining step. These chimeric proteins bind all E- and P-ligs on the cells via functional binding. After washing the cells, they were left incubating with the secondary antibody anti-huIgG-PE to complete the stain of E- or P-ligs. The cells were then washed with HBSS and resuspended in PBA for flow cytometric analysis. Before analyzing the cells, DAPI was added to stain dead cells to exclude these from the analysis. An unstained sample was kept and used to set the voltage against samples with single stains of each fluorochrome. Samples of fluorescence minus one (FMO) controls were performed for each fluorochrome, which entailed leaving out one fluorochrome from the complete stain mixture. This was done to assess the level of spillover between the

different emission and excitation spectra of the fluorochromes, thereby ensuring correct compensation prior to analysis. The FMO control for E- and P-lig staining was performed with the antibodies in Ca^{2+}-depleted PBS+EDTA, as the binding between selectins and their ligands is Ca^{2+}-dependent. The FMO control for 1B11 was performed with an isotype antibody control. For cytometric analysis, a BD Canto (BD Biosciences) and subsequent FlowJo Software (Treestar Inc.) were used. Due to the staining panel, 1B11-PECy7 is always co-stained with P-lig or E-lig – both stained in PE. Figure 5.1 shows representative dot plots of the gating strategy for 1B11 and P-lig surface staining.

5.2.8 Cloning

The *fut7* orientation and position dependent CNS enhancer constructs were generated on a pGL3 plasmid already containing the *fut7* minimal promoter v1_1 cloned previously by Matthias Pink in our lab. The CNS region was amplified from mouse DNA using the indicated sets of primers (CNSeFO/RO upstream/downstream primers) given in Table 5.10 on page 63. The mouse DNA was previously isolated and purified from primary murine cells, that were discarded during the naive T cell sort, using the Nucleobond Blood kit as described by the manufacturer (Macherey-Nagel). The PCR master mix and cycling conditions were as described in Table 5.9 on page 59.

The resulting PCR products and the backbone vector were restricted (in 10,000 U/mL enzyme unless otherwise stated) by KpnI and SacI for 1 hr in the following mixture: 1µg insert or backbone vector were digested in a mixture of 0.5µL KpnI, 0.5µL SacI, 3µL NEB1.1 buffer with DEPC water in a volume of 30µL for 1 hr at 37°C. To prevent self-religation of the linearized backbone vector, this was additionally dephosphorylated for 1 hr at 37°C by addition of 3.5µL Antarctic phosphatase buffer and 1µL antarctic phosphatase. The vector was then resolved on a 1% agarose gel, cut out, and cleaned using the Gel and PCR clean-up kit by Macherey-Nagel as described by the manufacturer. The inserts were not resolved on a gel, but directly purified using the Gel and PCR clean-up kit.

The ligation between PCR products and linearized vector was performed in a 3:1 insert to vector molar ratio using the formula: ng of insert needed = (3× length (kb) of insert)/(length (kb) of vector) × ng of vector. The ligation reaction was set up in 10µL final volume with 1µL T4 DNA ligase and 1µL T4 DNA ligase buffer and allowed to ligate at 4°C O/N. The ligation mixtures were transformed into appropriate competent bacteria as described in section 5.2.8.4 "Transformation of competent *E. coli* and sequencing". The constructs where the enhancer/CNS region was inserted upstream of the luciferase coding region were checked by sequencing using the forward binding primer upstream of the luciferase gene. The constructs where the enhancer/CNS region was inserted downstream of the luciferase coding region were checked by sequencing with the forward or reverse

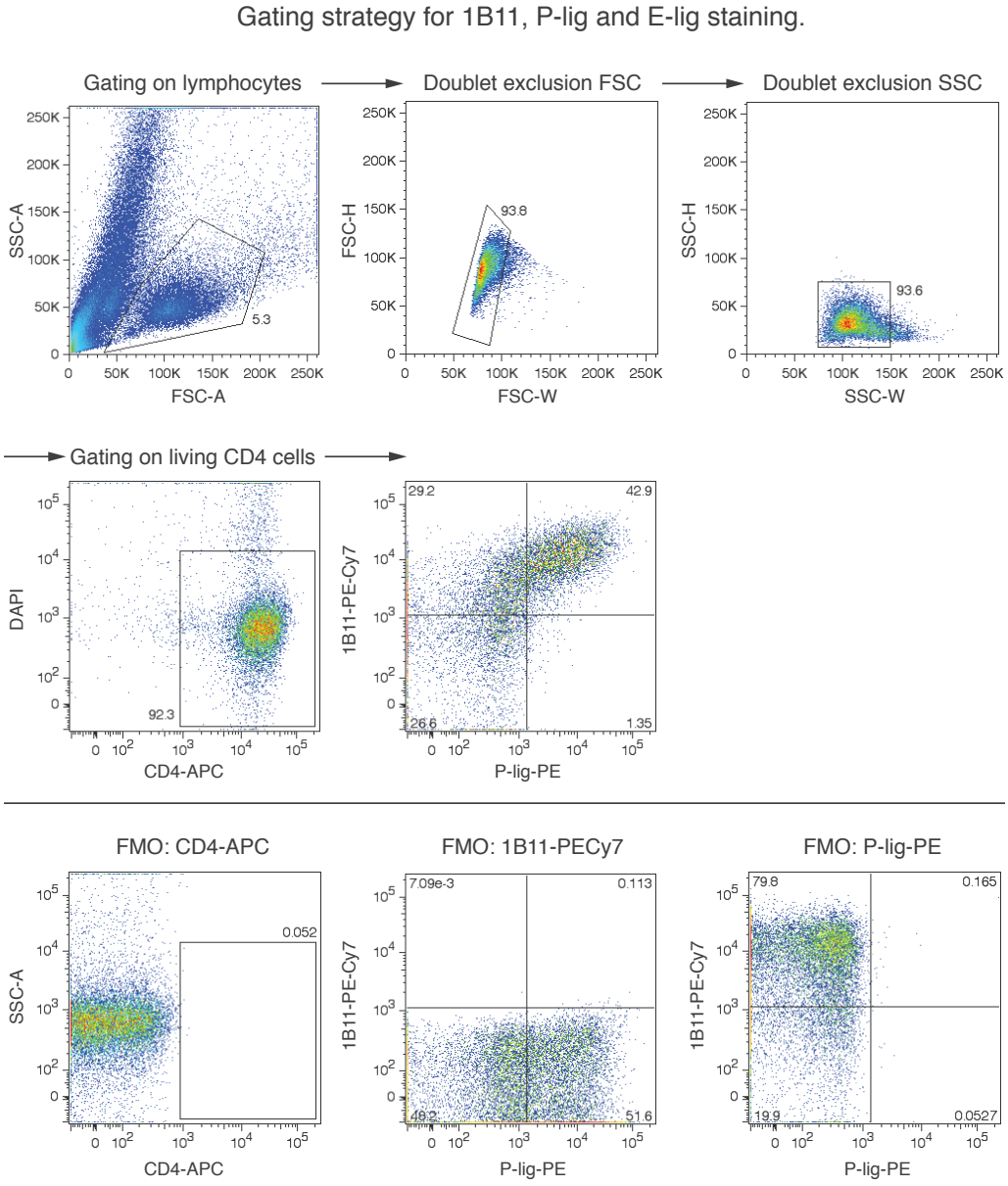

Figure 5.1: Gating strategy for 1B11, P-lig, and E-lig surface staining *Upper panel* shows a representative of the gating strategy. *Lower panel* shows representative fluorecence minus one (FMO) stainings that were preformed for all fluorochrome coupled antibodies and chimeras to ensure correct gating and compensation. In FMO 1B11-PE-Cy7, the isotype antibody IgG-PE-Cy7 was added. In FMO P-lig-PE, the staining was performed in a PBS Ca^{++} depleted buffer.

primers binding downstream of the luciferase gene – sequences of all primers are given in Table 5.10 on page 63.

5.2.8.1 Mutagenesis by overlap extension PCR

Regions of interest were mutated by overlap extension PCR using complementary mutated primers and a set of flanking primers in a two-step manner, first generating two PCR products (A and B) and then one final PCR product (AB) containing the mutation. PCR products A and B are generated by a PCR reaction with the mutated reverse primer and the forward flanking primer, and in a separate tube, the mutated forward primer is combined with the reverse flanking primer.

For example, to generate one product A, Fut7_STAT5_2 RV primer and the FW pCpGL flanking primer were used with the template. To generate the corresponding product B, the Fut7_STAT5_2 FW primer was used together with the RV pCpGL flanking primer on the same template. The template DNA was a plasmid containing the wild-type *fut7* enhancer/CNS + minimal promoter v1_2 immediately upstream of the luciferase coding region. Subsequently, products A and B were used as a template in an overlap extension PCR, using the flanking primers only, and generated a STAT5 mutation in the minimal promoter of *fut7* due to the complimentarity of the A and B product ends from the complimentary mutated primers. Sequences of the primers are given in Table 5.10 on page 63.

This WT construct was cloned previously in our lab by Matthias Pink and I, and is described in his thesis [75]. The PCR components and cycling conditions can be seen in Table 5.9 on page 59. PCR products were resolved as described in the previous section. The resulting AB products were restricted and ligated into the linearized and dephosphorylated backbone vector pCpGL-basic that is CpG free. To linearize the PCR products and the backbone vector, 1µg DNA was double digested at 37°C for 1 hr in 0.5µL BamHI, 0.5µL Hind·HF, 3µL CutSmart buffer, and DEPC water up to 30µL. The backbone vector was also dephosphorylated, as described in the previous section, to prevent self-religation of the linearized backbone vector. The ligation was also performed as described in the previous section. The ligation mixtures were transformed into appropriate competent bacteria as described in the section 5.2.8.4 "Transformation of competent *E. coli* and sequencing".

CRE-mutation and -deletion mutants were generated with the same flanking primers for the pCpGL plasmid as described above, but replacing the mutated primers specific for the CRE modification required. pCpGL plasmids were checked by sequencing using forward and reverse flanking primers binding upstream of the luciferase gene.

The STAT4 mutant was generated on the WT construct cloned previously by Micha

Schröter in our lab. This construct contained the promoter for *gcnt1* and the enhancer for *gcnt1* upstream and downstream of the luciferase coding region, respectively. The mutated PCR products were amplified from the WT contruct using the flanking primers for pGL3-vector and the primers containing a mutated STAT4 binding motif. The PCR products and the backbone vector were restricted using BamHI and SalI in a similar manner as described above. STAT4 constructs were checked by sequencing using forward and reverse primers binding downstream of the luciferase gene in the pGL3 plasmid. Sequencing was always performed in both directions when possible.

Table 5.9: Q5 PCR reaction setup and PCR cycling conditions

Components	**Volume (concentration)**		**PCR temperatures**	**time min:sec**
5 × Q5 reaction buffer	5 µL		98°C	01:00
10 mM dNTPs	0.5 µL		98°C	00:10
FW primer (10 µM)	1 µL (400 nM)	25 × cycles	64 + G 1°C**	00:30
RV primer (10 µM)	1 µL (400 nM)		72°C	00:45*
Template DNA	50 ng*		72°C	02:00
Q5 polymerase	0.25 µL		4°C	∞
DEPC water	add up to 25 µL			

* For the second PCR, the overlap extension PCR, a mix of products A and B were added as template DNA in a 1:1 molar ratio based on the following formula: and the elongation time increased to 01:30.

** G 1°C = the PCR machine is programmed to heat in a gradient fashion going from 64±1°C along the heating block.

5.2.8.2 *fut7* minimal promoter *in vitro* methylation

To methylate only CpGs of the *fut7* minimal promoter v1_2 within the *fut7* CNS+minimal promoter v1_2, the CpG methylase enzyme M.SssI was used in the following protocol.

90µg of the *fut7* CNS+minimal promoter v1_2 was digested for 1 hr at 37°C in a master mix composed of 22.5µL BamHI (10,000 U/mL), 2.25µL BglII (100,000 U/mL), 25µL NEB3.1 10x buffer, and DEPC water up to a final volume of 250µL. The minimal promoter v1_2 was separated from the rest of the vector by agarose gel electrophoresis and both bands (insert and vector separately) cut out and cleaned using the Gel and PCR clean-up kit (Macherey-Nagel). This was scaled up twice to have enough to methylate and mock methylate in the next part of the protocol.

90µg insert was subsequently methylated or mock methylated in a master mix of 11.25 µL methylase enzyme M.SssI (DEPC water instead for the mock methylation), 1.65µL methyl donor S-adenosyl methionine (SAM) (pre-diluted 2µL + 6.45µL DEPC water),

18μL NEB2 buffer, and water up to a final volume of 180μL. *in vitro* methylation was performed at 37°C for 4 hrs. After 2 hrs, another 0.55μL SAM was mixed into the mastermix. The methylation was checked by restricting 0.5μL of the methylated or mock methylated DNA with 1μL AvaI, a CpG methylation sensitive restriction enzyme, in a mixture of 3μL NEB4 buffer and 26.5μL DEPC water. After 1 hr at 37°C, the DNA was visualized on a gel. The methylation was successful if only 1 band appeared on the gel at 1 kb due to the inability of AvaI to cleave methylated CpGs. The mock methylation yielded two bands around 400bp and 600bp due to cleavage by AvaI.

Meanwhile, the remaining vector was diluted in 280μL DEPC water and dephosphorylated with 10μL Antarctic phosphatase buffer and 10μL Antarctic phosphatase for 2 hrs at 37°C. The methylated and mock methylated inserts as well as the phosphorylated vector were then purified using the Gel and PCR clean up kit according to the manufacturer's instructions (Macherey-Nagel) eluting with 20μL DEPC water through two columns per sample (the column has a maximum binding capacity of 25μg - here we assume some loss during restriction of the plasmid).

Ligation of the backbone vector with the methylated or mock methylated insert was performed in a molar ratio of 1:1, according to that described in the "Cloning" section earlier, but in a 50μL reaction volume with 5μL T4 DNA ligase (2,000,000 U/mL) and 5μL T4 DNA ligase buffer. Ligation mixture was left at 4°C for 3 days, after which the ligation was verified by observing coiled and supercoiled bands on a 1% agarose gel. The remaining ligation mixture was purified on 2 columns of the Gel and PCR clean up kit eluting with 15μL DEPC water.

5.2.8.3 Agarose gel electrophoresis

Linearized vectors and restricted inserts as well as sonicated cells prior to ChIP were resolved in 1x orange dye with DEPC water on a 1% agarose gel that was cast from 1 g of agarose with 100mL 1× TAE buffer. The gel was run at 150 Volts for 45 min, after which the DNA was visualized by UV-light.

5.2.8.4 Transformation of competent *E. coli* and sequencing

Ligation reactions with the CpG-free plasmid pCpGL were transformed into 25μL competent PIR1 *E.* coli from Invitrogen that had been thawed on ice, and left incubating with plasmid on ice for 30 min. The cells were subsequently heat shocked for 45 sec at 42°C, left on ice again for 2 min, and then left shaking (∼300 rpm) for 1 hr at 37°C after addition of 250μL SOC media. Finally, the cells were centrifuged at 500×g for 5 min, the supernatant discarded, and the cells plated on ampicillin selective low-salt LB agar

plates. The plates were positioned upside-down in 37°C O/N. Single colonies were then amplified in O/N low-salt LB cultures after which extraction and purification of the plasmids was performed using the Nucleobond Maxiprep kit as described by the manufacturer (Macherey-Nagel). pGL3 vector ligations were transformed into 50µL competent TOP10f' *E.* coli that had been thawed on ice, and left incubating with plasmid on ice for 15 min. The cells were subsequently heat shocked for 45 sec at 42°C, left on ice again for 2 min, and then left shaking (∼300 rpm) for 1 hr at 37°C after addition of 250µL SOC media. Finally, the cells were centrifuged at 500×g for 5 min, the supernatant discarded, and the cells plated on ampicillin selective LB agar. Single colonies were amplified in LB media. All constructs were verified by sequencing at LGC genomics in Berlin.

5.2.9 Reporter gene assays

The Luciferase assay is a reporter assay using a Firefly Luciferase expression vector to assess the ability of a genetic region to drive Luciferase gene expression from that plasmid. If the region cloned into the plasmid is a promoter or enhancer region, the cell will express Luciferase enzyme from the plasmid – if the region is a silencer on the other hand, the Luciferase enzyme will not be expressed and the suppressive activity of the silencing region should be tested by other methods.

We used a dual-luciferase reporter system from Promega that compares the activity of Firefly Luciferase from a vector with a gene region of interest cloned into it, to that of an unmanipulated control vector that expresses Renilla Luciferase driven by a known promoter. Co-transfection of the Firefly and Renilla Luciferase vectors ensures that the variances observed between samples in one experiment is not due to variances in transfection efficiencies. The enzymatic activity of Firefly Luciferase and Renilla Luciferase leads to the oxidation of the substrates Beetle Luciferin and Coelenterazine, respectively, resulting in the emission of photons that are detected as luminescence by a luminometer machine. The components LARII, and STOP&Glo are solutions that contain Beetle Luciferin and Coelenterazine, respectively. Their usage and the measurement of Luciferase activity is explained after the next section, that describes how the cells are transfected with expression vectors.

5.2.9.1 Transfection

1pmol pCpGL or 3pmol pGL3 plasmid were transfected into 1×10^6 *in vitro* polarized T_H1 or T_H2 cells 48hrs after antiCD3/antiCD28 stimulus, using the NEON transfection system (Invitrogen, Carlsbad, CA). Prior to transfection, the cells were washed twice with PBS, centrifuging 500× g for 5 min at RT in between washing steps. Immediately before the transfection, the cells were resuspended in 110µL R buffer from the NEON Kit and trans-

fected as described with electroporation 2× 20ms at 1350V. Cells were cotransfected with 25 ng of a CMV-promoter-driven Renilla luciferase reporter vector pGL4.75*[hRluc/CMV]* (Promega). Due to severe trans effects observed between promoter elements on the pGL3 and pGL4.75 plasmids when comparing regulatory activity T_H1 and T_H2 cells, either treated or untreated with RA, we switched to 200 ng of pRL-TK as the internal renilla expressing control plasmid. After transfection, the Th cells were stimulated for another 24 hrs on anti-CD3/anti-CD28 antibody coated 24-well plates in cRPMI media without antibiotics. The transfected cells were then given Gentamycin and removed from stimulus for 24 hrs before measuring the resulting Luciferase activity (see next section).

5.2.9.2 Determination of Luciferase activity

Luciferase activity was determined using the Dual-Luciferase Reporter Assay System as described by the manufacturer (Promega) and a luminometer plate reader from Berthold. Briefly, cells were centrifuged at 500×g for 5 min at RT. The cell pellets were resuspended and lysed for 15 minutes at RT with 60µL of 1× Passive Lysis Buffer.After lysis, cell debris was removed by centrifugation at 13000×g for 1 min at RT. The supernatant was then transferred to a luminometer plate and left in the dark before measuring. Meanwhile, the luminometer's two tubings were cleaned with 4mL 70% Ethanol and distilled H_2O prior to use. Tubing no. 1 was inserted into a 15mL falcon containing LARII and tubing no. 2 was inserted into a 15mL falcon containing 1× STOP&Glo. Both substrate solutions were prepared as described by the manufacturer. The luminometer was set to dispense 50µL LARII and wait 2.05 sec before making the first luminescence measurement of Firefly Luciferase activity for 10 sec. 8 seconds pass to allow the signal to dissipate, before adding STOP&Glo, which quenches Firefly Luciferase enzyme activity and provides the substrate for Renilla Luciferase. After STOP&Glo addition, a second measurement is recorded by the machine for 10 seconds. This results two values for each sample, representing the activity of Firefly Luciferase and Renilla Luciferase. To obtain interpretable values, the Firefly values are divided by the Renilla value in each sample (in short FL/RL). Next the samples can be compared or normalized to each other. When reporting that the activity is relative to that of the empty vector, each sample's FL/RL is divided by that of the sample containing an empty Firefly Luciferase vector. When reporting that the activity is relative to that of the promoter vector, each sample's FL/RL is divided by that of the sample containing the given promoter in Firefly Luciferase vector.

5.2.10 Primer design and plasmid sequencing

Primer-BLAST was used to design primers for mRNA analysis [94]. The UCSC genome browser's built-in *in silico* PCR tool was used to design primers for cloning [95]. Primers were synthesized by Eurofins, MWG, Operon in Ebersberg, Germany. Plasmids were

sequenced by LGC Genomics in Berlin, Germany.

5.2.11 *In silico* analysis

Conservation/homology analyses was performed using the ECR browser [96]. Transcription factor binding sites were predicted using MatInspector from Genomatix [97] and PROMO [98].

5.2.12 Software and statistics

BD FACSDiva was used on the BD FACS Canto during acquisition of stained FACS samples, after acquisition the software FlowJo from Tree Star was used. MxPro QPCR Software was used to analyze qPCR data. Graphpad PRISM was used for statistical analysis. The statistical tests used are indicated in each figure legend where appropriate.

Table 5.10: Primers for cloning of Luciferase reporter constructs

Final construct	Sequence (5'-3')	Name of primer
gcnt1 STAT4 mutant	Fw: CTATAAAAGGTTTGTCAACAGGAGTTTCC (29)	STAT4_4_antisense
	Rv: GGAAACTCCTGTTGACAAACCTTTTATAG (29)	STAT4_4_sense
pGL3 flanking primers	Fw: AGTGGATCCTGAAGACTTGAGGGATGGAA (29)	2kbS4_Rv8BamHI_FO
	Rv: AGTGTCGACCTGCCCTTTCCAAATTCTTG (29)	2kbS4_fw1SalI_FO
pGL3 upstream_Luc seq primer	Fw: CTAGCAAAATAGGCTGTCCC (23)	RVprimer3
pGL3 downstream_L seq primers	Fw: AACCATTATAAGCTGCAATAAAC (23)	EGFP-C1_R
	Rv: GACGATAGTCATGCCCCGCG (29)	RVprimer4
CNSeFO upstream primers	Fw: CGTAGGATCCCTGGTTGGACGAG (23)	CNSe_KpnI_FO_FW
	Rv: CATGGAGCTCTCAGTTACTCTGTGCTTA (28)	CNSe_SacI_FO_RV
CNSeRO upstream primers	Fw: CGTAGAGCTCCTGGTTGGACGAG (23)	CNSe_SacI_RO_FW
	Rv: CATCGGATCCTCAGTTACTCTGTGCTTA (28)	CNSe_KpnI_RO_RV
CNSeFO downstream primers	Fw: AGTGGATCCCTGGTTGGACGAGGG (23)	CNSe_FO_BamHI_Fwd
	Rv: AGTGTCGACTCAGTTACTCTGTGC (28)	CNSe_FO_SalI_RV
CNSeRO downstream primers	Fw: AGTGGATCCTCAGTTACTCTGTGC (23)	CNSe_RO_BamHI_Fwd
	Rv: AGTGTCGACCTGGTTGGACGAGGG (28)	CNSe_RO_SalI_RV
fut7 STAT5 mutant	Fw: GGATGACAATGCTGACAACAAGGCATT (27)	Fut7_STAT5_2_FW
	Rv: AATGCCTTGTTGTCAGCATTGTCATCC (27)	Fut7_STAT5_2_RV
*fut7*_mtCRE substitution mutant	Fw: CAAGTGCTGTGGCTCCATCAGAC (23)	Fut7_CREmut_FW
	Rv: GTCTGATGGAGCCACAGCACTTG	Fut7_CREmut_RV
*fut7*_ΔCRE deletion mutant	Fw: TCAGGGCAAGTG_CTCTCCATCAGACTG (27)	Fut7_CREdel_FW
	Rv: CAGTCTGATGGAGAG_CACTTGCCCTGA (27)	Fut7_CREdel_RV
pCpGL flanking and seq primers	Fw: TAAATCTCTTTGTTCAGCTCTCTG (24)	pCpGS
	Rv: CATCTTCCAGAGGGTAGAATGG (22)	pCpGR

Table 5.11: Primers for mRNA quantification by RT-qPCR

mRNA target	Sequence	Source
Gcnt1	Fw: CAGGAGTCAGAGCCTCAAAG (20) Rv: TGCCAGTTTAACAGCGGGAC (20)	Syrbe et al. (2004) [2]
Gcnt1 – mRNA isoform E1E2E3	Fw: GCTCCAGGCTGTTGGAAAG (20) Rv: TTTGCACTATAGAACAGGGC (20)	M. Schröter PhD thesis [53]
Gcnt1 – mRNA isoform E1.1E2E3	Fw: ACAAGTGCTCAACTGGCTGT (20) Rv: TTTGCACTATAGAACAGGGC (20)	M. Schröter PhD thesis [53]
Gcnt1 – mRNA isoform E3.1	Fw: TTTTGAGCCCGAGAAACACT (20) Rv: CCTTTGTAGTAACCGTAAGT (20)	M. Schröter PhD thesis [53]
Fut7	Fw: CAGATGCACCCTCTAGTACTCTGG (24) Rv: TGCACTGTCCTTCCACAACC (20)	Syrbe et al. (2004) [2]
Itgα	Fw: AATTGGACCAAGTGAGGGACAA (22) Rv: TCGCTAGATCCATACACAAATGAAGT (20)	DeNucci et al. (2010) [99]
Ccr9	Fw: TGCCATGTTCATCTCCAACTG (21) Rv: GAACTGGGTTCAGACAACTGTGG (23)	Hoffmann et al. (2013) [40]
Il4	Fw: TCCACGGATGCGACAAAAAT (23) Rv: TTCTTCTTCAAGCATGGAGT (26)	Brenner et al, 2004 [100]
Rarα	Fw: GACTTGGTCTTTGCCTTCGC (20) Rv: ATGTCCACCTTGTCTGGCTG (20)	Primer-BLAST
Rarγ	Fw: TATGGGGTCAGCTCCTGTGA (20) Rv: CGTTCCTTACAGCTTCCTTGG (21)	Primer-BLAST
Rxrα	Fw: TACCCACCACACCCACATTG (20) Rv: ACCTTGAGGACGCCATTGAG (20)	Primer-BLAST
Rxrβ	Fw: TTTAATCCAGACGCCAAGGGC (21) Rv: TGACACTCGGTGTGCATCTG (20)	Primer-BLAST
18S ribosomal RNA	Fw: GATCCATTGGAGGGCAAGTCT (21) Rv: GCAGCAACTTTAATATACGCTATTGC (26)	M. Pink PhD thesis [75]
Hprt	Fw: ATCATTATGCCGAGGATTTGGAA (23) Rv: TTGAGCACACAGAGGGCC (18)	M. Pink PhD thesis [75]

Table 5.12: Primers for ChIP-qPCR of the *Gcnt1* enhancer and control regions

ChIP-qPCR amplicons	**Sequence**	**Binding location**
gcnt1 enhancer – I (270bp)	Fw: AAAACGCCAACCATTCTTTTT (21) Rv: TGAAGACTTGAGGGATGGAA (20)	chr19:17456010+17456279
gcnt1 enhancer – II (280 bp)	Fw: GCTCTGCCCACTGACAATCT (20) Rv: AAAAAGAATGGTTGGCGTTTT (21)	chr19:17455751+17456030
gcnt1 enhancer – III (230bp)	Fw: TCAGCATCTGCCTGACTTTT (20) Rv: AGATTGTCAGTGGGCAGAGC (20)	chr19:17455541+17455770
gcnt1 enhancer – IV (244bp)	Fw: CCCCGCTTTGAGAACACTAA (20) Rv: TGGGATTAAAAGTCAGGCAGA (21)	chr19:17455324+17455567
gcnt1 enhancer – V (251bp)	Fw: CAGAACCACAGGGATGGTCT (20) Rv: CCATGAGAGCGCTGTGAGTT (20)	chr19:17455111+17455361
gcnt1 enhancer – VI (222bp)	Fw: CCTCCACATTGACTTAGGGAAC (22) Rv: AGACCATCCCTGTGGTTCTG (20)	chr19:17454909+17455130
gcnt1 enhancer – VII (239bp)	Fw: GAGATGTCATGCTCTCTTCTGG (22) Rv: TTCCCTAAGTCAATGTGGAGGT (22)	chr19:17454691+17454929
gcnt1 enhancer – VIII (215bp)	Fw: CTGCCCTTTCCAAATTCTTG (20) Rv: AGCATGACATCTCATCCCATT (21)	chr19:17454489+17454703
ifnγ – DHS(I)	Fw: CTGCCCTTTCCAAATTCTTG (20) Rv: AGCATGACATCTCATCCCATT (21)	chr19:17454489+17454703

6. Results

6.1 Regulation of *gcnt1* and *fut7* in T_H1 cells

6.1.1 Regulation of *gcnt1* in T_H1 cells

6.1.1.1 Verification of *gcnt1* enhancer activity in T_H1 cells

Our group has recently identified two regulatory regions within the *gcnt1* gene. A promoter was identified by *in silico* conservation analyses and reporter assays using truncated reporter constructs designed to cover the conserved regions found. One region was able to induce promoting activity in reporter assays in all helper T cell subsets tested – T_H1, T_H2, and T_H0 cells. However, it has been established with *in vitro* primary polarized helper T cells subsets that IL-12 induces *gcnt1*, but that the polarizing cytokine driving the T_H2 fate, IL-4, cannot [51, 68]. Therefore, despite the activity of the newly identified promoter region, this region is not responsible for the polarization-dependent induction of *gcnt1*.

T_H1 cells that express P-lig also express Gcnt1 mRNA, while P-lig$^-$ T_H1 cells do not [68]. Such a difference in expression can be due to differences in transcriptional or chromatin-modifying events within the cell. To find a T_H1-dependent regulatory region controlling induction of *gcnt1* and subsequently P-lig, we used the knowledge that distal regulatory regions are often discernible by distinct histone marks. In particular, it has been shown that enhancers in the human genome carry tissue/cell-specific chromatin marks, while promoters are invariant in this respect [101]. To that end, former students in the lab performed a *gcnt1* locus-wide ChIP-on-chip for the active histone methylation mark, H3K4me2, and the repressive histone methylation mark, H3K27me3, on five-day *in vitro* generated T_H1 cells that were were FACS-sorted according to their expression of P-lig – giving rise to P-lig$^+$ and P-lig$^-$ subsets. This experiment revealed an interesting region about 20 kb distal to the *gcnt1* transcriptional start site (TSS) with prominent H3K27me3 marks in P-lig$^-$ cells (data not shown). The promoter and the distal upstream region, depicted as an enhancer, are shown in a schematic of the *gcnt1* gene locus (Figure 6.1 - upper panel), followed by a conservation alignment of the *gcnt1* gene locus between the mouse genome, database mm10, and the human genome, database hg19 (Figure 6.1 - lower panel).

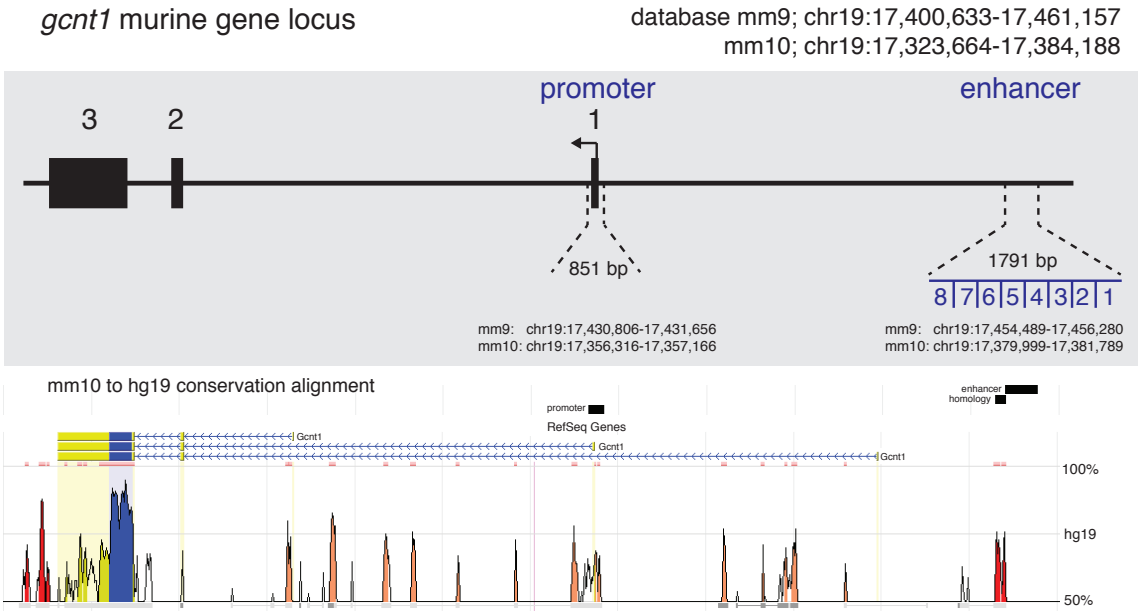

Figure 6.1: *gcnt1* gene locus and mouse-human conservation alignment. *Upper panel* schematic of the locus with exons numbered and regulatory regions with chromosomal locations on two murine genome databases, mm9 and mm10, indicated. The enhancer is highlighted to depict the 8 qPCR amplicons used in further analyses. *Lower panel* shows the conservation alignment from mouse (mm10) to human (hg19). Black boxes above the plot indicate location of the regulatory regions that are also highlighted in the upper panel. The middle transcript of the RefSeq genes represents the dominating transcript in T cells.

The ChIP-on-chip results were verified by histone-ChIP in cooperation with a former student, Micha Schröter, using eight primer pairs spanning the distal region. To address the changes that ensue upon polarization from the naive T cell state, we included naive T cells and T_H1 cells sorted for their P-lig expression on day 3 and day 5 of culture by our in-house FACS core facility. In line with a lack of *gcnt1* transcription, naive T cells exhibited a closed histone configuration with low H3K4me2 and prominent H3K27me3 marks (Figure 6.2). We observed that the active H3K4me2 mark in this region increased in a time-dependent manner during T_H1 differentiation (Figure 6.2 – upper panel). The active histone mark did not differ between P-lig$^+$ and P-lig$^-$ T_H1 cells on day 3. It was even significantly higher on day 5 of culture in P-lig$^-$ T_H1 cells compared to P-lig$^+$ T_H1 cells. Therefore, H3K4me2 does not seem to be the responsible mark for the differential expression of P-lig observed in these T_H1 cell populations. On the other hand, a significantly lower H3K27me3 mark was observed in P-lig$^+$ T_H1 cells compared to naive T cells on both day 3 and day 5 of culture. This mark was also significantly lower in day 3 P-lig$^-$ T_H1 cells compared to naive T cells. However, on day 5, the amount of repressive mark seen in P-lig$^-$ T_H1 cells approached that observed in naive T cells. This suggested that the presence of the repressive mark at this distal region governs transcription of *gcnt1* in T_H1 cells.

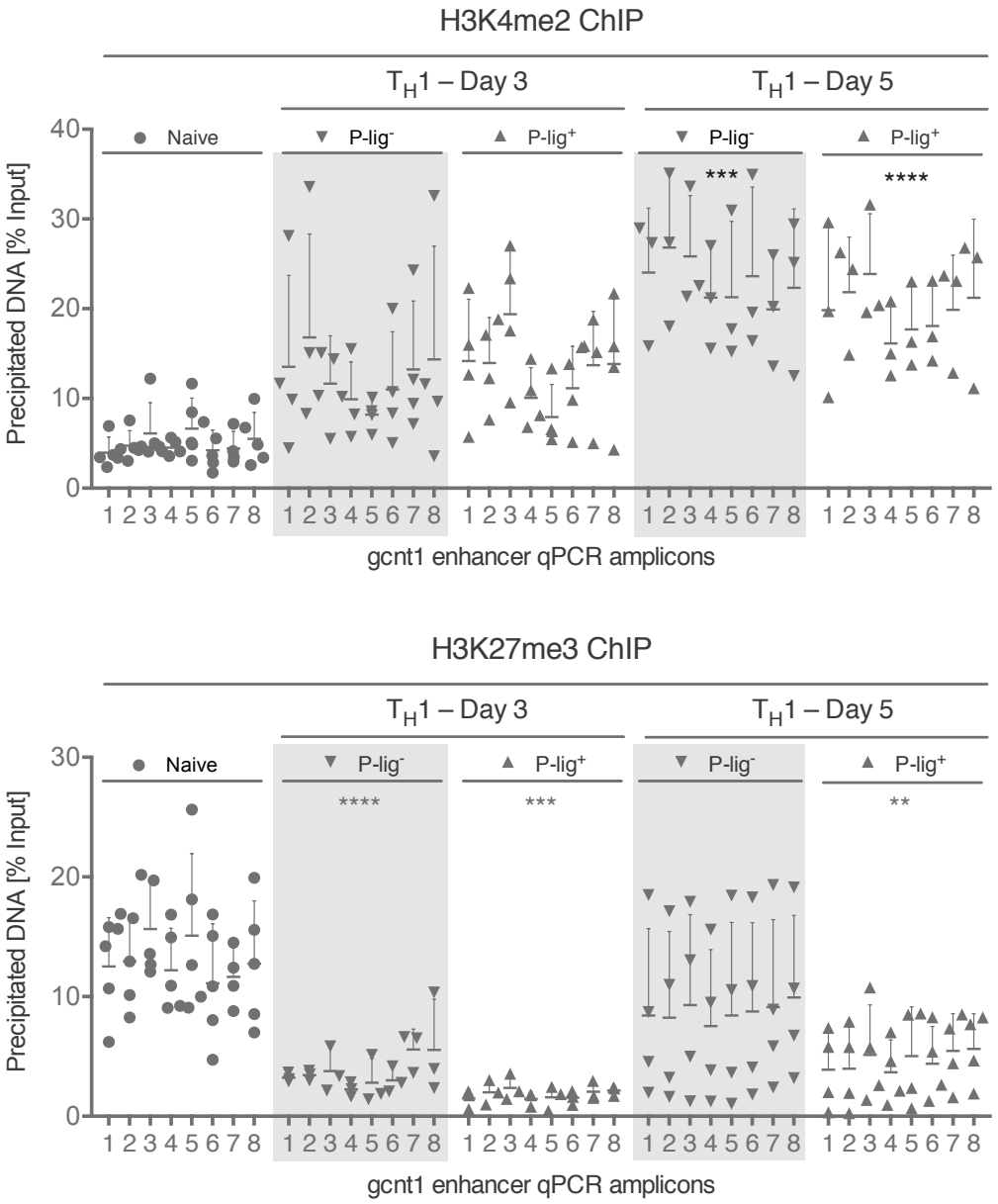

Figure 6.2: Histone methylation of the *gcnt1* enhancer in P-lig$^+$ and P-lig$^-$ T_H1 cells. Naive T cells from WT mice were used immediately for ChIP or polarized under T_H1 conditions for 3 or 5 days. Prior to the ChIP of the polarized T_H1 cells, the cells were sorted by FACS for expression of P-lig. *Upper panel* ChIP of the open/active histone methylation mark, H3K4me2; *lower panel* ChIP of the closed/repressive histone methylation mark, H3K27me3. Both panels show the % of input DNA that each qPCR amplicon primer pair was able to pull down from the indicated sample (n≥3; Mean+SD shown;*p≤0.05, **p≤0.01, ***p≤0.001, ****p≤0.0001; Kruskal-Wallis with Dunn's Multiple Comparison's test results shown in the graph compared to naive). These experiments were performed in cooperation with a previous PhD student in the lab, Micha Schröter.

The enhancer maps close to a region of homology between mouse and human as shown in fig. 6.1 bottom right. It is commonly believed that conserved regions possess regulatory activity, and this is how the promoter was found initially. Therefore, we cloned the distal enhancer along with the homology region, in both directions, into a reporter vector already containing the *gcnt1* promoter. The activity of these constructs was tested in T_H1 cells in two independent pilot experiments (Figure 6.3). Furthermore, truncated versions were generated without the homology region to assess the contribution to activity of the homology region. We found that the constructs without the homology region did not differ significantly in activity from those containing the homology region (Figure 6.3). Therefore, we conclude that the homology region does not represent a regulatory region controlling *gcnt1* induction and continued to characterize the putative enhancer alone.

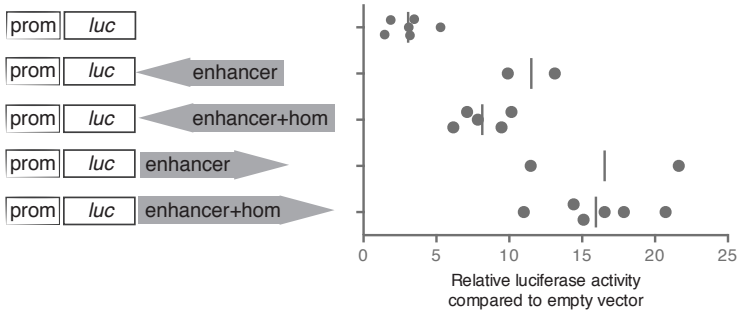

Figure 6.3: Activity of a conserved region downstream of a *gcnt1* enhancer. Naive T cells from WT mice were polarized under T_H1 conditions, transfected with the indicated constructs on day 2, after which the luciferase assay was performed on day 4 (n=2 homology constructs, n≥5 promoter and prom+enhancer constructs; line in each dataset represents the mean). The gene location of the homology region, hom, is depicted in the lower panel of fig. 6.1 as a small black box.

6.1.1.2 STAT4 and T-bet binding to the *gcnt1* enhancer

IL-12 is required for the induction of the surrogate marker for C2-GlcNAcT-I (encoded by *gcnt1*) activity, 1B11 (glycosylated CD43) [72]. Additionally, it has been shown that the downstream signaling molecule of IL-12, STAT4, controls induction of *gcnt1* in T_H1 cells [72]. Therefore, we investigated whether STAT4 acts on the identified *gcnt1* enhancer. First, *in silico* analyses of the enhancer region, using the prediction software MatInspector [97] and PROMO [98], revealed several conserved and non-conserved STAT4 binding motifs. A site was considered conserved when predicted by both software programs. Second, reassessment of publically available STAT4 ChIP-seq data revealed binding of STAT4 in and around amplicon 4 of the putative *gcnt1* enhancer – a binding that is lost in ChIP-seq of $stat4^{-/-}$ T_H1 cells [102] (data not shown). The schematic result of these analyses are shown in Figure 6.4.

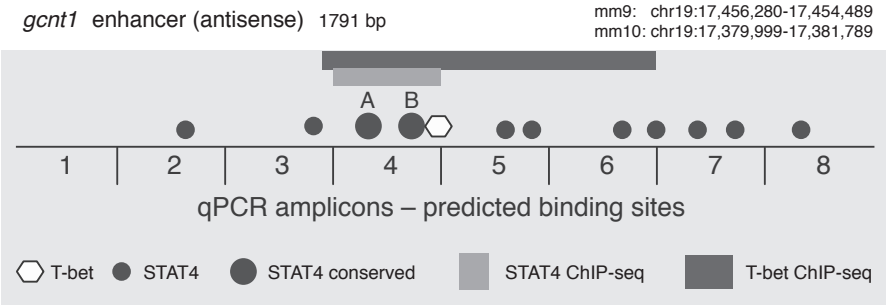

Figure 6.4: Predicted STAT4 motifs and T-bet binding within the *gcnt1* enhancer. Binding motifs were considered conserved after prediction by at least two of the software programs used – MatInspector [97] and Promo [98].The T-bet binding prediction was found by manual search for the T-bet binding motif based on two previous publications [103, 8]. The location of STAT4 and T-bet binding from reanalyzed ChIP-seq datasets performed in T_H1 cells cultured in cRPMI [102] and [104, 105] is also shown.

To determine whether the reported inductive properties of STAT4 on *gcnt1* activity are caused by a transactivation of STAT4 on the *gcnt1* enhancer, we performed reporter assays in WT and *stat4*$^{-/-}$ T_H1 polarized cells. The reporter vectors were cloned with the *gcnt1* promoter region upstream of the luciferase gene, while the enhancer was inserted downstream of the luciferase gene. These plasmids were cloned in cooperation with Micha Schröter as described [53]. Both the promoter and enhancer were inserted in the forward orientation toward the direction of transcription and checked by sequencing before use. We compared the reporter activity of the "promoter+enhancer" (also referred to as prom+enh and p+enh) vector to that of the vector without the enhancer, i.e. "promoter only" (also referred to as prom). The "promoter+enhancer" construct has significantly more activity than the "promotor only" as shown in fig. 6.3.

Compared to WT T_H1 cells, we observed that the promoter+enhancer activity was 3-fold lower in *stat4*$^{-/-}$ T_H1 cells (Figure 6.5 – upper panel). To determine whether the activity level of the *gcnt1* prom+enh construct correlated with the amount of P-lig expressed on the cell surface, WT and *stat4*$^{-/-}$ T_H1 cells were cultured in parallel with the reporter assay and assessed for P-lig expression on day 5 of culture. This culture was kept one day longer than the culture of the cells used in the reporter assay for historical reasons. As expected, adding IL-12 to the culture on day 3 gave rise to 30% and 50% P-lig in WT T_H1 cells. However, in *stat4*$^{-/-}$ T_H1 cells, this was more than 3-fold lower (Figure 6.5 – lower panel). Therefore, we concluded that STAT4 indeed possesses transactivating effects on the *gcnt1* enhancer which translates into changes in P-lig expression.

The transactivating effect of STAT4 can arise from a direct binding to the enhancer or an indirect binding of STAT4 to a larger co-activating complex. We hypothesized that STAT4

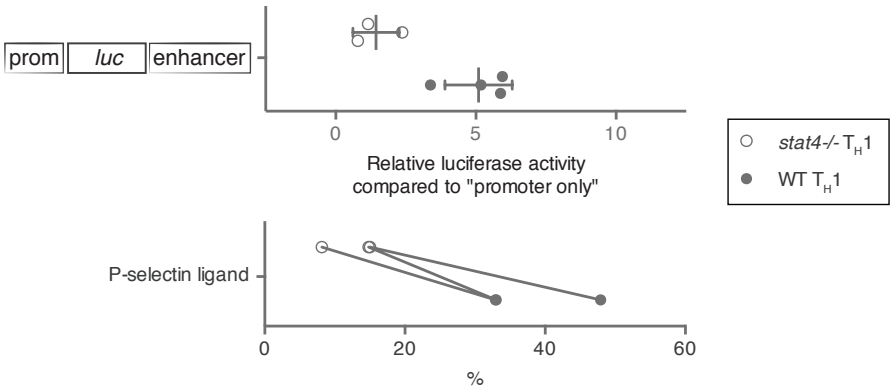

Figure 6.5: Activity of the *gcnt1* enhancer in *stat4*$^{-/-}$ T_H1 cells and P-lig expression. *Upper panel* naive T cells from *stat4*$^{-/-}$ and WT mice were polarized under T_H1 conditions, transfected with the "promoter+enhancer" and "promoter only" constructs on day 2, after which the luciferase assay was performed on day 4. "Promoter+enhancer" construct compared to "promoter only" for *stat4*$^{-/-}$ T_H1 cells is shown (n≥3; Mean±SD). *Lower panel* P-lig expression on day 5 of *stat4*$^{-/-}$ and WT T_H1 cells (n=3).

binds directly to the enhancer. Therefore, we mutated the conserved STAT4 binding motif marked "A" in fig. 6.4 in the prom+enh vector, and assessed the resulting reporter activity in WT T_H1 cells. The site was mutated by overlap extension PCR introducing two substitution mutations that changed the sequence from TTCTCAAAA to TTgTCAAcA in line with [106]. The results revealed significantly lower activity of the mutated construct compared to the WT construct (Figure 6.6). This indicated that binding of STAT4 to the mutated site was prevented, thus supporting a direct binding mode for STAT4 in the induction of *gcnt1*.

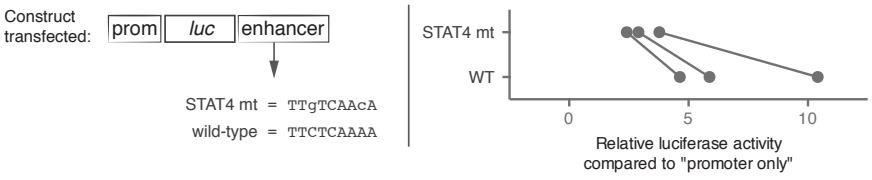

Figure 6.6: Activity of the *gcnt1* enhancer with a mutated STAT4 binding site. Naive T cells from WT mice were polarized under T_H1 conditions, transfected with the mutated or WT "promoter+enhancer" and "promoter only" constructs on day 2, after which the luciferase assay was performed on day 4. "Promoter+enhancer" construct compared to "promoter only" is shown (n=3).

STAT4 requires phosphorylation before being able to bind DNA and drive transcription. STAT4 is phosphorylated (pSTAT4) in the presence of IL-12 [13, 107]. Previous studies in our lab have shown that once P-lig is expressed on the surface, it remains on a subset of effector/memory T cells despite the absence of IL-12 signaling in these cells [93]. This leaves the question of how long STAT4 activates the *gcnt1* enhancer and what transcription factor(s) drive long-term induction of *gcnt1* and, in turn, maintenance of P-lig

expression. To determine whether and when STAT4 binds to the *gcnt1* enhancer, we performed ChIP experiments with antibodies against STAT4 on WT T_H1 cells cultured for 1, 3, or 5 days without adding fresh IL-12 to the culture from day 3 to day 5. This enabled us to study the binding kinetics also when IL-12 is no longer present in the culture. The results showed that STAT4 did not bind any of the amplicons of the enhancer on day 1 (Figure 6.7). On day 3, however, the binding of STAT4 increased significantly to amplicon 3, 4, and 5 compared to day 1. This binding declined on day 5 (Figure 6.7). Furthermore, on day 3 and day 5, binding to amplicon 4 was significantly greater than to amplicon 8. Amplicon 8 served as a negative control as STAT4 ChIP-seq did not reveal binding to that region, despite the prediction of a binding site in this region (shown in fig. 6.4). The binding of STAT4 to amplicon 4 was comparable to that of a positive control region within a DNAse hypersensitivity region DHS(I) of the *ifng* locus that showed STAT4 binding in ChIP-seq data (ChIP-seq data not shown).

On day 5 of this culture, IL-12 was no longer present, and was associated with a decline in STAT4 binding to the *gcnt1* enhancer. This is in line with the aforementioned importance of IL-12 in the activation of STAT4. Supporting this notion, we observed that when IL-12 is added to the T_H1 culture during the expansion phase (day 3 to day 5), the binding of STAT4 to the enhancer increases dramatically (data not shown). This is similar to what was reported for the binding of pSTAT4 to the *Tbx21* locus [13]. As IL-12 is induced early during T_H1 dominated immune responses but then declines throughout the course of the response, other factors must drive long-term expression of *gcnt1* and P-lig. Another

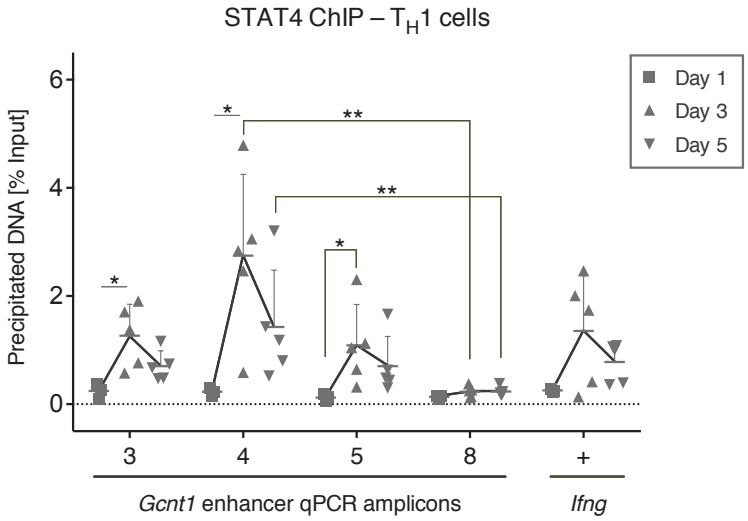

Figure 6.7: Kinetics of STAT4 binding to the *gcnt1* enhancer in T_H1 cells. Naive T cells from WT mice were polarized under T_H1 conditions for 1, 3, or 5 days before harvesting the cells for STAT4-ChIP.Shown is the % of input DNA that each qPCR amplicon primer pair was able to pull down from the indicated sample – a region on the *ifng* gene locus was used as a positive control ($n \geq 3$, Mean+SD shown;*$p \leq 0.05$, **$p \leq 0.01$; Kruskal-Wallis with Dunn's Multiple Comparison's test results shown between days for each amplicon, and for all amplicons for each day).

important contributing factor to the imprinting of the T_H1 lineage is the master transcriptional regulator of T_H1 cells, T-bet, encoded by the *Tbx21* gene. Like STAT4, T-bet was shown to be essential for the induction of the surrogate marker for C2-GlcNAcT-I activity, 1B11, and for T_H1 cell rolling events on P-selectin *in vitro* [73, 74]. In contrast, we found no difference between *tbx21*$^{-/-}$ T_H1 cells and WT T_H1 cells in terms of Gcnt1 mRNA and P-lig expression on day 3 of a T_H1 culture [68]. However, this does not rule out that T-bet may have an effect on transcription during later stages of activation.

To assess the contribution of T-bet in comparison to STAT4 on the regulation of *gcnt1* at the trancriptional level, we analyzed the expression of Gcnt1 mRNA in WT, *stat4*$^{-/-}$, and *tbx21*$^{-/-}$ T cells polarized under T_H1 conditions for 3 or 5 days. The cells were either supplemented with fresh IL-12 on day 3 or not. While there were minor differences on day 3 after activation, expression of Gcnt1 mRNA on day 5 was lower in *stat4*$^{-/-}$ as well as *tbx21*$^{-/-}$ T_H1 cells compared to WT T_H1 cells regardless of the presence of IL-12 in the culture (Figure 6.8). Despite lacking repetitions of this experiment, it suggests that both STAT4 and T-bet play a considerable role in transcriptional activity after cessation of TCR activation, which occurs from day 0 to day 3. Taken together, these results suggest that both STAT4 and T-bet play a role in the induction of Gcnt1 mRNA.

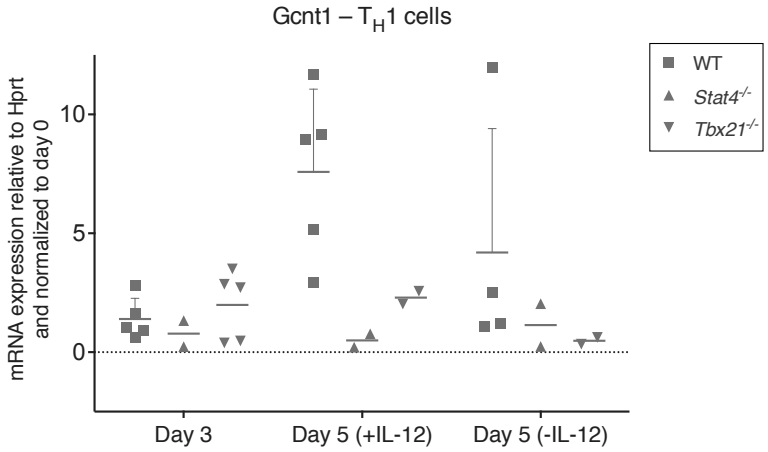

Figure 6.8: Expression of Gcnt1 mRNA in *stat4*$^{-/-}$ and *tbx21*$^{-/-}$ T_H1 cells. Naive T cells from WT, *stat4*$^{-/-}$, and *tbx21*$^{-/-}$ were polarized under T_H1 conditions for 3 or 5 days before harvesting the cells for mRNA analysis. Cells that were cultured until day 5 were either supplemented with IL-12 on day 3 (hi) or not (lo). Gcnt1 mRNA levels are reported relative to the housekeeping gene Hprt and normalized to naive levels (n≥2, Mean+SD shown for WT).

Our own T-bet binding site prediction as well as T-bet ChIP-seq data have suggested binding of T-bet within the *gcnt1* enhancer (fig. 6.4). To determine whether and when T-bet binds directly to the *gcnt1* enhancer, we performed T-bet ChIP on T_H1 cells cultured

for 1, 3, or 5 days (without supplementing the culture with IL-12 on day 3). As expected, there was no binding on day 1. On day 3, T-bet binding to amplicon 4 and the positive control region within the *ifng* locus increased, compared to amplicon 8 (Figure 6.9). This narrowed down the binding site of T-bet from T-bet ChIP-seq data available [104, 105]. Most notably, and in contrast to the STAT4 ChIP, T-bet remained bound to the enhancer from day 3 to day 5. This suggests that T-bet, unlike STAT4, is able to stay bound to the *gcnt1* enhancer in the absence of IL-12.

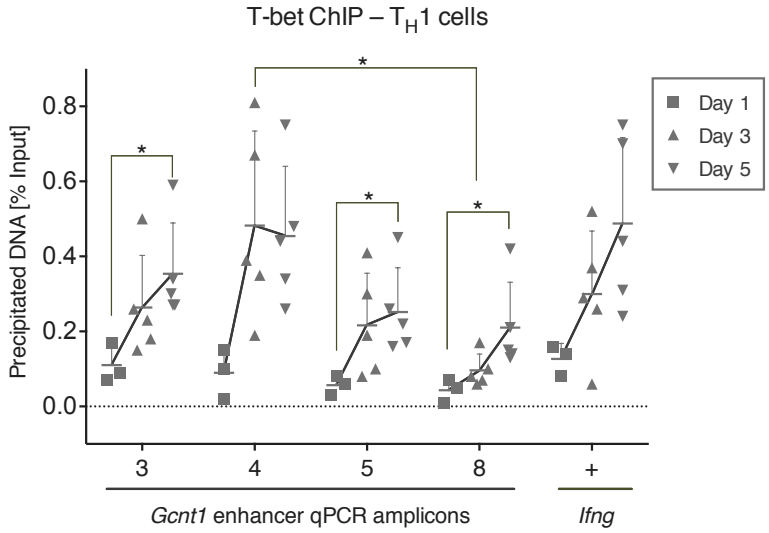

Figure 6.9: Binding of T-bet to the *gcnt1* enhancer in T_H1 cells. Naive T cells from WT mice were polarized under T_H1 conditions for 1, 3, or 5 days before harvesting the cells for T-bet-ChIP. Shown is the % of input DNA that each qPCR amplicon primer pair was able to pull down from the indicated sample – a region on the *ifng* gene locus was used as a positive control (n=3 day 1, n=5 day 3 and 5; Mean+SD shown;*p≤0.05, **p≤0.01; Kruskal-Wallis with Dunn's Multiple Comparison's test results shown between days for each amplicon).

6.1.1.3 STAT4 and early chromatin modifications of the *gcnt1* locus

STATs have previously been implicated in the opening of the chromatin by recruitment of p300. p300 is a coactivator with intrinsic histone deacetylase activity, enhancing expression of target genes [108]. To estimate the functional effects of STAT4 on the chromatin configuration, we reanalyzed publically available ChIP-seq datasets of WT and *stat4*$^{-/-}$ T_H1 cells, comparing the following histone methylation marks present on the *gcnt1* gene locus: H3K4me3, a putative promoter mark, and H3K36me3, a mark indicating RNA polymerase II activity. In WT T_H1, the promoter and enhancer are decorated with H3K4me3 marks, and the coding region is flanked by H3K36me3 marks, indicating that transcription is active in these cells (Figure 6.10 – upper panel). In T_H1 cells, but not in naive T cells, the regions overlap with DNAse hypersensitivity sites. In *stat4*$^{-/-}$ T_H1 cells, both histone

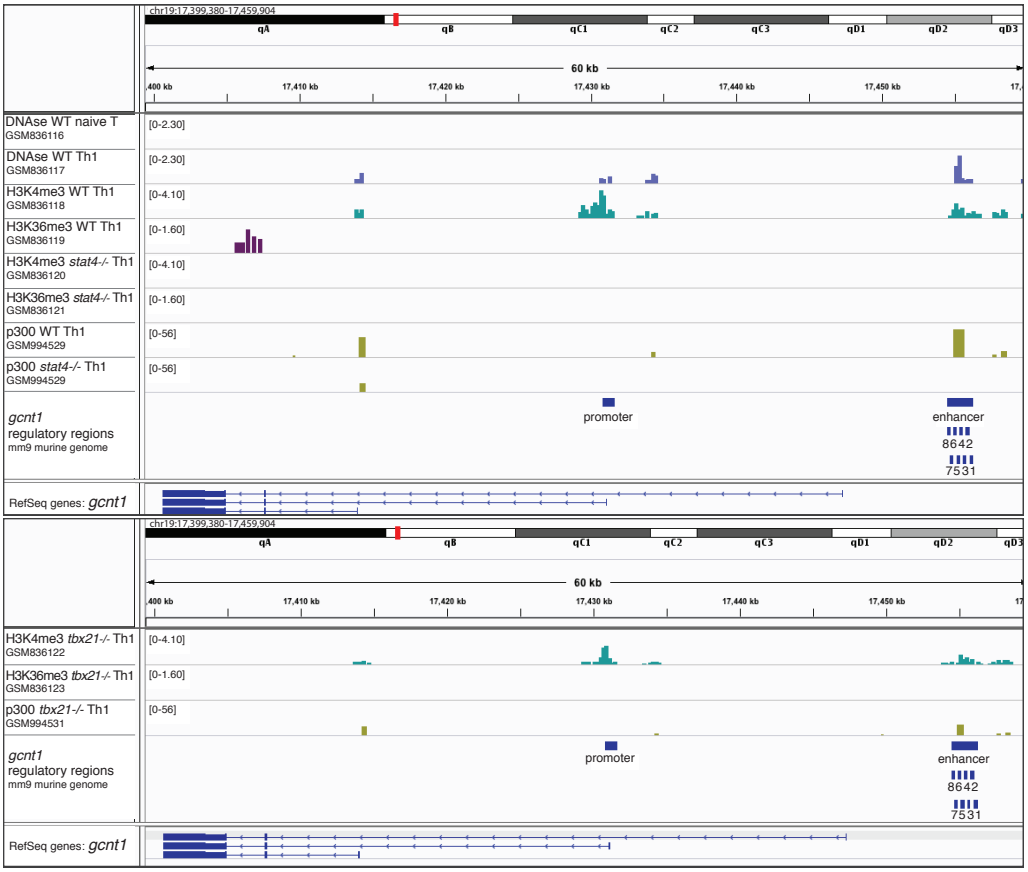

Figure 6.10: Epigenetic regulation of *gcnt1* – public ChIP-seq data. *Upper panel* shows DNAse hypersensitivity assays in naive and T_H1 cells (purple/blue); H3K4me3 (turquoise) and H3K36me3 (purple) ChIP-seq data in WT and then *stat4*$^{-/-}$ T_H1 cells; p300 (olive) ChIP-seq in WT and then *stat4*$^{-/-}$ T_H1 cells. *Lower panel* shows H3K4me3, H3K36me3, and p300 ChIP-seq data from *tbx21*$^{-/-}$ T_H1 cells with the same color-code as the upper panel. DNAse hypersensitivity assays and histone ChIP-seq reanalyzed from [105]; p300 ChIP-seq from [108].

marks are absent on the gene, which correlates with a lack of p300 binding in *stat4*$^{-/-}$ compared to WT T_H1 cells. These results confirm the functional importance of STAT4 on *gcnt1* induction and suggest that STAT4 plays a role in chromatin modification at the *gcnt1* enhancer, which in turn confirms the crucial role of this region as an enhancer for *gcnt1* expression.

As in *stat4*$^{-/-}$ T_H1 cells, *tbx21*$^{-/-}$ T_H1 cells also lack the H3K36me3 mark, but unlike *stat4*$^{-/-}$$T_H1$ cells, they do possess H3K4me3 marks. This indicates that some chromatin remodeling is occurring in the absence of T-bet, which corroborates other datasets showing that binding of p300, although less than in WT, is still present in *tbx21*$^{-/-}$ T_H1 cells compared to *stat4*$^{-/-}$ T_H1 cells (Figure 6.10 – lower panel), even though the majority of STAT4 signaling is not present in these cells [72]. Taken together, this indicates that although both STAT4 and T-bet bind to the enhancer, STAT4 seems to be an early reg-

ulating factor that modulates the chromatin to promote an accessible locus for long-term regulating factors, such as T-bet. T-bet can then remain bound to the enhancer at later time points in the absence of inflammatory cytokines, such as IL-12, likely promoting transcription and/or further chromatin remodeling without requiring STAT4 or p300.

6.1.2 Regulation of *fut7* in T_H1 cells

6.1.2.1 Verification and characterization of *fut7* regulatory regions

In contrast to Gcnt1, primary $CD4^+$ T cells express multiple Fut7 mRNA transcripts, transcribed from the *fut7* gene locus (schematic in Figure 6.11 – upper panel). In a project undertaken by a former PhD student in our lab, Matthias Pink, it was found that the Fut7 transcripts begin either upstream of exon 1 or upstream of exon 4, henceforth referred to as group 1 and group 4 transcripts. All transcripts express exon 5, which encodes the Golgi-localized catalytic domain that makes the enzyme FucT-VII functional. FucT-VII plays a critical role in the generation of E- and P-lig in T cells, but the regulation of its gene, *fut7*, is not well understood. Therefore, we aimed to identify regions on the *fut7* locus with regulatory activity to examine the possible signaling pathways converging onto *fut7*. By conservation analyses, a highly conserved non-coding 705 bp region (henceforth referred to as CNS) was found proximally upstream of exon 1 (Figure 6.11 – middle panel). In reporter assays, however, this region alone did not have any activity (data not shown).

In a second attempt to identify regulatory regions, a ChIP-on-chip was performed with antibodies against the histone methylation marks, H3K4me2 and H3K27me3, similar to that shown earlier for *gcnt1*. This array-based screening revealed that the histone methylation pattern does not differ between naive T cells and polarized cell subsets, that do or do not express Fut7 mRNA, such as P-lig^+ T_H1 and P-lig^- T_H1 cells, respectively. All subsets revealed an open *fut7* locus with H3K4me2 marks and a lack of repressive H3K27me3 marks. This was not the case for fibroblasts that exhibited a closed chromatin configuration with relatively few H3K4me2 marks and many H3K27me3 marks.

Finally, the level of group 1 and group 4 Fut7 mRNA transcripts were determined in the aforementioned T cell subsets, where it was found that group 4 transcripts dominate in P-lig^+ T cells. This prompted the study and identification of an alternative minimal promoter immediately surrounding exon 4 (Figure 6.11 – middle panel, second black box). This region maps to chr2: 25,279,490-25,280,285 on the mm9 murine genome database and had activity in reporter assays when a plasmid with an internal SV40 enhancer was used (data not shown).

We next tested whether the CNS region, identified earlier, possessed regulatory activ-

ity on the newly identified minimal promoter. Therefore, the CNS region was cloned into a reporter vector containing the minimal promotor upstream or downstream of the luciferase gene, in both orientations, as depicted in the lower panel of Figure 6.11. The results showed that the CNS has position- and orientation-independent enhancing activity compared to the promoter alone.

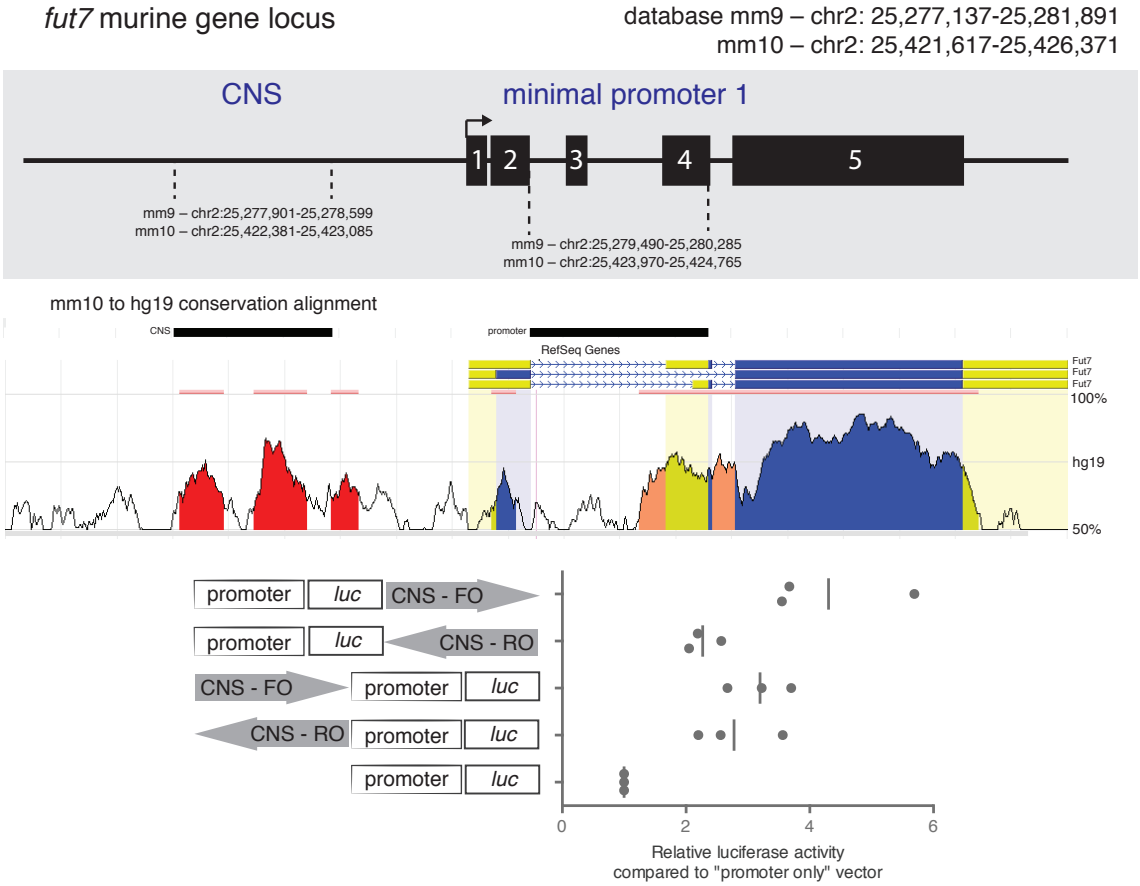

Figure 6.11: Activity of the *fut7* CNS in a pGL3 vector. *Upper panel* schematic of the five-exon *fut7* gene locus with regulatory regions indicated by dashed lines and their chromosome locations according to the murine genome database mm9 and mm10, respectively. *Middle panel* shows the conservation alignment from mouse (mm10) to human (hg19). Black boxes above the plot indicate location of the regulatory regions that are also highlighted in the upper panel. *Lower panel* naive T cells from WT mice were polarized under T_H1 conditions, transfected with the indicated constructs on day 2, after which the luciferase assay was performed on day 4 (n=3, line at mean).

6.1.2.2 DNA methylation and *fut7* expression

Previously, our lab has shown that the induction of selectin ligands in $CD4^+$ T cells requires cell division, which is considered a window for epigenetic changes [2]. Epigenetic changes leading to stable gene up- or down-regulation have been linked to the topographical memory that a subset of effector T cells acquire and retain as memory T cells. This enables the cells to recirculate the tissue in which they were activated initially.

As described earlier, the histone methylation pattern within the *fut7* gene does not change during T cell differentiation; however, artificial methylation of cytosines within the DNA with 5-Aza-deoxycytidine promotes expression of P-lig in T cell cultures [2]. To elucidate the impact of DNA methylation on Fut7 expression, earlier bisulfite sequencing studies were performed in the lab on *ex vivo* isolated effector/memory T cells ($T_{eff/mem}$) FACS-sorted into P-lig$^+$ and P-lig$^-$ subsets. The gut homing receptor $\alpha4\beta7$ is only expressed on P-lig$^-$ $T_{eff/mem}$ because P-lig and $\alpha4\beta7$ are induced under different priming-dependent environments. Moreover, under homeostatic conditions, these molecules are largely mutually exclusive in their expression [1, 6]. Therefore, we also stained this marker prior to the FACS sort to further distinguish P-lig$^+$ $T_{eff/mem}$ from P-lig$^-$ $T_{eff/mem}$ cells.

It was shown that the amplicon for bisulfite sequencing covering the minimal promoter for *fut7* was substantially demethylated in the skin- and inflammation-seeking P-lig$^+\alpha4\beta7^-$ $T_{eff/mem}$ compared to the gut homing P-lig$^-\alpha4\beta7^+$ $T_{eff/mem}$ cells. This indicated a clear role for DNA methylation in the control of *fut7* gene regulation (data not shown – Pink et al. submitted). The amplicons for the bisulfite sequencing experiments were designed by the company Epiontis. The amplicon covering the minimal promoter flanked +∼160 bp upstream and is henceforth investigated as the minimal promoter 1_v2 for *fut7* (Figure 6.12 – upper panel).

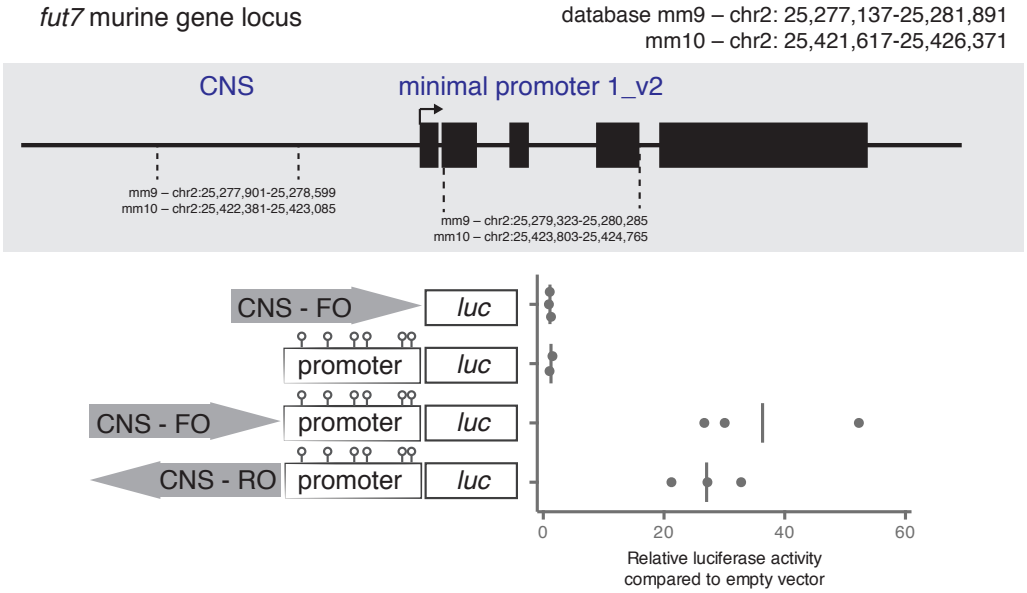

Figure 6.12: Activity of the *fut7* CNS and promoter in a pCpGL CpG-free vector. Naive T cells from WT mice were polarized under T_H1 conditions, transfected with the indicated constructs on day 2, after which the luciferase assay was performed on day 4 (n=3, line at mean).

To clarify the impact of DNA methylation on the *fut7* in more detail, the minimal promoter 1_v2, as well as the CNS region, were cloned into a CG-free plasmid for further *in vitro* methylation assays combined with reporter assays. This was done because the original pGL3-plasmid contains CpGs and is methylated during bacterial amplication. Therefore, to determine the effect of DNA methylation within the minimal promoter 1_v2, the minimal promoter 1_v2 and the CNS were separately transferred into a CG-free plasmid upstream of the luciferase gene, yielding two constructs. The activity of the constructs, without prior *in vitro* methylation, was then determined in reporter assays. The luciferase assay revealed that separately the two regions had no activity compared to the empty vector (Figure 6.12). The CNS region was then inserted in either orientation upstream of the minimal promoter 1_v2. The resulting constructs, containing both the CNS and the minimal promoter 1_v2, displayed greatly enhanced activity, independent of the orientation of the CNS.

Unlike minimal promoter 1_v2, the CNS region alone was not differentially methylated in the aforementioned bisulfite sequencing array. To determine the effect of methylation of minimal promoter 1_v2 in reporter assays, without compromising the enhancing activity of the demethylated CNS region, we performed selective *in vitro* methylation of the minimal promoter 1_v2 prior to reporter assays. First, the minimal promoter was restricted out of the vector and subjected to *in vitro* methylation with M.SssI, a CpG methyltransferase, or mock methylation, without enzyme added. Then the insert was ligated back into the vector, after which the activity of the ligated constructs were determined in reporter assays with polarized T_H1 cells. The reporter assays revealed that the activity of the construct with the methylated minimal promoter 1_v2 was significantly lower than the activity of the construct containing the mock methylated minimal promoter 1_v2 (Figure 6.13). This further indicates a clear role for DNA methylation in controlling *fut7* gene regulation.

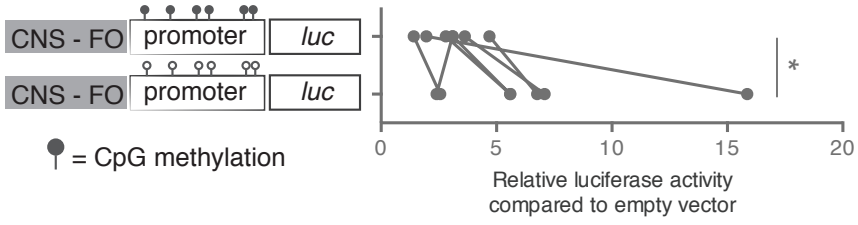

Figure 6.13: *in vitro* methylation of the *fut7* promoter and activity in T_H1 cells. Naive T cells from WT mice were polarized under T_H1 conditions, transfected with the indicated constructs on day 2, after which the luciferase assay was performed on day 4 (n=6, *p<0.05; Wilcoxon mathed pairs signed rank test).

6.1.2.3 CREB and STAT5 and transcriptional activity of *fut7*

It is known that IL-4 and retinoic acid (RA) are suppressors of E- and P-lig induction [52]. As such, these factors are key players in regulating signaling pathways during the activation of cells within LNs, and therefore contribute to establishing a stable linage commitment. A former PhD student in our lab, Matthias Pink, showed that the *fut7* minimal promoter 1_v2 is methylated in naive T cells, which correlates with a lack of Fut7 transcription. Once naive T cells are activated and express P-lig, the minimal promoter 1_v2 is de-methylated, which correlates with Fut7 transcription activation. When RA was present in a T_H1 culture, the activation-dependent de-methylation of the minimal promoter 1_v2 was abrogated, as assessed by bisulfite sequencing of T_H1 cultures treated with RA or not (Pink et al. submitted). He showed that RA prevents active de-methylation of the minimal promoter 1_v2 already on day 4 of a T_H1 culture, which spreads to flanking regions on day 9 of a T_H1 culture. This correlated with reduced Fut7 mRNA transcription on both day 4 and 9. The opposite was observed when treating the T_H1 culture with LE540, a RAR antagonist, that blocks RA signaling in FCS-containing media. Addition of LE540 resulted in progressive de-methylation originating within the minimal promoter 1_v2, which correlated with increased Fut7 mRNA transcription. The early de-methylation within the minimal promoter 1_v2 suggested an important regulatory function for this region.

An *in silico* transcription factor motif search revealed a cAMP responsive element (CRE) motif spanning the second CpG (CpG 844) within the minimal promoter 1_v2. A recent publication showed HTLV-1 tax-dependent activation of CREB, which induced expression of Fut7, by binding to a CRE site upstream of the *fut7* locus in human T cells [109]. This study suggested a function for CREB also in the regulation of *fut7* in murine T cells. In a preliminary CREB-ChIP, we also observed binding of CREB to the minimal promoter 1_v2 of *fut7* in the absence of RA (data not shown). Due to difficulties in repeating the CREB-ChIP, we mutated the CRE site by substitution or deletion in the CNS+minimal promoter 1_v2 CG-free plasmid and assessed the activity of these non-methylated constructs compared to the WT construct in reporter assays in T_H1 cells. Both the mutation and deletion mutants displayed lower activity than the WT CNS+minimal promoter 1_v2 construct (Figure 6.14). This indicates that CREB, which binds unmethylated DNA, is implicated not only in the regulation of *fut7* in human primary T cells, but also in murine T cells.

Recent experiments from our group have shown that IL-2 signaling is also implicated in Fut7 induction [68]. It was shown that the absence of IL-2, by treatment with a STAT5 inhibitor, reduced Fut7 mRNA transcription in a dose-dependent manner in T_H1 cells. Moreover, preliminary ChIP experiments showed binding of STAT5 to the *fut7* minimal

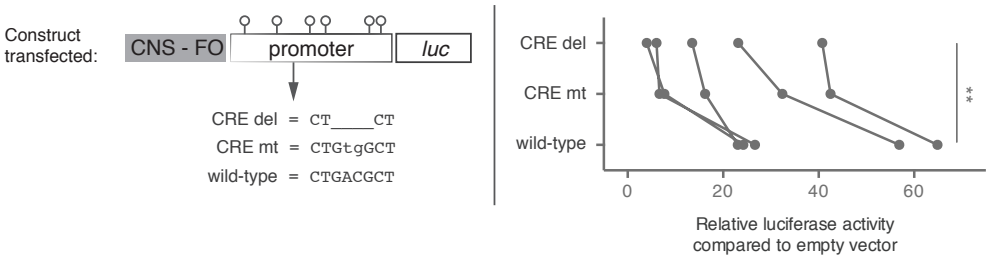

Figure 6.14: Activity of the *fut7* promoter with a mutated or deleted CRE binding site. Naive T cells from WT mice were polarized under T_H1 conditions and transfected with the indicated constructs, after which luciferase assays were performed (n=5, **p<0.01; Friedman test with Dunn's Multiple Comparisons test results shown).

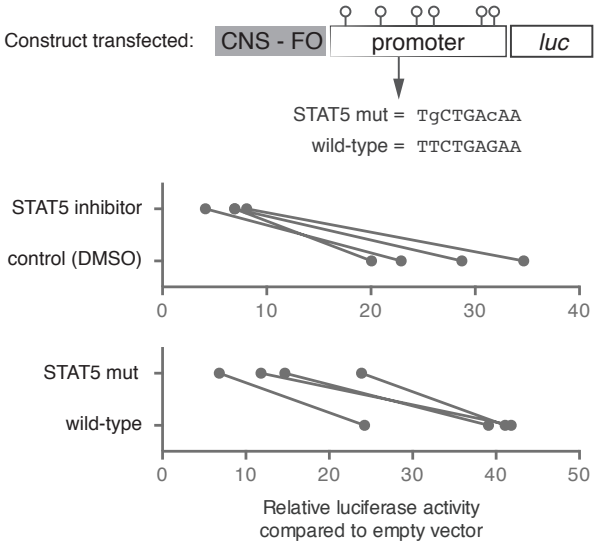

Figure 6.15: Activity of the *fut7* minimal promoter 1_v2 in the absence of STAT5. Naive T cells from WT mice were polarized under T_H1 conditions and transfected with the indicated constructs, after which luciferase assays were performed. The cells treated with the STAT5 inhibitor or DMSO were transfected with the WT construct (n=4). These experiments were performed together with a former PhD student in the lab, Matthias Pink.

promoter 1_v2 in the absence of RA [75]. Because these results indicated that the effect of IL-2 on *fut7* regulation proceeded through STAT5, we next investigated whether STAT5 has a transactivating effect on the *fut7* minimal promoter 1_v2. In cooperation with a former PhD student in lab, Matthias Pink, we performed reporter assays with the CNS+minimal promoter 1_v2 WT construct in T_H1 cells treated either with a STAT5 inhibitor or DMSO. We clearly saw a lower activity of the WT construct in the STAT5 inhibitor treated T_H1 cells compared to the DMSO control (Figure 6.15 – middle panel). This prompted the *in silico* analysis of STAT5 binding motifs within minimal promoter 1_v2, specifically around the STAT5 binding site determined by STAT5 ChIP (data not shown). As the result of binding was not significant, we verified the implication of STAT5 by mutational studies. The site was mutated from TTCTGAGAA to TgCTGAcAA using

the same principles as for the STAT4 binding site mutation shown earlier for the regulation of *gcnt1*. We found diminished activity of the mutated construct compared to the WT construct (Figure 6.15 – lower panel). Taken together, we conclude that CREB, as well as STAT5, play a direct role in the regulation of *fut7* in T_H1 cells.

6.2 Regulation of *gcnt1* and *fut7* in T_H2 cells

Previously, our group has shown that, in contrast to T_H1 cells, T_H2 cells do not express *gcnt1* and P-lig in *in vitro* cultures [51]. As such, these molecules were thought to be T_H1 lineage-specific molecules. However, further *in vivo* studies in our group contradicted this notion, because $CD4^+$ IFNγ, IL-4, and IL-10 producers, *ex vivo* isolated from the pLN, mLNs, or spleen, were observed to express P-lig at similar levels [1]. To understand the mechanisms behind this discrepancy, we first characterized the levels of Gcnt1 and Fut7 mRNA in T cells polarized *in vitro* under either T_H1 or T_H2 conditions, and compared the results to that of the naive T cells from which they differentiated. The results showed that Gcnt1 mRNA levels increase significantly during differentiation into the T_H1 cell fate, whereas it did not become expressed in T_H2 cells. Gcnt1 mRNA expression *in vitro* was significantly greater in T_H1 cells compared to T_H2 cells (Figure 6.16). On the other hand, Fut7 mRNA was similarly expressed in T_H1 and T_H2 cells.

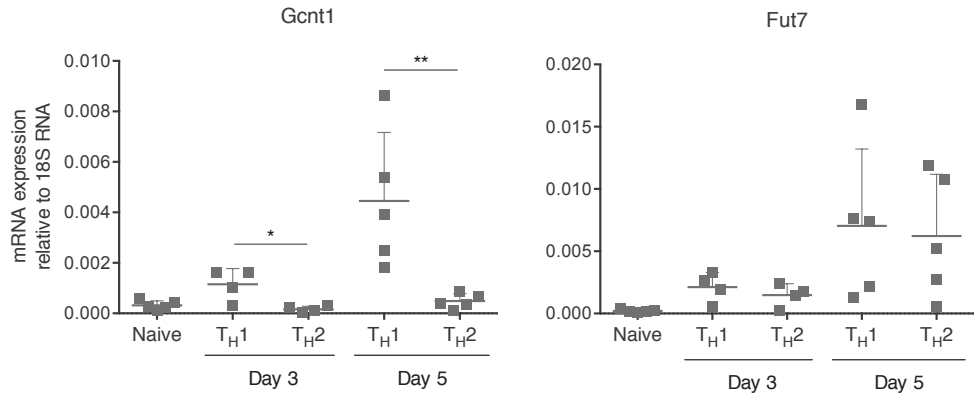

Figure 6.16: Expression of Gcnt1 and Fut7 mRNA in T_H1 versus T_H2 cells *in vitro*. Naive T cells from WT mice were harvested immediately or polarized under T_H1 or T_H2 conditions for 3 or 5 days before harvesting the cells for mRNA analysis. Cells that were cultured until day 5 were supplemented with polarizing cytokines on day 3. Gcnt1 and Fut7 mRNA is shown relative to the housekeeping gene 18S RNA ($n \geq 4$; mean+SD shown; *$p<0.05$, **$p<0.01$; Mann-Whitney test).

To verify the relation between Gcnt1 and Fut7 mRNA expression and selectin ligand expression in T_H1 and T_H2 cells cultured *in vitro*, we determined the expression of 1B11, the surrogate marker for C2GlcNAcT-I activity, as well as P-lig and E-lig in these cells. As expected, 1B11, P-lig, and E-lig increased during differentiation to T_H1 cells (summa-

rized data in Figure 6.17). However, already on day 3 of culture, expression of 1B11 was significantly lower in T_H2 cells compared to T_H1 cells. P-lig and E-lig were expressed at low, but similar levels on day 3 on T_H1 and T_H2 cells. This confirms a correlation between low Gcnt1 mRNA and low 1B11, but not selectin ligand generation. Representative flow cytometry dot plots (Figure 6.18) show that most E- and P-ligs are generated on 1B11 positive cells in T_H1 cells, but that not all 1B11 positive cells are also positive for E- and P-lig. In day 3 T_H2 cells, E- and P-ligs are generated in the absence of 1B11, i.e. *gcnt1* expression. On day 5, however, all ligands were significantly reduced on T_H2 cells compared to T_H1 cells.

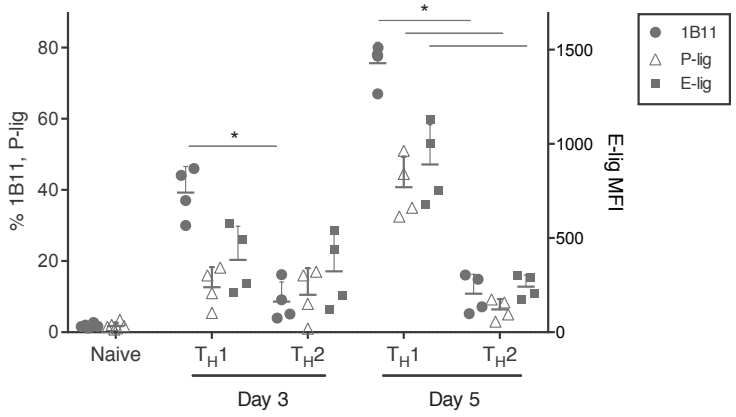

Figure 6.17: Expression of 1B11, P-lig, and E-lig in T_H1 versus T_H2 cells *in vitro*. Naive T cells from WT mice were harvested immediately or polarized under T_H1 or T_H2 conditions for 3 or 5 days before harvesting the cells for 1B11, P-lig, and E-lig staining. Cells that were cultured until day 5 were supplemented with polarizing cytokines on day 3. % 1B11 and P-lig are plotted on the left Y-axis, whereas mean fluorescent intensity (MFI) of E-lig is plotted on the right Y-axis (n=4; mean+SD; *p<0.05; Mann-Whitney test).

As shown earlier in this section, Gcnt1 mRNA is significantly greater in *in vitro* cultured T_H1 cells compared to T_H2 cells. This is reflected in the P-lig expression of the same cells. Therefore, we next investigated whether the chromatin configuration of the *gcnt1* enhancer is closed in T_H2 cells compared to T_H1 cells. We either isolated naive T cells or polarized them for 3 to 5 days under T_H1 and T_H2 cells conditions. We then performed histone ChIPs with antibodies against the active mark, H3K4me2, and the repressive mark, H3K27me3. Already on day 3, we observed that the *gcnt1* enhancer in T_H1 cells acquired significantly more H3K4me2 marks than the T_H2 cells, compared to naive T cells. This difference was even more pronounced for T_H1 in the day 5 cultured cells. The *gcnt1* enhancer in T_H1 cells had significantly more H3K4me2 marks than T_H2 on both day 3 and day 5. T_H2 cells appeared to have a slower kinetic because H3K4me2 marks on day 5 were significantly greater than that in naive T cells (Figure 6.19 – upper panel). The level of H3K27me3 marks on the *gcnt1* enhancer was significantly lower in T_H1 cells compared to naive T cells already on day 3, and this level remained low on day 5. For T_H2 cells,

H3K27me3 did not significantly differ from that of naive cells on day 3 or day 5. In the day 3 and day 5 T_H2 cells, there were significantly more H3K27me3 than that observed in T_H1 cells (Figure 6.19 – lower panel). These results indicate that *gcnt1* transcription is permissive in *in vitro* generated T_H1 cells, but not in *in vitro* generated T_H2 cells. This is likely controlled at the epigenetic level by H3K4me2 and H3K27me3.

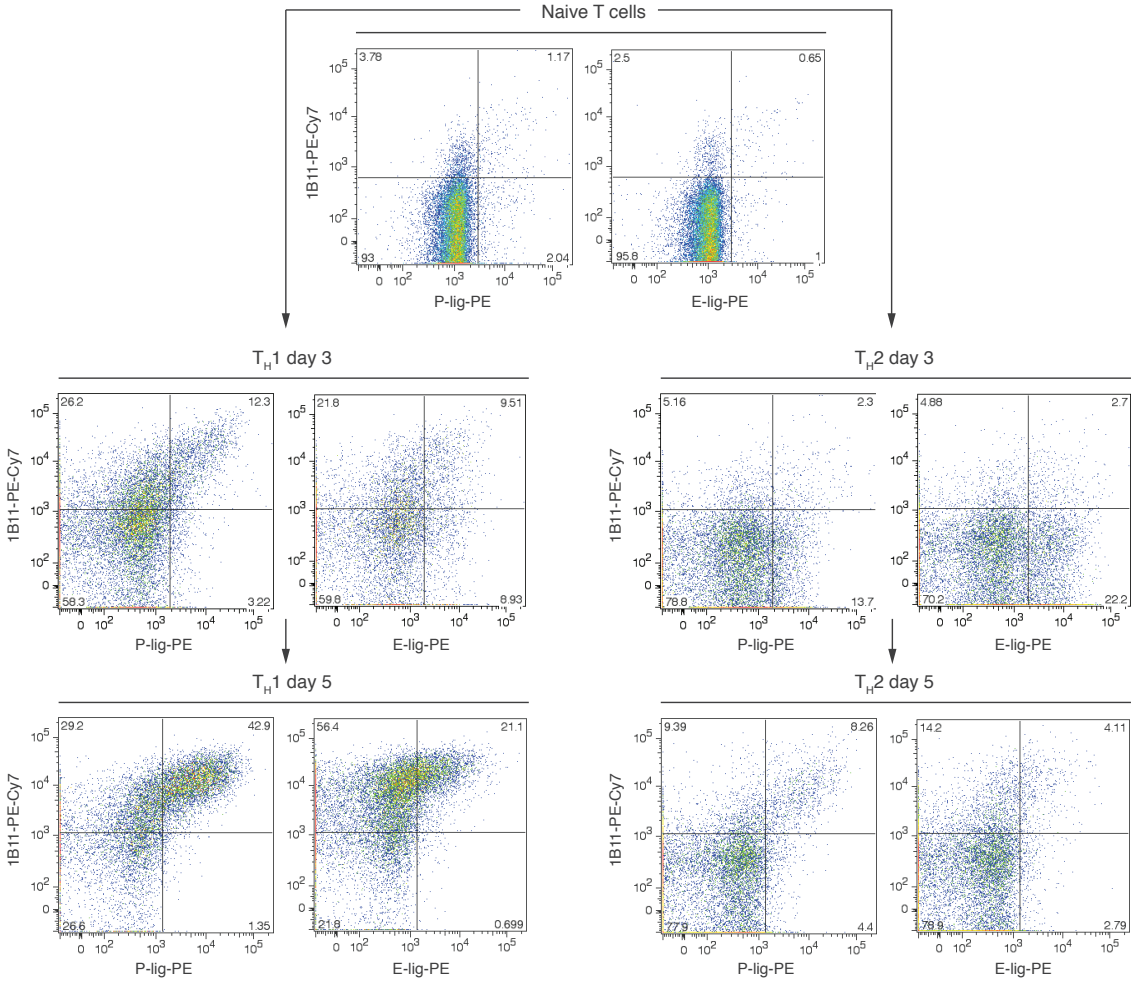

Figure 6.18: Representative dot plots of ligand staining in T_H1 and T_H2 cells. Representative FACS plots of one experiment; all of the experiments are summarized in fig. 6.17. Naive T cells from WT mice were harvested immediately or polarized under T_H1 or T_H2 conditions for 3 or 5 days before harvesting the cells for 1B11, P-lig, and E-lig staining. Cells that were cultured until day 5 were supplemented with IL-12 on day 3.

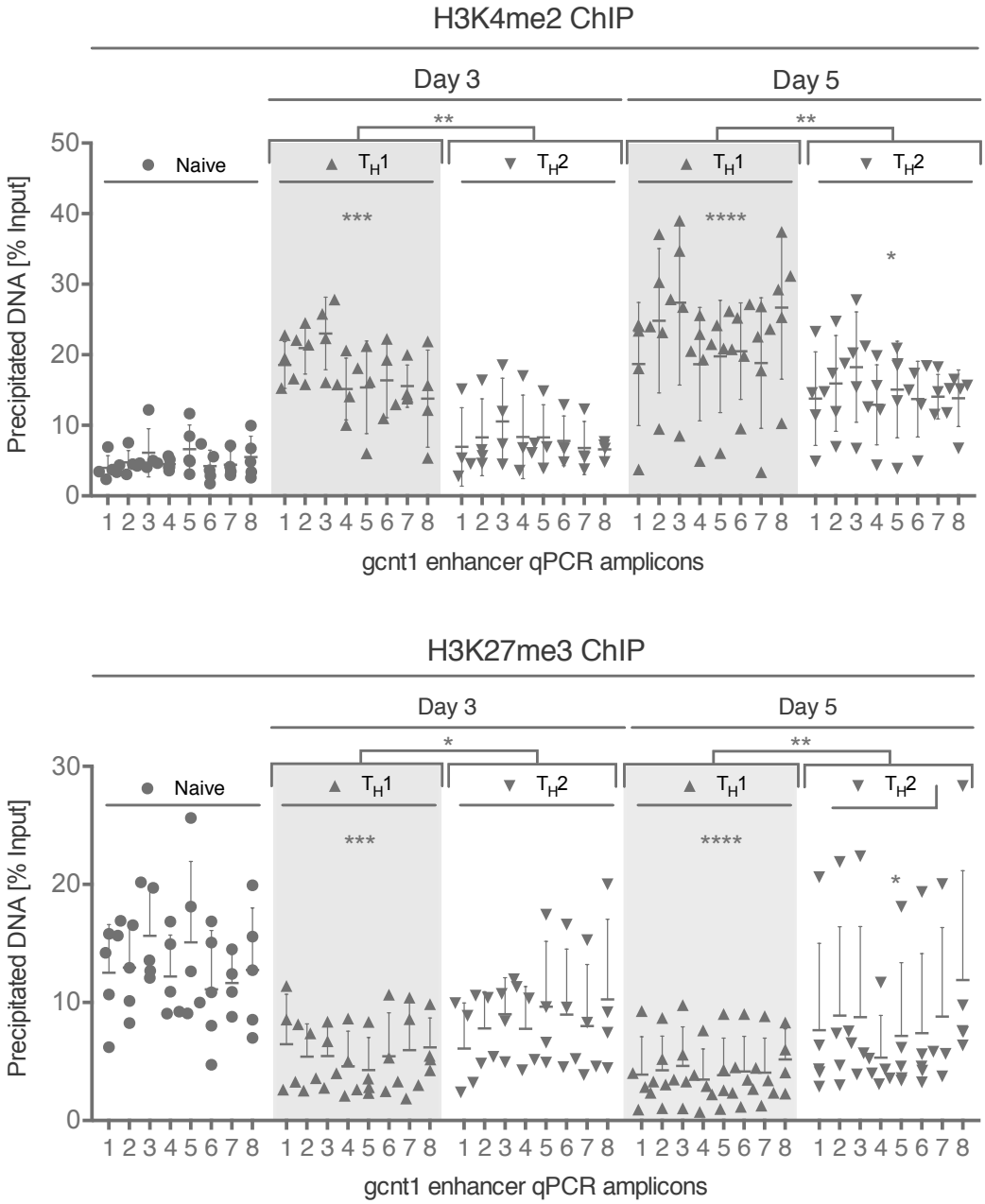

Figure 6.19: Histone methylation of the *gcnt1* enhancer in T_H1 versus T_H2 cells. Naive T cells from WT mice were harvested immediately or polarized under T_H1 or T_H2 conditions for 3 or 5 days before harvesting the cells for histone ChIP. Cells that were cultured until day 5 were supplemented with IL-12 on day 3. *Upper panel* H3K4me2-ChIP; *lower panel* H3K27me3-ChIP. % of input DNA is shown ($n \geq 4$; mean+SD; *$p \leq 0.05$, **$p \leq 0.01$, ***$p \leq 0.001$, ****$p \leq 0.0001$; Wilcoxon matched-pairs signed rank test results shown above, and Kruskal-Wallis with Dunn's Multiple Comparison's test results shown in the graph compared to naive).

6.2.1 Microenvironmental differences between pLN and mLN

As mentioned earlier, there are microenvironmental differences between LNs that play a significant role in the priming/activation of naive T cells to promote tissue-specific recirculation/homing. This most likely developed to promote faster antigen response in the future in the tissue of first antigen encounter, which is mediated by the surviving memory compartment of effector T cells. Two of the most well-characterized lymphoid compartments are the peripheral and mesenteric lymph nodes (pLNs and mLNs). The major differences between these compartments are the availability of RA and IL-4 [52, 110, 111]. RA is predominately generated by DCs in the mLNs. These microenvironmental differences promote seemingly mutually exclusive homing receptor repertoires on T cells after activation: the gut homing receptors $\alpha_4\beta_7$ and CCR9 are induced on T cells primed in the presence of RA, i.e. in the mLNs, whereas the skin- and inflammation-seeking homing receptors E- and P-ligs are upregulated on T cells primed in pLNs lacking RA [32, 6].

RA and IL-4 have both previously been suggested to suppress E-lig [112, 113], however, the effect on Gcnt1 mRNA and P-lig has not been clarified. This prompted us to determine the effect of RA on the regulation of *gcnt1*, *fut7*, and the selectin ligands. To that end, we cultured naive T cells for 4 days under T_H2 polarizing conditions in the presence or absence of RA. We used two ways of RA depletion: either the cells were cultured in cRPMI with the RAR antagonist, LE540, added, or the cells were cultured in serum-free XVIVO media. Subsequently, Gcnt1 and Fut7 mRNA expression was measured.

On day 5 of *in vitro* cultures, a large part of the T cells were dying; therefore prior to this experiment, we changed the experimental setup after determining that the level of P-lig was substantial enough to measure on day 4 instead of day 5. Compared to T_H1 cells, we found no expression of Gcnt1 and some expression of Fut7 mRNA in T_H2 cells cultured in cRPMI (Figure 6.20 – left panel). Induction of both Gcnt1 and Fut7 mRNA was observed in T_H2 cells when RA was inhibited by LE540, although for Gcnt1 this did not reach the level observed in the positive control T_H1 cells cultured in parallel. When we repeated the experiment with T_H2 cells cultured in RA-free medium, XVIVO, we observed a high expression of both Gcnt1 and Fut7 mRNA. This expression was completely abrogated if RA was added to the XVIVO culturing medium (Figure 6.20 – right panel). This clearly indicates a role for RA as a suppressor, in combination with IL-4, of both *gcnt1* and *fut7*, which explains the lack of E- and P-lig on T_H2 cells generated *in vitro*, as most often primary T cells are cultured in cRPMI.

From the results presented earlier, it is clear that IL-4 has suppressive effects on *gcnt1* expression and subsequently 1B11, P-lig, and E-lig in a RA-dominated environment. Reports have suggested that IL-4 is present in abundance in mLNs, but not in pLNs [111].

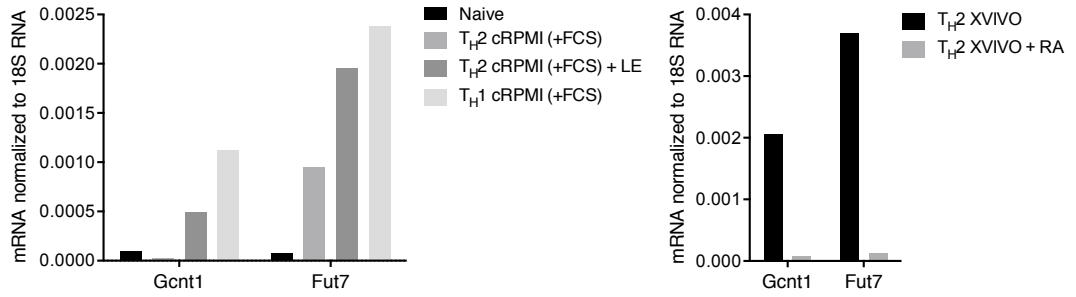

Figure 6.20: RA suppresses Gcnt1 and Fut7 mRNA in T_H2 cells. Naive T cells from WT mice were harvested immediately after naive sort or polarized under T_H1 or T_H2 conditions in the presence or absence of 10 nM RA or 0.5 μM of the RAR antagonist, LE540. The cells were cultured in FCS-containing cRPMI (*left panel*) or RA-free XVIVO medium (*right panel*) (n=1). These experiments were performed together with a master student, Julia Hackbusch.

This could explain why IL-4 producers express less P-lig in mLNs than in pLNs *in vivo*. Therefore, we next asked whether IL-4 is present in higher levels in mLNs than pLNs, hypothesizing that IL-4 could be a cause of the suppressed P-lig levels observed in mLN *in vivo*. This prompted us to determine IL-4 availability and Gcnt1 mRNA levels in the pLNs vs. mLNs. To that end, we performed separate crude isolations of cells from inguinal pLNs and mLNs of four mice, and subjected the cell suspensions to erylysis prior to Il4 and Gcnt1 mRNA analyses. We observed a significantly lower level of Il4 in inguinal pLNs compared to mLNs. In contrast, Gcnt1 mRNA was significantly lower in mLNs compared to pLNs (Figure 6.21). This supports our hypothesis, and the results of others, that IL-4 dominated environments could play a role in the suppression of *gcnt1*, which can be related to a suppression of the skin-and inflammation-seeking homing receptors, E- and P-lig, in the gut.

6.2.2 RA and induction of *gcnt1* and *fut7* in T_H2 cells *in vitro*

To determine the effect of RA on the expression of Gcnt1 and Fut7 mRNA and P-lig *in vitro* in more detail, we polarized T_H1 and T_H2 cells from naive T cells in serum-free medium (XVIVO) for 5 days in the absence or presence of titrated amounts of RA (0.1 nM, 1 nM, 10 nM, or 100 nM). We observed that Fut7 mRNA was suppressed by low levels of RA (1 nM) in both T_H1 and T_H2 cells, whereas Gcnt1 mRNA was only significantly suppressed in T_H2 cells and only in the presence of $\geq$1 nM RA in T_H2 cells (Figure 6.22 – upper panel). The suppression by RA was also evident at the ligand level, where low levels of E-lig, P-lig, and 1B11 were observed in T_H2 cells compared to T_H1 cells, regardless of the presence of RA. In T_H1 cells, only E-lig was suppressed by RA (Figure 6.22 – lower panel), while 1B11 seemed to decrease with added amounts of RA in T_H2 cells.
Low Fut7 mRNA levels is in line with the suppression of E-lig in both T_H1 and T_H2 cells.

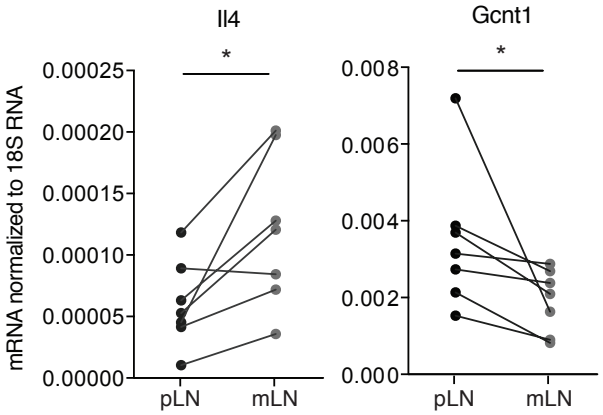

Figure 6.21: pLN have lower Il4 mRNA and greater Gcnt1 mRNA compared to mLN. Levels of Il4 and Gcnt1 mRNA were measured in crude cell isolates from pLN and mLN from separate WT mice. Lines connect measurements from one mouse (n=7; *p<0.05; Wilcoxon matched-pairs signed rank test). These experiments were performed together with a master student, Julia Hackbusch.

Remarkably, in the absence of RA, T_H2 cells displayed an overall lower baseline of the homing receptors compared to T_H1 cells, even though the enzymes responsible for their synthesis are available at the same levels in both cell subsets. This suggests a possible slower kinetics of 1B11, P-lig, and E-lig synthesis in T_H2 cells. Altogether, these results suggest that IL-4 can drive the induction of Gcnt1, but only in the absence of RA. These results clearly show that low doses of RA have suppressive effects on Gcnt1 and Fut7 expression, particularly in T_H2 cells.

6.2.3 Mechanism underlying RA suppression of Gcnt1 and Fut7 mRNA

6.2.3.1 RAR and RXR isotype expression

We have shown that RA suppresses Gcnt1 and Fut7 mRNA as well as E- and P-lig induction in T_H2 cells, but the mechanism of this suppression is unknown. This prompted us to investigate whether RA regulates RAR/RXR isotype expression during T_H2 differentiation, as a potential mechanism of Gcnt1 and Fut7 mRNA suppression. To that end, we measured the expression levels of the known RAR and RXR isotypes in T_H2 cells cultured in the absence or presence of titrated amounts of RA (0, 0.1, 1, 10, 100 nM). The mRNA levels of all isotypes were determined in naive T cells and in T_H2 cells cultured until day 3 or 5.

The results show that RARβ and RXRγ are not expressed in naive and T_H2 cells (data not shown), as has been shown by others previously [114]. Despite considerable variability in the values measured on day 5, it became apparent that RARα was the most expressed in naive T cells and in T_H2 day 5 cells. Remarkably, during the TCR stimulation pe-

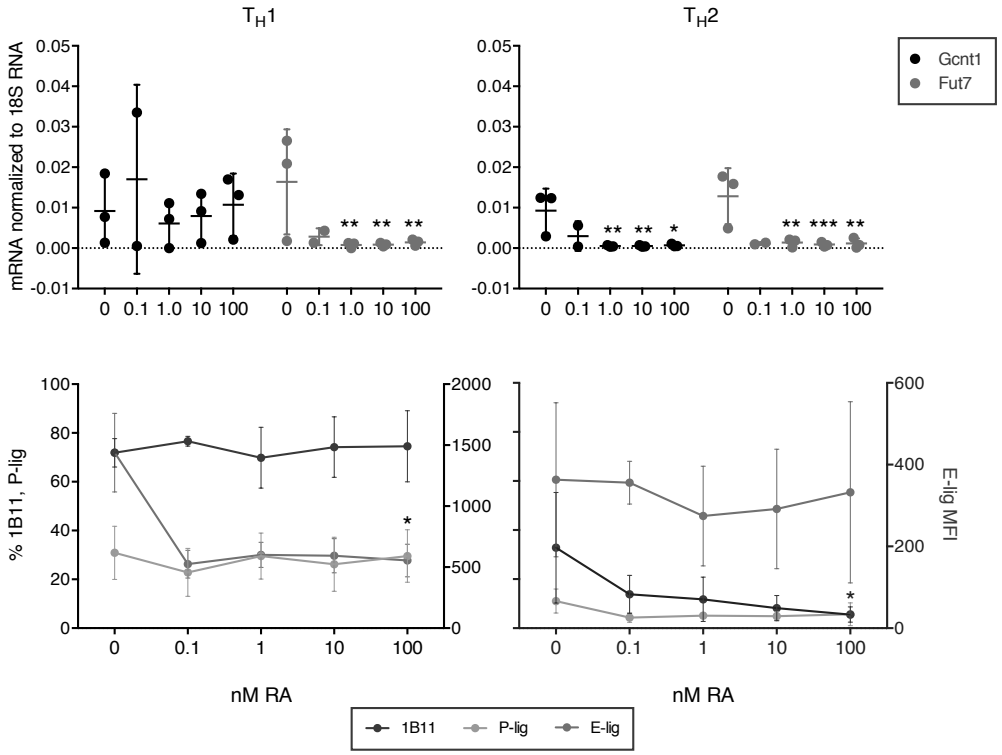

Figure 6.22: RA suppresses expression of Gcnt1 and Fut7 mRNA in a dose-dependent manner. Naive T cells from WT mice were polarized under T_H1 or T_H2 conditions for 5 days in XVIVO media with titrated amounts of RA added. *Upper panel* Gcnt1 and Fut7 mRNA in T_H1 (left) and T_H2 (right) cells. *Lower panel* 1B11, P-lig, and E-lig in T_H1 (left) and T_H2 (right) cells. (n=2 for [RA]=0.1 nM; n=3 for [RA]=0, 1, 10, 100 nM; *p<0.05 for E-lig in T_H1 and 1B11 in T_H2; Mean±SD; 2way RM-ANOVA with Sidak multiple comparisons test results shown between [RA]=0, 1, 10, 100). These experiments were performed together with a master student, Julia Hackbusch.

riod, the level of RARα decreased dramatically (Figure 6.23). Like RARα, RARγ was expressed in naive T cells, but its levels dropped during TCR stimulus, only to increase again on day 5 in the absence of RA. RXRα was the lowest expressed RXR isoform, which increased in expression in the absence of RA during T_H2 differentiation. In the presence of RA, RXRα remained at naive levels during T_H2 differentiation. The levels of RXRβ exhibited a similar expression pattern to RARα, where initially, expression was high in naive T cells, which reduced only during TCR stimulation, after which it increased expression above naive levels. Remarkably, for RARα and RXRβ, the dose of RA was not a regulating factor in their expression, indicating that another factor or mechanism is involved in the suppressive mechanism of RA on *gcnt1* transcription. However, this experiment does highlight that the suppressive mechanism of RA on Gcnt1 mRNA and P-lig expression might proceed through RARα:RXRβ heterodimers or homodimers. These nuclear receptors do not appear to be regulated by the dose of RA, however, by the TCR stimulus. RXRα, as the only nuclear receptor isoform appeared to be suppressed by 1 nM

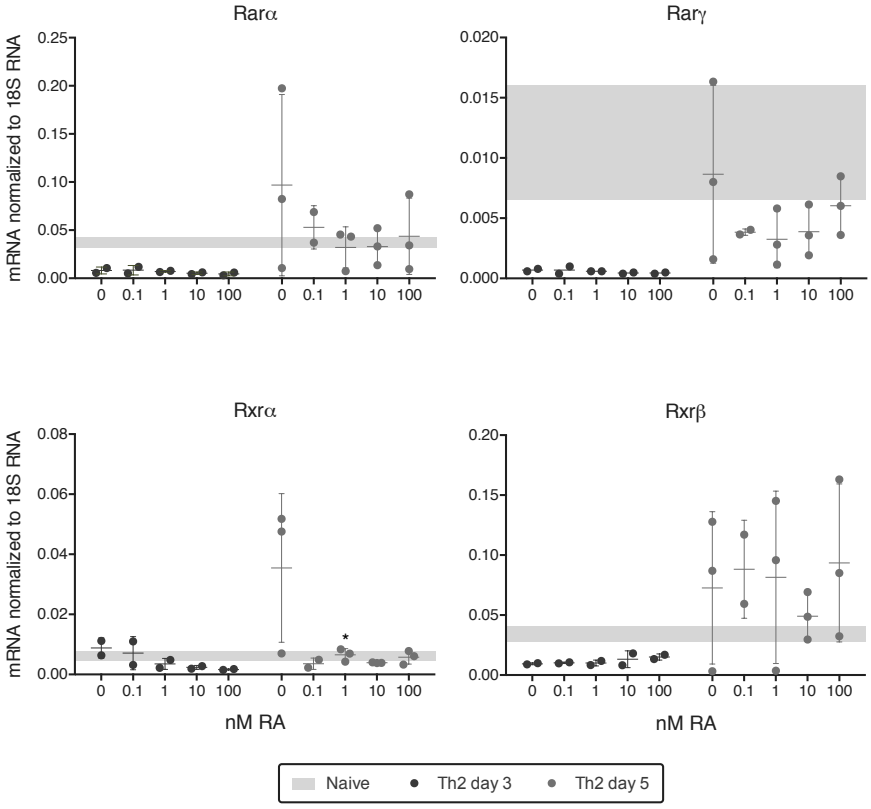

Figure 6.23: RA and the expression of RAR and RXR isoforms in T_H2 cells. Naive T cells from WT mice were either harvested immediately or polarized under T_H2 conditions for 3 or 5 days in XVIVO media with titrated amounts of RA added. *Upper panel* RAR isoform mRNA levels; RARβ was undetected and therefore not shown. *Lower panel* RXR isoform mRNA levels; RARγ was undetected and therefore not shown (day 3 and day 5 0.1 nM: n=2; day 0 and day 5 0, 1, 10, 100 nM: n=3; Mean±SD; *$p<0.05$; Friedman test with Dunn's Multiple Comparisons test of day 5: 1, 10, and 100 nM compared to 0 nM shown.). These experiments were performed together with a master student, Aneta Ziolkowska.

RA, which could also be a reason for the suppressive effect of RA on Gcnt1 mRNA and P-lig expression.

6.2.3.2 RAR and RXR agonists and expression of homing receptors

To verify the contribution of the RAR and RXR receptors on the suppression of *gcnt1* and P-lig, we performed experiments where we cultured T_H2 cells in the presence of the RARα specific agonist, AM80, and the pan-RXR agonist, HX630, as well as a combination of these. One study has reported that RAR and RXR isoforms promote induction of the gut homing receptor α4β7, and that treatment with both a RAR and a RXR agonist simultaneously has a synergistic inducing effect. This implicated both RAR and RXR isoforms in the regulation of gut homing [112]. Despite their report that suppressive effects on E-lig were similar under RAR agonist or RXR agonist treatment compared to

treatment with both, we wanted to clarify the effect of RAR and RXR agonist treatment on Gcnt1 and Fut7 mRNA during T_H2 cell differentiation. As a control, we measured the levels of Itga4 and Ccr9 because these are upregulated in the presence of RA. We polarized naive T cells under T_H2 conditions in serum-free media until day 5 of culture with the agonists added at 10 nM or 100 nM. In the groups where both a RAR agonist and HX630 are added, they were added at 10 nM each.

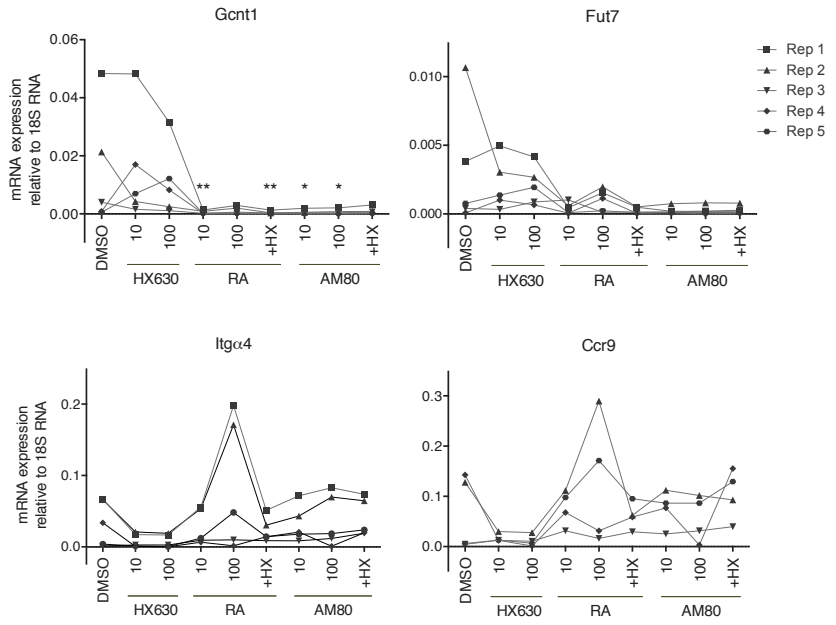

Figure 6.24: RAR and RXR agonists and expression of Gcnt1, Fut7, Itga4, and Ccr9 mRNA in T_H2 cells. Naive T cells from WT mice were polarized under T_H1 or T_H2 conditions for 5 days in XVIVO media with either the RAR agonists RA or AM80 (10 or 100 nM), or the RXR agonist HX630 (10 nM), or a combination of RAR agonist and HX630 (10 nM each) added, after which cells were harvested for mRNA analysis. Naive and DMSO-treated cells were used as controls. *Upper panel* Gcnt1 and Fut7 mRNA responsible for skin- and inflammation-seeking homing receptors. *Lower panel* Gut homing receptors Itga4 and Ccr9 mRNA. (n=5; Mean±SD; Friedman test with Dunn's Multiple Comparisons test results compared to DMSO shown). These experiments were performed together with a master student, Aneta Ziolkowska.

The results showed that the RAR agonists suppressed Gcnt1 and Fut7 mRNA completely, while the pan-RXR agonist was not able to suppress Gcnt1 or Fut7 transcription compared to the DMSO control. Therefore, when given simultaneously, the suppressive effects of RA and the RAR agonist AM80 did not have a synergistic effect with the RXR agonist HX630 (Figure 6.24 – upper panel). Because FucT-VII is largely responsible for the induction of E-selectin ligand, these results contradict those of Takeuchi et al. (2011) where they used another pan-RXR agonist, PA024, and observed a decrease in E-lig induction compared to the control.

As expected, both Itga4 and Ccr9 were induced by RAR agonist treatment, however, not by RXR agonist treatment alone (Figure 6.24 – lower panel). The combination of a RAR agonist and HX630 treatment did not lead to a synergistic effect on the induction of Itga4 and Ccr9. This is in contrast to that observed by Takeuchi et al. where a synergistic inductive effect is reported for CCR9. These results support our hypothesis that the suppressive effects of RA proceed only through RAR nuclear isoforms and specifically through the RARα isoform.

6.2.3.3 Gcnt1 transcript expression in T_H1 cells versus T_H2 cells

Previously, our lab has shown that one Gcnt1 mRNA transcript variant dominates in P-lig$^+$ T_H1 and effector/memory T cells. It was unclear whether the suppression of Gcnt1 mRNA in T_H2 cells by RA could be due to an alternative transcript being used in T_H2 cells. This prompted us to determine the level of the different transcripts in T_H2 cells cultured in the absence and presence of RA. We looked for three transcripts that had been described using RACE-PCR studies by a previous PhD student in the lab, Micha Schröter. The first of these transcripts consists of the known exons 1, 2, and 3, E1E2E3. The second transcript begins at a newly identified exon between exon 1 and 2 called "E1.1", and also contains exons 2 and 3, E1.1E2E3. The final transcript includes another newly identified exon, located immediately upstream of the largest exon 3, E3.1. Earlier, it was found that the transcript consisting of the classical exons, E1E2E3, dominated in T_H1 cells and in P-lig$^+$ memory T cells (CD4$^+$CD45RB^{low}P-lig$^+\alpha_4\beta_7{}^-$). However, because all transcripts contain the protein coding sequence present in exon 3, all transcripts can theoretically translate into a Core 2 branching enzyme with a functional catalytic domain.

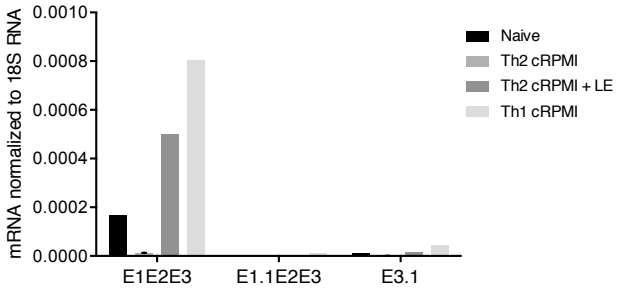

Figure 6.25: Gcnt1 transcript expression in T_H2 cells.

Naive T cells from WT mice were harvested immediately or polarized under T_H1 or T_H2 conditions for 4 days before harvesting the cells for transcript analysis. T_H1 cells were cultured in cRPMI medium, whereas T_H2 cells were cultured in cRPMI medium or cRPMI medium with the RAR antagonist, LE540, added (n=1). These experiments were performed together with a master student, Julia Hackbusch.

We cultured T_H2 cells in serum-free media, XVIVO, and in normal cRPMI media supplemented with FCS, thus containing RA, with or without the RAR antagonist LE540 added

to the culture. We used T_H1 as a positive control and naive T cells as a negative control for E1E2E3 expression. We found that T_H2 cells cultured in the absence of RA express high levels of E1E2E3 and not any of the other Gcnt1 mRNA transcripts (Figure 6.25). Most notably, all transcripts were absent in T_H2 cells cultured in the presence of RA. Despite the lacking repetitions of this experiment, it clearly demonstrates that the Gcnt1 mRNA transcript isoform is the same in T_H1 cells and T_H2 cells cultured without RA, and that in the presence of RA, T_H2 cells are unable to produce Gcnt1 transcripts.

6.2.3.4 *gcnt1* promoter and enhancer activity in T_H2 cells

Because the Gcnt1 transcript appeared to be the same in both T_H1 and T_H2 cells, we next tested the activity of the regulatory regions identified in T_H1 cells, in T_H1 and T_H2 cells cultured in the presence of RA or the RAR antagonist, LE540. The results show that the promoter construct has similar activity (notice the Y-axis scale) in both T_H1 and T_H2 cells. The LE540-treated samples appear to have higher activity of the promoter construct in both T_H1 and T_H2 cells. Although this is not significant, it could suggest that RA suppresses the activity of the promoter. As expected, in both RA- and LE540-treated cells, the promoter+enhancer construct has higher activity in T_H1 cells than the promoter construct. In remarkable contrast, regardless of RA or LE540 treatment, the promoter+enhancer construct has lower activity than the promoter construct in T_H2 cells. This suggests that either the "enhancer" has a silencing effect in T_H2 cells, or that an additional region, required to promote transcription, is not present in the reporter construct.

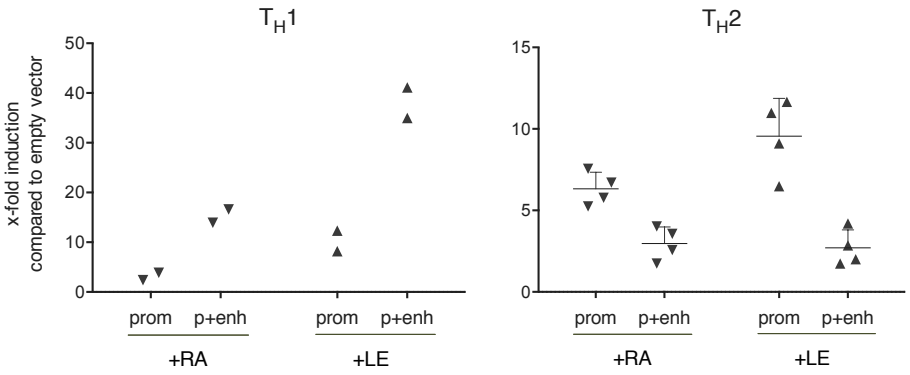

Figure 6.26: *gcnt1* enhancer activity in T_H1 and T_H2 cells.
Naive T cells from WT mice were polarized under T_H1 or T_H2 conditions, treated either with RA or LE540, and transfected with the indicated constructs, after which luciferase assays were performed (n=2 for T_H1, n=4 for T_H2, mean+SD).

6.2.3.5 TF and nuclear receptor binding sites within the *gcnt1* promoter and enhancer

The reporter assays in RA- and LE540-treated T_H1 and T_H2 cells suggested that the promoter might be affected by RA signaling. This prompted the search of RAR and RXR binding sites as well as T_H2-specific TF binding sites to elucidate the mechanism of IL-4-mediated RA suppression of *gcnt1*. We searched for binding motifs in the promoter and enhancer using MatInspector and Promo software. A depiction of the results can be seen in Figure 6.27. Although there are no RARα binding sites within the promoter, there are two binding sites predicted within the enhancer. These binding sites are flanked by NFAT and GATA3 binding sites, and proximal to a predicted STAT6 binding site where proven STAT6 binding has been shown by STAT6 ChIP-seq data performed by others [102]. Taken together, the transcription factor binding search does not suggest a direct effect of RA on the promoter (see fig. 6.26).

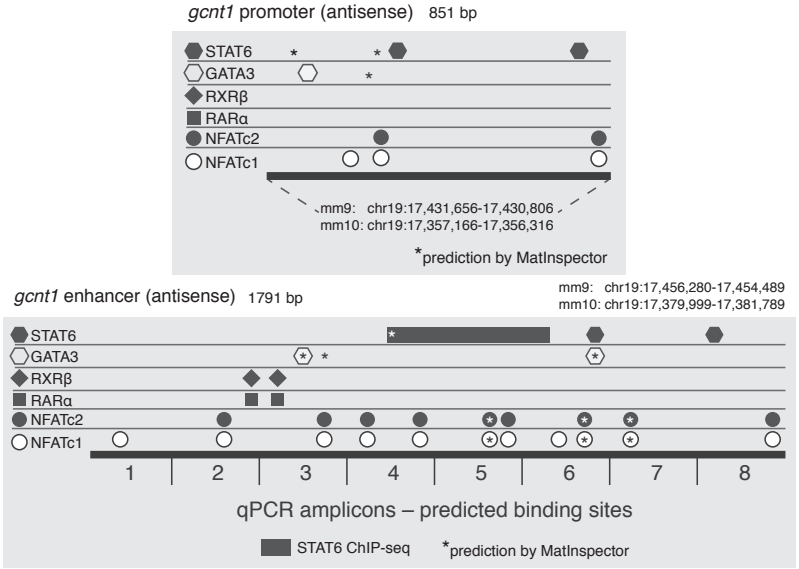

Figure 6.27: Predicted TF motifs and binding within the *gcnt1* promoter and enhancer. Binding motifs were predicted using MatInspector [97] and PROMO [98]. Symbols indicate binding predicted by Promo, and * indicate prediction by MatInspector. Prediction by both software is shown by a symbol and a star in the opposite color. The location of STAT6 binding from reanalyzed ChIP-seq datasets performed on T_H2 cells cultured in cRPMI [102] is shown.

7. Discussion

Until recently, based on *in vitro* experiments, P-lig expression was thought to be restricted to the T_H1 lineage [51]. Since the discovery that P-lig is expressed on both T_H1 and T_H2 cells *in vivo*, the regulatory mechanism underlying this discrepancy has been investigated. For murine T cells, C2-GlcNAcT-I and FucT-VII are implicated as the rate-limiting enzymes in the generation of P-lig and E-lig epitopes because these are upregulated during TCR activation and differentiation.

To come closer to an understanding of the lack of P-lig expression in *in vitro* generated T_H2 cells and its expression in *in vitro* generated T_H1 cells, our first aim was to understand the molecular gene regulation of the enzymes crucial for P-lig expression, *gcnt1* and *fut7*, in T_H1 cells generated *in vitro*. Our second aim was to apply the knowledge we gained studying T_H1 cells to investigate mechanisms behind the discrepancy in *gcnt1*, *fut7*, and P-lig expression between T_H1 and T_H2 cells generated *in vitro* to explain the *in vivo* findings.

7.1 Molecular regulation of *gcnt1* in T_H1 cells

Two regulatory regions on the *gcnt1* gene locus were found by a previous PhD student in the lab, Micha Schröter, which laid the foundation for the work herein on the molecular regulation of *gcnt1*. Firstly, a polarization-independent promoter was found to have reporter activity in T_H0, T_H1, and T_H2 cells generated *in vitro*. Secondly, preliminary data revealed a distal regulatory region with differential histone modifications by mapping H3K4me2 (active) and H3K27me3 (repressive) marks across the gcnt1 gene locus, that could explain the induction of *gcnt1* and lack thereof in P-lig$^+$ and P-lig$^-$ T cells, respectively [68]. Notably, the presence of the repressive mark H3K27me3 at this site in P-lig$^-$ cells seemed to correlate with a lack of *gcnt1* transcription. This was supported by a similar strong repressive H3K27me3 peak in naive T cells, consistent with low *gcnt1* transcription in these cells as well.

We verified the pattern of histone modifications across the newly identified region de-

scribed earlier using histone-ChIP-qPCR with qPCR amplicons covering the distal region. In addition, we followed the changes over time as the cells were activated from naive to day 3 T_H1 cells and after expansion from day 3 to day 5 T_H1 cells. Consistent with the preliminary data, we found a steady increase in the active mark, H3K4me2, as T_H1 differentiation progressed, irrespective of P-lig status. As expected, the repressive mark was absent in P-lig$^+$ T_H1 cells. P-lig$^-$ T_H1 cells, as well as the naive T cells from which they differentiated, were, however, clearly marked by H3K27me3 in the region (Figure 7.1).

Taken together, *gcnt1* transcription in P-lig$^+$ T_H1 cells correlated with an absence of the H3K27me3 mark at the distal region, rather than with the coexisting active mark H3K4me2 that was upregulated during and after TCR activation.

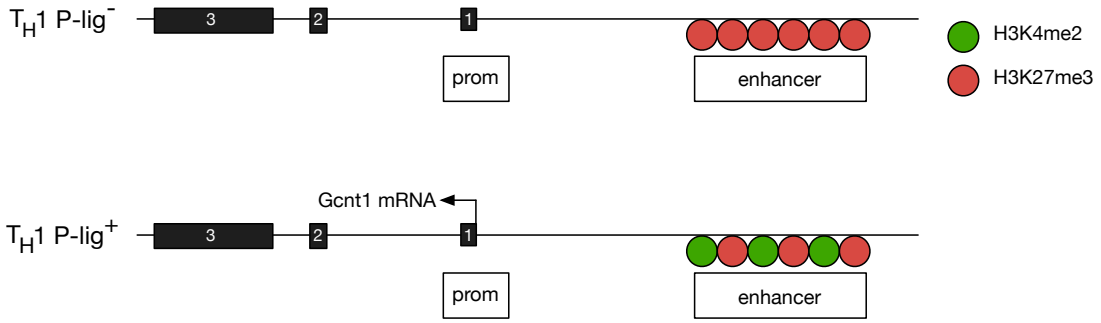

Figure 7.1: Histone methylation of the *gcnt1* enhancer in P-lig$^+$ and P-lig$^-$ T_H1 cells. Schematic of the *gcnt1* locus with the enhancer and promoter, prom, indicated. *Upper panel* shows that the histone modifications on the enhancer in P-lig$^-$ T_H1 cells are dominated by the repressive mark, H3K27me3. Gcnt1 transcription is not seen in these cells. *Lower panel* shows the histone modifications on the enhancer in P-lig$^+$ T_H1 cells. Both the active mark, H3K4me2, and the repressive mark, H3K27me3, decorate the enhancer in these cells, which also transcribe Gcnt1 mRNA.

Although the rationale for the heterogeneity in P-lig induction and *gcnt1* expression in T cells cultured under similar conditions is enigmatic, it seems to be fixed by the histone modification pattern and in particular during the expansion phase as our results reveal for *gcnt1*. Effector T cells arising from identical cultures also differ in effector cytokine production, a phenomenon that has been attributed to differences in expression of master transcription factors, such as T-bet or GATA-3 [115, 116, 117], however, it may also be highly dependent on the activation of STATs by cytokines through the JAK/STAT pathway [108, 102].

Further characterization of the distal region (henceforth referred to as enhancer) using reporter assays revealed enhancer activity selectively under T_H1 conditions [53] that was not influenced by a flanking homologous region.

IL-12 is crucial for differentiation of T cells into effector T_H1 cells and has been shown to promote P-lig and Gcnt1 mRNA expression as well [72, 71, 118]. Consistent with the IL-12-dependent enhancer activity of the *gcnt1* enhancer, we show that STAT4 is required for enhancer activity, with reporter assays performed in *stat4*$^{-/-}$ *in vitro* generated T_H1 cells. Similarly, the master transcriptional regulator for T_H1 cells, T-bet, has been shown by others to induce expression of Gcnt1 and P-lig [73, 74, 76], which is discussed later again.

In line with the trans-activating function of STAT4 for the expression of *gcnt1*, day 5 *in vitro* generated *stat4*$^{-/-}$ T_H1 cells expressed significantly less Gcnt1 mRNA and P-lig, compared to WT T_H1 cells – a difference that was not evident on day 3 (data not shown). These results implicated STAT4 in the induction of *gcnt1* transcription. To mimic physiological conditions, where IL-12 is no longer present during the expansion phase [13], we cultured *in vitro* generated T_H1 cells without further addition of IL-12 and IFNγ during the expansion phase from day 3 to day 5 and performed STAT4-ChIP on day 1, 3, and 5 to get an impression of the binding kinetics of STAT4 to the region over time. STAT4 binds to amplicon 4 in T_H1 cells and its binding peaks on day 3 of culture. If the cells were supplemented with additional IL-12 and IFNγ during the expansion phase, STAT4 binding increased dramatically (data not shown). Taken together, these results indicate an initial direct control of this enhancer by STAT4 in T_H1 cells, which maintained control of the enhancer as long as IL-12 is present.

As mentioned before, the removal of the repressive mark seems to be a prerequisite for transcription because the presence of the repressive H3K27me3 mark, even concomitant with an active H3K4me2 mark, as seen in P-lig$^-$ T_H1 cells, was associated with transcriptional repression of *gcnt1*. We have previously reported that P-lig$^+$ $T_{eff/mem}$ cells isolated *ex vivo* express significantly more Gcnt1 mRNA than their P-lig$^-$ counterparts [68]. Taken together, it may be speculated that STAT4 plays a pivotal role in promoting initial transcription of *gcnt1* through recruitment of chromatin modifiers, which can initiate opening of the chromatin on the *gcnt1* enhancer.

Reanalyzing publically available ChIP-seq data showed that p300 binds to the enhancer in WT T_H1 cells but not in *stat4*$^{-/-}$ T_H1 cells. Although p300 did not bind to the same level as in WT cells, it still bound the *gcnt1* enhancer in *tbx21*$^{-/-}$ T_H1 cells. This could indicate that STAT4 plays a role in triggering the induction of an epigenetically permissive locus state that results in the accessibility to other factors such as T-bet, the master transcriptional regulator of T_H1 cells. Supporting this hypothesis, reanalysis of another publically available ChIP-seq dataset revealed four DNAse hypersensitive sites, of which two have been identified in our group as regulatory regions of *gcnt1* that open during

the polarization of naive T cells into T_H1 cells. In addition, deposition of the histone methylation marker for enhancers, H3K4me3, on our identified enhancer, and the mark for active transcription, H3K36me3, on the CDS, was clearly visible. These two histone marks were not present in *stat4*$^{-/-}$ T_H1 cells, whereas H3K4me3 marks were present on the locus in *tbx21*$^{-/-}$ T_H1 cells. This is not in line with our unpublished histone ChIP experiments where we observed an upregulation of the active mark H3K4me2, which is similar to H3K4me3, in both Th0 and *stat4*$^{-/-}$ T_H1 cells comparable to the levels observed in WT T_H1 cells. We found that cells lacking IL-12 signaling, such as in Th0 and *stat4*$^{-/-}$ T_H1 cells, were rather marked by higher H3K27me3 levels than in WT T_H1 cells. This means that while the ChIP-seq data supports the hypothesis that STAT4 is involved in the deposition of H3K4me3, our data rather suggests that STAT4 is involved in the removal of H3K27me3. This could, however, also be due to lower T-bet levels in *stat4*$^{-/-}$ cells [72]. From the ChIP-seq data, it appears that T-bet is required to trigger transcription as evident from lack of H3K36me in T-bet-deficient T_H1 cells, which was also suggested by others [15]. This is in line with the lack of transcription in both STAT4- and T-bet-deficient T_H1 cells, further supporting the hypothesis that both of these factors play a role in making the locus accessible for transcription, but STAT4 potentially playing an earlier role together with p300.

In line with the notion that both STAT4 and T-bet are important in the control of *gcnt1* expression, a report by Thieu et al. (2008) revealed that commitment to the T_H1 fate not only involves T-bet as the main transcriptional regulator, but also requires STAT4-dependent gene regulation. The transcripts analyzed in that study were regulated solely by STAT4 or T-bet, or by both factors. Moreover, it was shown that both STAT4 and T-bet played a role as chromatin modifiers during the T_H1 polarization period, with STAT4 and T-bet both being able to recruit transcriptional modifiers that lead to hyperacetylation and H3K4 methylation, and the absence of STAT4 and T-bet being associated with the presence of repressive H3K27me3 marks [15]. Corroborating the importance of STAT4 and T-bet in the regulation of selectin ligand expression, it has previously been shown that STAT4- [72] and T-bet- [73, 74] deficient T_H1 cells lack the ability to roll on P-selectin *in vitro* and correlate with a lack of 1B11 and P-lig expression. This is further substantiated by a recent report that shows T-bet as an important factor in the homing of T cells to secondary sites after *Toxoplasma gondii* infection [119]. To determine if T-bet was directly involved in regulating *gcnt1* and P-lig expression during T_H1 lineage commitment, we performed T-bet-ChIP. We determined that T-bet binds to amplicon 4 in the *gcnt1* enhancer on day 3 of a T_H1 culture, but that this binding, unlike that of STAT4, does not decrease on day 5 of culture – implicating T-bet in regulation/maintenance of *gcnt1* expression in T_H1 cells during the expansion phase (Figure 7.2).

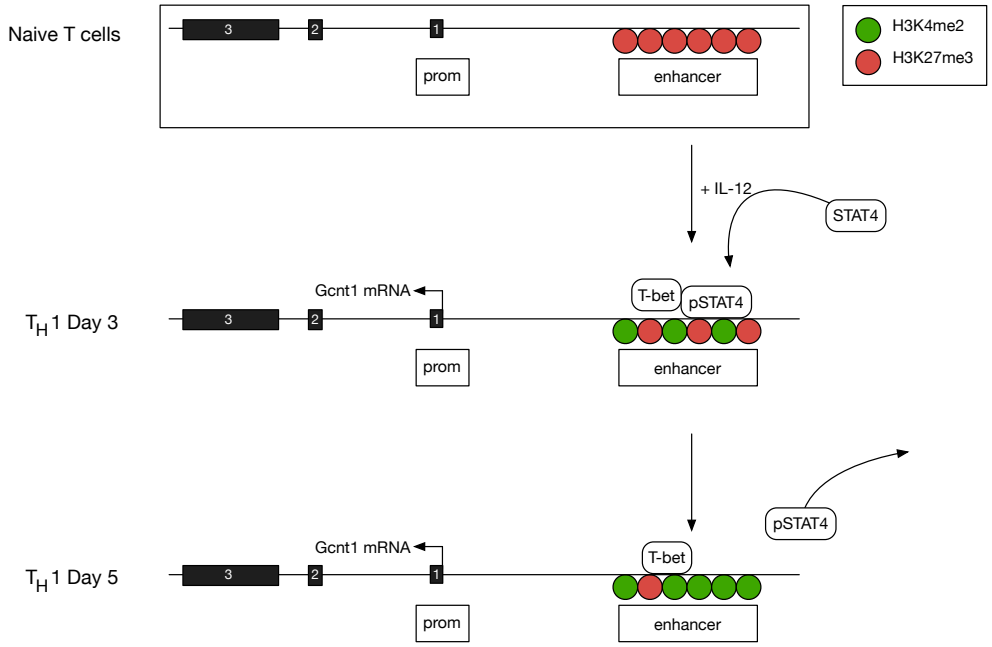

Figure 7.2: STAT4 and T-bet binding to the *gcnt1* enhancer in T_H1 cells. Schematic of the *gcnt1* locus with the enhancer and promoter indicated. *Upper panel* shows the histone modifications on the enhancer in naive T_H1 cells dominated by the repressive mark, H3K27me3. Gcnt1 transcription is not seen in these cells. *Middle panel* shows the histone modifications and binding of STAT4 and T-bet to the enhancer in *in vitro* generated day 3 T_H1 cells. *Middle panel* shows the histone modifications and binding of T-bet to the enhancer in *in vitro* generated day 5 T_H1 cells.

In conclusion, our data suggests a complex interplay of TCR signals [68], polarization-specific transcription factors STAT4 and T-bet, and remodeling of the histone modifications in the initiation of *gcnt1* transcription and P-lig induction during T_H1 differentiation. The correlation of *gcnt1* repression with the presence of the repressive histone mark, H3K27me3, at the herein identified distal enhancer, provides the first direct evidence for the epigenetic control of *gcnt1*, that we have previously postulated controls long-term expression of the pro-inflammatory homing receptor P-lig in memory $CD4^+$ T cells [2].

7.2 Molecular regulation of *fut7* in T_H1 cells

In contrast to *gcnt1*, expression of *fut7* is not regulated epigenetically by histone modifications in T cells, but rather by DNA methylation. Using locus-wide bisulfite sequencing, Matthias Pink and Boris Ratsch, former PhD students in our group, showed that an intragenic differentially methylated region (DMR), beginning at exon 2 and ending after exon 4, correlated with expression of P-lig in CD4+ T cells – dominated by expression of shorter Fut7 transcripts starting at exon 4 [120]. *ex vivo* isolated P-lig^+ $CD4^+$ T cells were demethylated within this region, whereas P-lig^- $CD4^+$ T cells were methylated,

which correlated with expression of *fut7* and lack thereof, respectively. Furthermore, they showed that this region was also methylated in naive T cells and stays methylated if the cells are activated in the presence of RA, in line with the lack of FucT-VII and E-lig in $CD4^+$ T cells that are primed in the gut.

The intragenic differentially methylated region (DMR) (henceforth referred to as the minimal promoter 1_v2) they described, showed activity in a reporter assay when using a CpG-containing pGL3-basic plasmid. Due to the significant differential methylation of this region in different T cell subsets, we questioned whether methylation within this region affects activity in reporter assays. The CNS (*fut7* enhancer) and minimal promoter 1_v2 were therefore transferred to a CpG-free plasmid. The CNS region has enhancing activity that has already been described [75], and is distinct in its regulation from the minimal promoter 1_v2 because it is demethylated in both P-lig^+ and P-lig^- T_H1 cells. As a consequence, methylating the entire CpG-free plasmid, including the CNS and the minimal promoter 1_v2, made it unclear whether activity would be affected by methylation of the CNS or the minimal promoter 1_v2, or both. Therefore, we had to confirm the methylation dependency of the minimal promoter 1_v2 by enzymatically cutting out the minimal promoter 1_v2 of the reporter plasmid to perform selective *in vitro* methylation of this region prior to religation with the backbone vector again before performing the reporter assay. This technique requires a lot of plasmid material and ligation without transformation into competent bacteria. This means that not all insert and backbone religate and this also explains the reduction in reporter activity compared to the untreated plasmid which has not been digested and religated (data not shown). The results showed reporter activity of the unmethylated minimal promoter 1_v2, which was reduced 10-fold upon selective *in vitro* methylation of the minimal promoter 1_v2. In conclusion, the reduction in reporter activity by *in vitro* methylation supports the hypothesis that DNA methylation within the minimal promoter 1_v2 plays a role in the regulation of *fut7*.

Within the minimal promoter 1_v2, a CRE site was found covering the CpG 844 that was most differentially methylated in P-lig^+ and P-lig^- T cells in the bisulfite sequencing experiment mentioned earlier. Moreover, this CpG showed the strongest difference in methylation upon *in vitro* T cell activation and differentiation. For example, T_H1 cells cultured in the absence of RA showed 20% methylation at this CpG compared to 80-90 % methylation in naive T cells and *in vitro* generated T_H1 cells cultured in the presence of RA. This indicated a role for CREB, a methylation sensitive protein in mouse and human [121, 122], in trans-activation of *fut7* when this region is demethylated – as it is in P-lig^+ T cells. This is supported by previous reports implicating CREB in driving constitutive Tax-dependent Fut7 induction in human T cell leukemia caused by the human T-cell leukemia virus-1 (HTLV-1) [109, 123]. A preliminary CREB-ChIP showed direct binding

of CREB to the minimal promoter 1_v2 in the absence of RA, i.e., on the demethylated locus – reinforcing the importance of CREB methylation-dependent CREB binding (data not shown). To confirm the preliminary ChIP-data, we mutated or deleted the CREB site in non-methylated reporter constructs. The deletion mutant exhibited significant reduction in activity of the minimal promoter 1_v2 in subsequent reporter assays. Taken together, this implicates the CRE site in the control of Fut7 transcription in murine T cells and suggests an inverse correlation between DNA methylation and transcriptional activity by most likely CREB binding to the CRE site.

Apart from the differences in epigenetic regulation of *gcnt1* and *fut7*, expression of both enzymes is controlled by different polarizing cytokines. While Gcnt1 is induced by IL-12, expression of Fut7 is promoted by IL-2 [72, 75, 53]. IL-2 signaling proceeds through STAT5, and preliminary data from our group show that STAT5 binds to the minimal promoter 1_v2 of *fut7* [75]. We showed that STAT5 enhances activity of the unmethylated *fut7* CNS+minimal_promoter_v2 construct, which was abolished by a STAT5 inhibitor. Furthermore, mutagenesis of the STAT5 binding motif within the minimal promoter 1_v2 led to a similar reduction in reporter activity. This clearly establishes a role for STAT5 in the induction of *fut7*. In our group, we have shown that STAT5 binds less to the *fut7* locus in RA-treated T_H1 cells than LE540-treated T_H1 cells. Interestingly, the gut homing receptor, Itga4 is regulated in a reciprocal manner, where RA induces its expression and IL-2 (via STAT5) inhibits it [124].

As differentiation in the presence of RA is correlated with maintenance of DNA methylation within the minimal promoter 1_v2 and a lack of *fut7* expression, it might be speculated that STAT5 binding is inhibited by DNA methylation around its binding site. However, the STAT5 binding site is located between two CpGs that are differentially regulated by methylation, making it more likely that STAT5 is sterically hindered from binding, either by RA or factors recruited to the DNA, such as DNA methylation maintenance proteins such as DNMT1 [75]. It is also unclear from other studies whether STAT5 is methylation sensitive like CREB, as one report describes STAT5 as activating Foxp3 expression despite methylation of its binding site [125], and another report suggests that STAT5 does not bind to methylated binding sites [121]. By binding of STAT5 to the *fut7* locus, RA could modulate the recruitment of coactivators by STAT5 such as Ten-eleven translocation (TET) enzymes that actively demethylate CpGs [126] or Dnmts that passively maintain the methylation status during cell cycling. As we have observed Fut7 expression only after cell division it is most likely that re-methylation of the *fut7* minimal promoter 1_v2 is prevented under permissive conditions, i.e., in the absence of RA. Permissive conditions, induced by STAT5, would allow binding of CREB, and in turn promote positive feedback allowing STAT5 to continuously bind the locus. Expression analysis of

Fut7 expression in TET- or Dnmt-deficient mice would clarify the underlying mechanism for control of the *fut7* by DNA methylation.

A final aspect of STAT5 signaling concerns histone acetylation. STAT5 is implicated in the induction of IL-4 responsiveness, and one study has shown that GATA-3, which is induced in T_H2 cells, can recruit HDAC to impose an open chromatin configuration of *fut7* in Jurkat cells [76]. This is not supported by our observations of unaffected Fut7 levels in T_H2 cells treated with the HDAC inhibitor, TsA, where GATA-3 is the main transcriptional regulator. This also stipulates the difference between using T cell lines and primary T cells for the study of gene regulation related to the immune response [75, 120].

Taken together, Fut7 mRNA expression is induced by CREB and STAT5 in T_H1 cells, and is imprinted epigenetically by removal of DNA methylation, which is sensitive to the presence of RA (Figure 7.3).

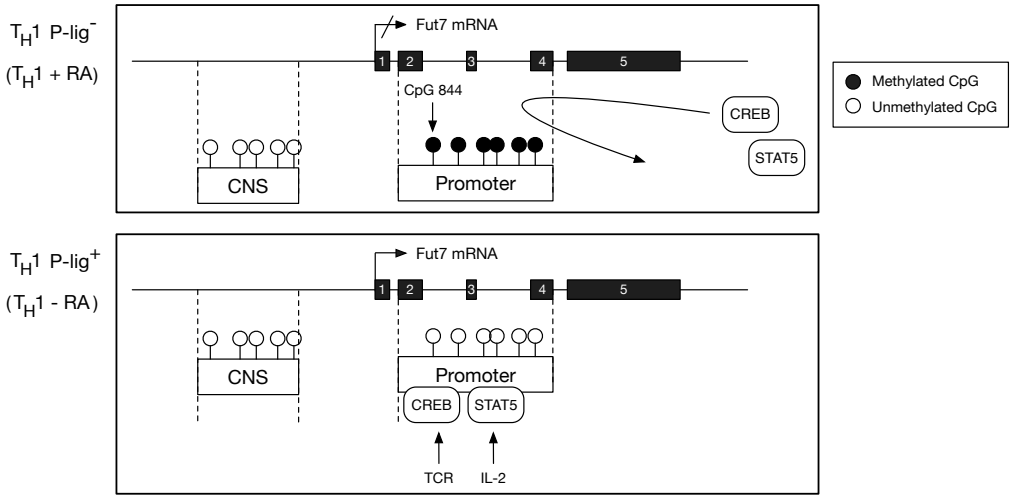

Figure 7.3: Regulation of *fut7* in P-lig$^+$ and P-lig$^-$ T_H1 cells. Schematic of the *fut7* locus with the CNS/enhancer and minimal promoter 1_v2 (promoter) indicated. *Upper panel* shows the DNA methylation on the promoter in *ex vivo* isolated P-lig$^-$ T_H1, which also illustrates what is observed in *in vitro* generated T_H1 cells cultured in the presence of RA. Fut7 transcripts are not seen in these cells. *Lower panel* shows lack of DNA methylation on the promoter in *ex vivo* isolated P-lig$^+$ T_H1, which is also observed in *in vitro* generated T_H1 cells cultured in the absence of RA, where CREB and STAT5 bind the promoter to drive transcription of *fut7* .

7.3 Molecular regulation of *gcnt1* and *fut7* in T_H2 cells

The second aim of this thesis was to understand the discrepancy in P-lig expression between T_H1 and T_H2 cells *in vitro* to clarify the expression of P-lig in both lineages *in*

vivo. Initial characterization of Gcnt1 and Fut7 mRNA in *in vitro* generated T_H1 and T_H2 cells showed that both increased in T_H1 cells, whereas Fut7 mRNA, but not Gcnt1 mRNA, increased in T_H2 cultures. Low to absent Gcnt1 mRNA expression was reflected in a significant lack of selectin ligand induction in the T_H2 cultures, compared to the T_H1 cultures, after the T cells had expanded from day 3 to day 5. This is in line with previous studies on *in vitro* T_H1 and T_H2 cultures reporting a lack of Gcnt1 and P-lig in *in vitro* generated T_H2 cells [51, 113]. Surprisingly, there was no difference between T_H1 and T_H2 cells regarding the expression of Fut7 mRNA. This is in contrast to the notion that IL-4 inhibits Fut7 expression [127, 113, 123]. The unexpected expression of Fut7 in these T_H2 cells might be due to the supplementation with IL-2, however, IL-4 has previously been observed in our group to suppress IL-2-induced Fut7 expression [68, 120]. The expression of selectin ligands in T_H2 cells also did not correlate with the expression of Fut7 mRNA because E-lig, mainly induced by *fut7*, was suppressed in T_H2 cells compared to T_H1 cells.

Remarkably, the expression of E-lig was similar in day 3 T_H1 and T_H2 cells, however, the FACS dot plots showed striking differences in co-expression with 1B11. In T_H1 cells, both E-lig and P-lig co-expressed with 1B11 on day 3 and day 5, however, it seems that in T_H2 cells, E-lig, and to some extent P-lig, can be built independently of 1B11 on day 3, but on day 5 the ligands are coexpressed with 1B11. This supports the notion that E-lig can be expressed independently of 1B11, which is more prominent in T_H2 cells where *gcnt1* expression is suppressed. By day 5, the T_H2 cells seemed to express sufficient amounts of *gcnt1* to induce expression of 1B11 and E- and P-lig built on 1B11. Moreover, this data suggests that TCR signaling is more important in the early induction of Fut7 mRNA and subsequent E-lig generation in T_H2 cells than cytokine signaling. This is in line with previous reports by others that antigen-stimulation alone is able to induce E-lig [113].

As there was no difference in Fut7 mRNA expression between T_H1 and T_H2 cells, and a low expression of P-lig, E-lig, and Gcnt1 was observed in T_H2 cells, the results indicated that something was interfering with *gcnt1* transcription and/or translation. As we know the *gcnt1* enhancer is regulated by histone methylation in P-lig$^+$ and P-lig$^-$ T_H1 cells, we examined its histone methylation profile in T_H1 vs. T_H2 cells. We found that the active mark, H3K4me2, increased significantly from naive T cells with differentiation into the T_H1 lineage compared to T_H2 cells on day 3, but not day 5. Moreover, naive T cells were marked by the repressive mark, H3K27me3, which is significantly lost in T_H1 cells compared to T_H2 cells on day 3, but not on day 5. This indicates that the chromatin does open in T_H2 cells, but is not reflected in Gcnt1 mRNA levels until after the T cells have expanded from day 3 to day 5. There is, however, a big standard deviation in replicates of the experiment and it should be mentioned that the Wilcoxon signed rank test, used in the statistical analysis, takes the mean across all amplicons in one cell type and compares

it with the mean of all amplicons of another cell type, making even discrete changes significant.

Taken together, this *in vitro* data suggests that Gcnt1 mRNA is suppressed in T_H2 cells due to the presence of the repressive histone mark, H3K27me3, on the *gcnt1* enhancer, which correlates with low 1B11 and P-lig levels in these cells.

7.3.1 Microenvironment-dependent expression of P-lig

Other groups and ours have previously reported a dramatic difference in P-lig expression in *ex vivo* isolated T_H1 and T_H2 cells from mLNs compared to those from pLNs [6, 51]. While T_H1 and T_H2 cells do not differ in the frequency of P-lig expression in one compartment, i.e., in either pLNs or mLNs, the expression in these lineages (defined by their expression of IFNγ and IL-4, respectively) is much higher in pLNs compared to their mLNs counterparts [1].

This difference is at least in part due to the greater availability of RA from mLN DCs vs pLN DCs [47, 46, 48] during priming/activating of naive T cells. mLN DCs have been shown by several studies to induce a gut homing phenotype characteristic of integrin $\alpha4\beta7$ and chemokine receptor CCR9 expression, while suppressing the skin homing receptor, E-lig [52, 46, 47]. T_H2 cells generated in conventional (cRPMI) *in vitro* culture, i.e., in FCS-containing media, express low levels of P-lig compared to T_H1 cells. However, we have shown, with *in vitro* cultures, that T_H1 and T_H2 cells polarized in the absence of RA express similar levels of Gcnt1 and Fut7 mRNA, transcripts of the rate-limiting enzymes in the generation of P-lig (fig. 6.22). If RA was present in combination with IL-4, however, both Gcnt1 and Fut7 mRNA were suppressed, whereas RA in combination with IL-12 led to suppression of only Fut7 mRNA. These results were observed when RA signaling was either inhibited by treatment with the RA-antagonist, LE540, or when serum-free media was used to cultivate the cells. As little as 0.1nM RA in serum-free media led to a reduction of Gcnt1 mRNA in the presence of IL-4, while RA, even at high doses did not impair IL-12-driven Gcnt1 induction.

Because it has been shown that IL-4 can instruct mLN DCs to express the enzymes aldehyde dehydrogenase and retinaldehyde dehydrogenase 2, necessary to synthesize RA [110, 128], we measured the level of IL-4 and Gcnt1 mRNA in crude isolates of mLN and pLN under homeostatic/non-inflammatory conditions, hypothesizing that IL-4 is available to a larger extent in mLNs than in pLNs, and that this might have an influence on levels of Gcnt1 mRNA. We observed that Il4 mRNA was indeed more available in mLN than pLN, which negatively correlated with the expression of Gcnt1 mRNA. This supports our hypothesis that IL-4 + RA availability in the gut suppresses Gcnt1 expression and is in

line with the requirement of IL-4 in the upregulation of the Vitamin A metabolizing enzyme, RALDH2, in mLN DCs prior to induction of CCR9 [110].

The constitutive availability of RA and IL-4 in mLNs might suggest that a tighter control of P-lig expression takes place in the non-inflamed gut. However, IL-12-dependent induction of P-lig is possible in the presence of RA *in vitro* and seems to occur *in vivo* also in the gut. Our group has previously observed P-lig expression on $CD4^+$ cells primed in the gut using a mouse disease model with a characteristic T_H1 response: large intestinal induced colitis by transfer of naive T cells into severe compromised immunodeficient (SCID) mice [40]. In this study P-lig was expressed and even co-expressed with the gut homing molecule $\alpha4\beta7$ despite the presence of RA. Despite the dampened Fut7 expression by RA, P-lig expression was unimpeded. Additional studies using a parasitic mouse model, with infection by the nematode *Nippostrongylus brasiliensis*, characterized by a strong T_H2 response, similarly showed that T_H2 cells in the lung of infected mice were able to express P-lig under inflammatory conditions in the presence of RA and did not require IL-12 [118]. Indeed recent reports by others have highlighted the mucosal lung tissue as a storage of vitamin A, containing DCs with RA-converting enzymes, and gut migratory inductive capacity (reviewed in [129]). Raune et al. (2013) showed that two subsets of DCs in the lung, $CD11b^+$ and $CD103^+$ DCs, can prime naive T cells in the lung and mediastinal LNs to upregulate $\alpha4\beta7$ and CCR9 and thereby promote migration to the gut after intranasal immunization [129].

If induction of Plig under T_H1 conditions is unrestricted even in the the presence of RA, why do T_H1 cells from pLNs and mLNs differ in P-lig expression under homeostatic conditions? Either P-lig^+ T cells induced during gut inflammation are preferentially recruited to the gut, i.e. leave the circulation, or priming in the presence of RA allows P-lig induction but prevents long-term expression, leading to the hypothesis that P-lig stabilization is regulated by RA. Taken together, RA and IL-4 suppresses induction of *gcnt1* (and most likely *fut7*) in mLNs in a homeostatic setting *in vitro*. However, in pLNs IL-4 can induce expression of P-lig under inflammatory settings, presumably due to a lack of RA presentation by DCs.

7.3.2 Mechanism of RA suppression of *gcnt1* and *fut7* transcription in T_H2 cells

To elucidate the mechanism underlying the RA-mediated suppression of Gcnt1 and Fut7 mRNA in T_H2 cells *in vitro*, we firstly investigated if there is a dose-dependent suppression of Gcnt1 and Fut7 mRNA and 1B11, E-, and P-lig by RA. Secondly, we measured mRNA levels of the nuclear receptors (RARs and RXRs) through which RA signals in the same T_H2 cells to determine which isoforms RA most likely signals through. Thirdly, we

examined the effects of pan-RAR and pan-RXR agonists on the suppression of Gcnt1 and Fut7 mRNA as well as the gut homing receptors-related transcripts Itga4 and Ccr9.

As expected, Gcnt1 mRNA was suppressed by all doses of RA in T_H2 cells, with a resulting inhibition of 1B11 and P-lig, while being unaffected in T_H1 cells, even in the presence of RA. This is in line with the *in vivo* data described in the previous section, where T_H1 cells primed in the presence of IL-12 in the gut and lung could express P-lig despite the presence of RA. Contrary to Gcnt1, Fut7 mRNA was suppressed by all doses of RA in both T_H1 and T_H2 cells. Despite the positive correlation between Fut7 mRNA and E-lig induction, the low Fut7 mRNA levels, however, only resulted in RA-mediated inhibition of E-lig induction in T_H1 cells. We cannot exclude that T_H2 cells express other Fut7- and Gcnt1-independent oligosacccharides, as the chimera used to bind and visualize E-ligs by FACS is an E-selectin ligand that binds all, also unidentified, E-selectin binding oligosaccharide epitopes that may require other genes than *gcnt1* and *fut7* for their expression.

Because RA signals as a ligand through RAR and RXR nuclear receptors, we wanted to confirm which RAR and RXR isoforms are important for RA signaling under T_H2 polarizing conditions. Therefore, we measured the mRNA levels of RARα, RARβ, and RARγ, as well as RXRα, RXRβ, and RXRγ isoforms in T_H2 cells cultured for 3 and 5 days in serum-free media with titrated amounts of RA added. We compared the levels measured to that in the naive T cells from which the cells differentiated. Compared to naive levels, all isoforms detected, RARα, RARγ, and RXRβ, except RXRα, decreased in expression during TCR stimulus, as indicated in other reports on nuclear isoform levels in T_H0 cells[114]. In day 5 T_H2 cells, all isoforms detected increased roughly to that of naive levels, except the RXR isoforms, which increased beyond that of the naive levels. RXRα was the only isoform that was significantly suppressed by RA (at 1 nM only due to few experiment repetitions), and RARα and RXRβ were the highest expressed of the RAR and RXR nuclear receptor isoforms induced by IL-4, even in the presence of RA. Ohoka et al. also measured RAR isoforms levels in T_H0 cells and found that RARα remains unchanged in expression during TCR stimulation, whereas we observe a downregulation in T_H2 cells during TCR stimulation. They, as we, observe a tendency towards RA-mediated downregulation of the RAR and RXR isoforms. The reduction of some RAR and RXR receptor transcripts that we observe during activation *in vitro* explains the lack of CCR9 induction during TCR stimulation originally observed by Ohoka et al. (2011). They found that NFATc1(NFAT2) and NFATc2(NFAT1) compete for the same binding site at the 5' UTR of the *ccr9* locus entering into a complex with the heterodimer RAR/RXR. Upon cessation of TCR stimulation, NFATc1(NFAT2) is exported out of the nucleus, and the competitive binder NFATc2(NFAT1) activates the *ccr9* promoter in cooperation with RA through a RARE half-site located between two NFAT binding sites. As such transcription

of the gut homing receptor CCR9 requires export of NFATc1(NFAT2) as well RA signaling for its expression in T_H0.

Taken together, the induction of the RAR and RXR isoforms during the expansion phase most likely leads to acquisition of RA responsiveness mediated by RARα and RXRβ in activated T cells (including T_H2 cells). Thus, there is no specific RA signaling pathway specifically promoted under T_H2 polarizing conditions i.e. as an effect downstream of IL-4 signaling. It could be speculated that RARα heterodimerizes with different RXRs depending on the presence of RA

Takeuchi et al. (2010) reported an inducing effect of RXR agonists for the homing receptors Itga4 and CCR9 in T_H0 cultures. They also reported a synergistic effect of RAR and RXR agonists on the induction of CCR9 expression and suppression of the skin-seeking homing receptor E-lig [112]. Yet another report implicates RXR signaling in the enhancement of T_H2 differentiation *in vitro* [130]. We were therefore interested in whether RA suppresses Gcnt1 mRNA expression under T_H2 conditions through both RAR and RXR nuclear receptors. Similar to the study by Takeuchi et al., we investigated whether a RA-mediated suppression of Gcnt1 induction can be induced by selective RAR or RXR agonists or by a combination of both. As in the Takeuchi study, we used a RARα/β specific agonist, Am80. Unfortunately, we were unable to obtain the same RXR agonists used in the study mentioned. We did, however, find another commercially available pan-RXR agonist, HX630, which is an analog of one of the RXR agonists, HX600, used in the Takeuchi study. Both HX600 and HX630 have been reported to bind to the RXR subunit of a RAR:RXR heterodimer and synergize with Am80 to promote transactivation of gene expression in the HL-60 cell line [131].

Our results showed that Am80 suppressed Gcnt1 induction similarly to RA. In contrast, HX630 was unable to induce or reduce transcription of Gcnt1 and Fut7 mRNA compared to the DMSO control – essentially displaying no effect at all. In line with the effect of HX600 shown by the Takeuchi study, HX630 alone also did not induce expression of the gut homing receptor CCR9, in this study in the presence of IL-4. Surprisingly, the combination of HX630 and Am80 did not lead to a synergistic activation of the gut homing receptor transcripts, Itga4 and Ccr9, as was reported for HX600+Am80 concerning CCR9 in T_H0 cells [112]. This is not surprising concerning Itga4 because IL-4 has been reported to suppress Itga4 [132]. The combination of HX630+Am80 also did not synergistically suppress the transcription of Gcnt1 or Fut7 in the presence of IL-4.

We cannot be sure that the HX630 pan-RXR agonist is as efficacious as HX600 reported in the Takeuchi study. We do not see any synergistic effect on the induction of gut homing

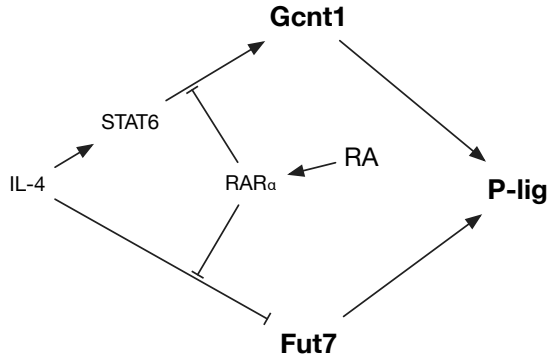

Figure 7.4: Model of RA-mediate suppression of Gcnt1 and Fut7 mRNA in T_H2 cells. RA suppresses IL-4 driven induction of Gcnt1 and Fut7 mRNA – most likely through RARα. This leads to a reduction of P-lig in *in vitro* generated T_H2 cells.

receptor transcripts when treating T_H2 cells with a combination of HX630 and the RAR agonist Am80. The discrepancy could be caused by different concentrations of agonists used in the Takeuchi study and ours. They used Am80 at a 1 nM concentration alone or in combination with 100 nM HX600. We used 10 nM of Am80 alone and in combination with 10 nM HX630. This was decided because 1 nM Am80 and 10 nM Am80 were similar in their effect on Ccr9 expression in the Takeuchi study and we wanted a comparable concentration to the 10 nM RA we used in our study. We used HX630 at 10 nM in combination with Am80 because 100 nM HX630 was toxic to the cells. In retrospect, HX630 should have been titrated more carefully because the concentration we used could be too low to take part in a synergistic effect with the RAR agonists. The combination of these agonists did not lead to further reduction in the level of Gcnt1 and Fut7 mRNA compared to RA alone, although a reduction in the Takeuchi study was reported for E-lig – although this study used naive T cells polarized in RPMI+FCS and as such cannot exclude a suppression of E-lig by RA.

Taking together, the results suggest that the suppression of Gcnt1 and Fut7 is mediated only by RAR signaling with no involvement of RXR signaling in T_H2 cells. High inter-experimental variation and poor agonist titration, however, does not exclude that RA signals through RXRs in addition to RARα and this should be addressed in future experiments.

7.3.3 Differential usage of *gcnt1* enhancer in T_H1 versus T_H2 cells

Transcriptional changes can occur in different cell types due to alterations in the turnover or property of the transcripts. We aimed to determine whether RA promotes alternative Gcnt1 transcript usage in T_H1 versus T_H2 cells. We found that the transcript was the same in T_H1 and T_H2 cells cultured in the absence of RA, but that the transcript was

absent in T_H2 cells cultured in the presence of RA.

Therefore, we next investigated the relationship between RA signaling and activity of the regulatory regions, the promoter and enhancer, we have identifed for Gcnt1 so far. We hypothesized that the same promoter and enhancer, originally identified in T_H1 cells, also drive IL-4-dependent induction of *gcnt1* in the absence of RA. To that end, we performed reporter assays with the *gcnt1* promoter and *gcnt1* promoter+enhancer construct in T_H2 cells polarized in the presence of RA or LE540, and compared it to that in T_H1 cells (fig. 6.26). As expected, the promoter+enhancer construct displayed greater activity than the promoter construct in T_H1 cells in the presence and absence of RA. Remarkably, the activity of the promoter construct is lower in RA-treated T_H1 cells than in LE540-treated T_H1 cells. This is also reflected in the activity of the promoter+enhancer construct, and indicates that RA can influence Gcnt1 transcription also in T_H1 cells. The reporter activity of the constructs in the presence or absence of RA resemble those of untreated T_H1 cells that we have studied in great detail, and is also shown earlier in this work (fig. 6.3).

RA signaling in the context of T cell lineage commitment is highly topical and recent reports suggest that RA promotes commitment to certain $CD4^+$ T cell phenotypes [107, 133]. One study reports that the T_H1 phenotype in the steady-state is maintained by RA signaling through RARα, which in turn prevents commitment to the T_H17 lineage [107]. As our T_H1 cells are not examined for the presence of T_H17-defining cytokines during our reporter assays, it could be argued that the LE540-treated samples might have shifted toward a T_H17 phenotype, also able to induce *gcnt1* and P-lig [70].

Regarding *gcnt1* regulatory activity in RA-treated vs. LE540-treated T_H2 cells, we unexpectedly observed greater activity of the promoter construct compared to the promoter+enhancer construct. In fact, it appears that the enhancer is rather a silencer in T_H2 cells regardless of the presence of RA. Moreover, the activity of the promoter is slightly downregulated in RA-treated vs. LE540-treated T_H2 cells, which could indicate that the IL-4-driven induction of *gcnt1* proceeds through different regulatory regions. Interestingly, loss of RARα, in the study mentioned earlier, did not have an effect on IL-4 or GATA3 expression [107]. This contradicts another recent study that suggests that IL-4 signaling is abrogated by RA signaling and that RA signaling promotes T_{reg} differentiation [133]. This suggests that RA prevents differentiation of the T_H2 lineage at the level of IL-4, which could be one explanation for why we are unable to see IL-4 driven induction of *gcnt1* in RA-treated T_H2 cells. Supporting this notion, *in vitro* generated *stat6*$^{-/-}$ T_H2 cells cultured in the absence of RA did not express Gcnt1 mRNA and had low P-lig expression, indicating that the RA disrupts IL-4-mediated Gcnt1 mRNA expression at the level of STAT6 (unpublished data). Altogether, this indicates a complicated relationship between

RA and induction of IL-4-driven gene regulation, that could be examined by following cytokine expression in T_H2 cells along with expression of *gcnt1*.

The pitfall of a reporter assay is that it isolates the region in question and therefore the contribution of other regions cannot be assessed. Other regions can be included, but often the position and directionality of each region has to be tested. Therefore, to minimize the workload it is essential to know which regions to look for, which is why one often chooses regions that 1) show predictions of cell-specific TF binding sites, 2) share homology with other species, or 3) contain chromatin-modified regions with distinct differences in different cell populations/subsets of interest. As we could only find two TF binding sites for RARα and RXRβ in the *gcnt1* enhancer, but none in the promoter, this could not explain the trend of RA-mediated regulation of the promoter, even though NFAT, STAT6, and GATA-3 binding motifs were found in both regulatory regions. Because the histone modifications on the regions tested did not show any differences in a preliminary ChIP-on-chip in RA-treated vs LE540-treated Th2 cells, this did not point us in the direction of additional lineage-specific regulatory regions. When further examining the reason for our reporter assay results, after, we found a RNA from a cDNA library that is being transcribed in the antisense direction on the *gcnt1* T_H1 enhancer in DC CD11b+ cells, which could be a potential lncRNA.

It could be speculated that IL-4 + RA promotes transcription of such a lncRNA. We know that the *gcnt1* enhancer region is demethylated in both P-lig$^+$ and P-lig$^-$ T_H1 cells from earlier studies in the group. This is in principle compatible with a polycomb response element that could repress transcription by recruiting a lncRNA to the region [134] (personal communication with Prof. Ringrose). The activity of a lncRNA could mediate suppression of Gcnt1 transcription in T_H2 cells cultured in the presence of RA, and thus explain the silencing effect we see in our reporter assays. Differences in such an expression would be determined by strand-specific RT-qPCR. If so, overexpression of this lncRNA should be done to analyze its effect on Gcnt1 transcription. Binding of STAT6 and RAR/RXR nuclear receptors to the enhancer should be clarified in future work to address the mode of action by this RNA. As shown earlier, STAT6 was seen in ChIP-seq performed on T_H2 cultured in cRPMI media, in the presence of RA, which does not clarify whether STAT6 acts as a repressor or activator of transcription. The level of Gcnt1 transcript in this ChIP-seq data could clarify if STAT6 is a silencer or activator of Gcnt1 transcription in the presence of RA.

Considering this in a broader biological context, it could be speculated that such a lncRNA is expressed and stabilized in the presence of RA and IL-4. Based on the recent reports suggesting that RA stabilizes the T_H1 and T_{regs} cell fate, global RA signaling might de-

crease T_H2 differentiation and induce a shift toward T_H1 or T_{regs} differentiation to promote tolerance to food allergens. As IL-4 is not a polarizing cytokine in the promotion of these cell lineages, this could mean that in the absence of IL-4, but presence of RA, the lncRNA is destabilized, leading to induction of *gcnt1*. As mentioned earlier, in T_H2 cells, the lncRNA might guide PcG to the region to deposit H3K27me3. Because PcG is attracted to H3K4me3 marks, this might explain why T_H2 cells initially have H3K4me2 marks but no H3K27me3 marks and then acquires H3K27me3 with no changes in H3K4me2 marks. In addition, this could explain the difference in P-lig expression in T_H1 and T_H2 generated *in vitro*. The difference between T_H1 and T_H2 regarding P-lig expression in mLN vs. pLN *in vivo* is most likely due to the difference in availability of IL-4 RA in these compartments.

In addition to the synthesis of RA, RA signaling is also regulated by members of the cytochrome P450 family 26 enzymes that catabolize RA when it is induced. Upon induction of RA signaling, Cyp26b1, but not Cyp26a1 or Cyp26c1, are induced in activated $CD4^+$ T cells isolated from mLNs, but not pLNs, which is in line with absence of RA signaling in the pLN compartment [50]. In the mLNs, the presence of TGFβ in combination with RA signaling, prevents induction of Cyp26b1. This is consistent with a role for RA in stabilizing the T_{reg} fate. Interestingly, this study found not only that TGFβ + RA, but also IL-12 + RA inhibited expression of Cyp26b1, supporting the aforementioned study showing that RA also stabilizes the T_H1 cell fate [107]. On the other hand, IL-4 + RA, as well as TNFα + RA, greatly induced Cyp26b1, indicating that RA signaling is quickly regulated in T_H2 cells and in T cells that are indicative of inflammation, the former to induce tolerance to food antigens and the latter to prevent inflammatory conditions in, e.g., the gut [50]. This is consistent with data showing that RA prevents induction of pathogenic T_H2 cells in response to oral antigens [135].

Altogether, our reporter assay suggests that enhancer identified to drive Gcnt1 expression in T_H1 cells has a silencing effect in T_H2 cells regardless of the presence of RA. Additionally, taken together with recent publications on RA signalling, it seems that a quick turnover of P-lig in T cells activated in the gut under inflammatory conditions or in the presence of IL-4 might explain the low levels of P-lig observed in mLN *ex vivo* isolated $CD4^+$ helper T cells compared to those from pLN.

7.4 Conclusions

This work furthers our understanding of the distinct mechanisms that induce and imprint the expression of *gcnt1* and *fut7* in T_H1 and T_H2 cells generated *in vitro*. These are the genes that encode the rate-limiting enzymes, C2-GlcNAcT-I and FucT-VII, crucial for the generation of E- and P-selectin ligands that mediate the skin- and inflammation-seeking

homing phenotype. Whereas P-lig is expressed in non-inflammatory and, is highly induced, in inflammatory models in both T_H1 and T_H2 cells, this could never be recapitulated *in vitro*.

In T_H1 cells, we have shown that *gcnt1* expression is induced and maintained by STAT4 and T-bet, respectively. Furthermore, using available ChIP-seq data, we observed that these transcription factors are implicated in the opening of the *gcnt1* locus by histone methylation that promote its transcription. This is pivotal to the understanding of how selectin ligands, such as P-lig, are induced long-term to give T cells a topographical migratory memory, which enables them to recirculate the tissue of first antigen encounter. For *fut7*, we have shown that initial activation in T_H1 cells is induced by the TFs CREB and STAT5, the actions of which are inhibited by DNA methylation and the presence of RA, respectively. Unlike *gcnt1*, the imprinting of *fut7* long term is therefore regulated by DNA methylation.

In T_H2 cells, we have aimed to solve the long-standing discrepancy between expression of P-lig *in vitro* and *in vivo*, by studying the regulation of *gcnt1* and *fut7* in *in vitro* generated T_H2. We have shown that RA suppresses expression of *gcnt1* and *fut7* in T_H2 cells, and that the mechanisms underlying the suppression proceeds through RARα potentially heterodimerizing with different RXR isoforms in the absence and presence of RAFurthermore, we have shown that despite the usage of the same Gcnt1 transcript in T_H1 cells and in T_H2 cells cultured in the absence of RA, the enhancer for *gcnt1* in T_H1 cells acts as a silencer in T_H2 cells.

This work entailed mostly the study of *gcnt1* gene regulation. Taken together, we envision three possibles ways how RA affects Gcnt1 under Th2 conditions. 1) differential NFAT signalling in T_H1 vs. T_H2 cells. Previous work in our group showed that while Gcnt1 was downregulated in Cyclosporine A (CsA)-treated T_H1 cells, it was upregulated in CsA-treated T_H2 cells [53]. This indicates that NFAT signaling might block IL-4-driven expression of Gcnt1. 2) A lncRNA might regulate *gcnt1*. As such, future studies on *gcnt1* regulation would benefit from investigating the involvement of a potential ncRNA in its regulation. This could be done using the CRISPR-Cas technology to determine the outcome of removing this region from the *gcnt1* locus in both T_H1 and T_H2 cells and comparing the results with overexpression studies. Furthermore, additional regulatory regions within the *gcnt1* locus could be discovered by querying looping databases for interactions between regions on the *gcnt1* locus. 3) Differential regulation of RA signaling in T_H1 vs. T_H2 cells regarding either the binding of RXRα- vs. RXRβ-dependent dimers to *gcnt1* enhancer in the absence or presence of RA, respectively, or regulation of the RA-catabolizing Cyp26b1 enzyme, which seems to be important in the regulation of RA

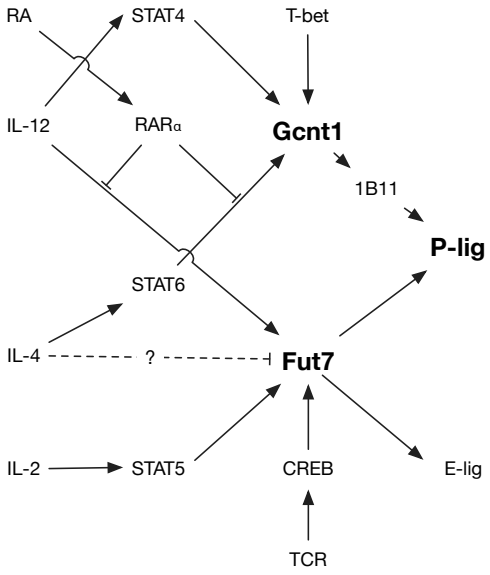

Figure 7.5: Model of molecular regulation of Gcnt1 and Fut7 mRNA in CD4$^+$ T cells generated *in vitro*. In T_H1 cells, IL-12 drives Gcnt1 transcription through STAT4 together with T-bet as shown in Figure 7.2. This leads to 1B11 and P-lig expression. Provided that the minimal promoter 1_v2 of *fut7* is not methylated, transcription is driven by STAT5 and CREB, induced respectively by IL-2 and TCR signaling, as shown in Figure 7.3. Fut7 transcription is suppressed by RA in T_H1 cells. In T_H2 cells cultured in the absence of RA, IL-4 drives Gcnt1 transcription, and subsequently P-lig expression, through STAT6 (unpublished data). When present in the T_H2 culturing media, RA suppresses both Gcnt1 and Fut7 transcription through RARα. While IL-4 has been postulated to have a role in suppressing Fut7 expression by our group and others, this was not the case in this work.

signaling. As such, Cyp26b1 would be an ideal candidate to measure in *in vitro*-generated T_H1 and T_H2 cells to determine whether lineage-specific regulation of RA signaling occurs.

Taken together, our findings firstly confirm that epigenetic regulation of *gcnt1* and *fut7* are regulated by distinct mechanisms. While *gcnt1* is governed by histone methylation, *fut7* expression is controlled by DNA methylation. Secondly, different polarizing cytokines regulate the transcriptional activation or maintenance of expression of *gcnt1* and *fut7*. p300 binds to the *gcnt1* enhancer, which is also bound by STAT4 and T-bet in T_H1 cells. On the other hand, while we could not confirm that *fut7* is repressed by IL-4, STAT5 and CREB are implicated in its induction downstream of IL-2 and TCR signaling (Figure 7.5). Thirdly, our findings confirm that microenvironmental factors, such as RA, play a crucial role in the suppression of *gcnt1* in *in vitro* generated T_H2 cells and Fut7 in both T_H1 and T_H2 *in vitro* generated cells. This suggests that a complex interplay between epigenetic modifications, cytokine signaling, and microenvironmental factors control the molecular regulation/induction of *gcnt1* and *fut7*, and subsequently P-lig on developing effector cells that are distinct in T_H1 and T_H2 *in vitro* generated cells (Figure 7.5).

References

1 Kretschmer U, Bonhagen K, Debes GF, Mittrucker HW, Erb KJ, Liesenfeld O, et al. Expression of selectin ligands on murine effector and IL-10-producing CD4+ T cells from non-infected and infected tissues. Eur J Immunol. 2004 Nov;34(11):3070–3081.

2 Syrbe U, Jennrich S, Schottelius A, Richter A, Radbruch A, Hamann A. Differential regulation of P-selectin ligand expression in naive versus memory CD4+ T cells: evidence for epigenetic regulation of involved glycosyltransferase genes. Blood. 2004 Nov;104(10):3243–3248.

3 Rivas FV, O'Keefe JP, Alegre ML, Gajewski TF. Actin cytoskeleton regulates calcium dynamics and NFAT nuclear duration. Mol Cell Biol. 2004 Feb;24(4):1628–1639.

4 Hogan PG, Chen L, Nardone J, Rao A. Transcriptional regulation by calcium, calcineurin, and NFAT. Genes Dev. 2003 Sep;17(18):2205–2232.

5 Macian F. NFAT proteins: key regulators of T-cell development and function. Nat Rev Immunol. 2005 Jun;5(6):472–484.

6 Campbell DJ, Butcher EC. Rapid acquisition of tissue-specific homing phenotypes by CD4(+) T cells activated in cutaneous or mucosal lymphoid tissues. J Exp Med. 2002 Jan;195(1):135–141.

7 Zhu J, Yamane H, Paul WE. Differentiation of effector CD4 T cell populations. Annu Rev Immunol. 2010;28:445–489.

8 Szabo SJ, Kim ST, Costa GL, Zhang X, Fathman CG, Glimcher LH. A novel transcription factor, T-bet, directs Th1 lineage commitment. Cell. 2000 Mar;100(6):655–669.

9 Miller CMD, Smith NC, Ikin RJ, Boulter NR, Dalton JP, Donnelly S. Immunological interactions between 2 common pathogens, Th1-Inducing Protozoan *Toxoplasma gondii* and the Th2-Inducing Helminth *Fasciola hepatica*. PLoS ONE. 2009;4(5):e5692.

10 Salgame P. Host innate and Th1 responses and the bacterial factors that control Mycobacterium tuberculosis infection. Current Opinion in Immunology. 2005;17(4):374 – 380.

11 Jiang S, Dong C. A complex issue on CD4+ T-cell subsets. Immunological Reviews. 2013;252(1):5–11.

12 Kanhere A, Hertweck A, Bhatia U, Gokmen MR, Perucha E, Jackson I, et al. T-bet and GATA3 orchestrate Th1 and Th2 differentiation through lineage-specific targeting of distal regulatory elements. Nat Commun. 2012;3:1268.

13 Schulz EG, Mariani L, Radbruch A, Hofer T. Sequential polarization and imprinting of type 1 T helper lymphocytes by interferon-gamma and interleukin-12. Immunity. 2009 May;30(5):673–683.

14 Becskei A, Grusby MJ. Contribution of IL-12R mediated feedback loop to Th1 cell differentiation. FEBS Lett. 2007 Nov;581(27):5199–5206.

15 Thieu VT, Yu Q, Chang HC, Yeh N, Nguyen ET, Sehra S, et al. Signal transducer and activator of transcription 4 is required for the transcription factor T-bet to promote T helper 1 cell-fate determination. Immunity. 2008 Nov;29(5):679–690.

16 Chen F, Liu Z, Wu W, Rozo C, Bowdridge S, Millman A, et al. An essential role for TH2-type responses in limiting acute tissue damage during experimental helminth infection. Nat Med. 2012 Feb;18(2):260–266.

17 Cote-Sierra J, Foucras G, Guo L, Chiodetti L, Young HA, Hu-Li J, et al. Interleukin 2 plays a central role in Th2 differentiation. Proc Natl Acad Sci U S A. 2004 Mar;101(11):3880–3885.

18 Zhu J, Cote-Sierra J, Guo L, Paul WE. Stat5 activation plays a critical role in Th2 differentiation. Immunity. 2003 Nov;19(5):739–748.

19 Swain SL, McKinstry KK, Strutt TM. Expanding roles for CD4+ T cells in immunity to viruses. Nat Rev Immunol. 2012 02;12(2):136–148.

20 Khader SA, Gopal R. IL-17 in protective immunity to intracellular pathogens. Virulence. 2010 Sep-Oct;1(5):423–427.

21 Whibley N, Gaffen SL. Brothers in arms: Th17 and Treg responses in *Candida albicans* immunity. PLoS Pathogens. 2014 12;10(12):e1004456.

22 Sakaguchi S. Regulatory T cells: history and perspective. Methods Mol Biol. 2011;707:3–17.

23 Mosmann TR, Kobie JJ, Lee FEH, Quataert SA. T helper cytokine patterns: defined subsets, random expression, and external modulation. Immunol Res. 2009 Dec;45(2-3):173–184.

24 Bromley SK, Mempel TR, Luster AD. Orchestrating the orchestrators: chemokines in control of T cell traffic. Nat Immunol. 2008 09;9(9):970–980.

25 Ebnet K, Vestweber D. Molecular mechanisms that control leukocyte extravasation: the selectins and the chemokines. Histochem Cell Biol. 1999 Jul;112(1):1–23.

26 Vestweber D. How leukocytes cross the vascular endothelium. Nat Rev Immunol. 2015 Nov;15(11):692–704.

27 Vestweber D, Wessel F, Nottebaum AF. Similarities and differences in the regulation of leukocyte extravasation and vascular permeability. Semin Immunopathol. 2014 Mar;36(2):177–192.

28 Zarbock A, Kempf T, Wollert KC, Vestweber D. Leukocyte integrin activation and deactivation: novel mechanisms of balancing inflammation. J Mol Med (Berl). 2012 Apr;90(4):353–359.

29 Chow Z, Banerjee A, Hickey MJ. Controlling the fire–tissue-specific mechanisms of effector regulatory T-cell homing. Immunol Cell Biol. 2015 Apr;93(4):355–363.

30 Marelli-Berg FM, Cannella L, Dazzi F, Mirenda V. The highway code of T cell trafficking. J Pathol. 2008 Jan;214(2):179–189.

31 Firner S, Onder L, Nindl V, Ludewig B. Tight control – decision-making during T cell-vascular endothelial cell interaction. Frontiers in Immunology. 2012;3(279).

32 Sigmundsdottir H, Butcher EC. Environmental cues, dendritic cells and the programming of tissue-selective lymphocyte trafficking. Nat Immunol. 2008 Sep;9(9):981–987.

33 Borchers AT, Shimoda S, Bowlus C, Keen CL, Gershwin ME. Lymphocyte recruitment and homing to the liver in primary biliary cirrhosis and primary sclerosing cholangitis. Seminars in Immunopathology. 2009 09;31(3):309–322.

34 Ley K, Kansas GS. Selectins in T-cell recruitment to non-lymphoid tissues and sites of inflammation. Nat Rev Immunol. 2004 May;4(5):325–335.

35 Schneider-Hohendorf T, Rossaint J, Mohan H, Boning D, Breuer J, Kuhlmann T, et al. VLA-4 blockade promotes differential routes into human CNS involving PSGL-1 rolling of T cells and MCAM-adhesion of TH17 cells. J Exp Med. 2014 Aug;211(9):1833–1846.

36 Wolber FM, Curtis JL, Maly P, Kelly RJ, Smith P, Yednock TA, et al. Endothelial selectins and alpha4 integrins regulate independent pathways of T lymphocyte recruitment in the pulmonary immune response. J Immunol. 1998 Oct;161(8):4396–4403.

37 Mangan PR, O'Quinn D, Harrington L, Bonder CS, Kubes P, Kucik DF, et al. Both Th1 and Th2 cells require P-selectin glycoprotein ligand-1 for optimal rolling on inflamed endothelium. Am J Pathol. 2005 Dec;167(6):1661–1675.

38 Bonder CS, Norman MU, Macrae T, Mangan PR, Weaver CT, Bullard DC, et al. P-selectin can support both Th1 and Th2 lymphocyte rolling in the intestinal microvasculature. Am J Pathol. 2005 Dec;167(6):1647–1660.

39 Rijcken EM, Laukoetter MG, Anthoni C, Meier S, Mennigen R, Spiegel HU, et al. Immunoblockade of PSGL-1 attenuates established experimental murine colitis by reduction of leukocyte rolling. Am J Physiol Gastrointest Liver Physiol. 2004 Jul;287(1):G115–24.

40 Hoffmann U, Pink M, Lauer U, Heimesaat MM, Winsauer C, Kruglov A, et al. Regulation and migratory role of P-selectin ligands during intestinal inflammation. PLoS One. 2013;8(4):e62055.

41 Tietz W, Allemand Y, Borges E, von Laer D, Hallmann R, Vestweber D, et al. CD4+ T cells migrate into inflamed skin only if they express ligands for E- and P-selectin. J Immunol. 1998 Jul;161(2):963–970.

42 Gironella M, Molla M, Salas A, Soriano A, Sans M, Closa D, et al. The role of P-selectin in experimental colitis as determined by antibody immunoblockade and genetically deficient mice. J Leukoc Biol. 2002 Jul;72(1):56–64.

43 Wan MX, Riaz AA, Schramm R, Wang Y, Vestweber D, Menger MD, et al. Leukocyte rolling is exclusively mediated by P-selectin in colonic venules. Br J Pharmacol. 2002 Apr;135(7):1749–1756.

44 Mora JR, Iwata M, von Andrian UH. Vitamin effects on the immune system: vitamins A and D take centre stage. Nat Rev Immunol. 2008 09;8(9):685–698.

45 Agace WW. Tissue-tropic effector T cells: generation and targeting opportunities. Nat Rev Immunol. 2006 09;6(9):682–692.

46 Molenaar R, Greuter M, van der Marel APJ, Roozendaal R, Martin SF, Edele F, et al. Lymph node stromal cells support dendritic cell-induced gut-homing of T cells. J Immunol. 2009 Nov;183(10):6395–6402.

47 Edele F, Molenaar R, Gutle D, Dudda JC, Jakob T, Homey B, et al. Cutting edge: instructive role of peripheral tissue cells in the imprinting of T cell homing receptor patterns. J Immunol. 2008 Sep;181(6):3745–3749.

48 Molenaar R, Knippenberg M, Goverse G, Olivier BJ, de Vos AF, O'Toole T, et al. Expression of retinaldehyde dehydrogenase enzymes in mucosal dendritic cells and gut-draining lymph node stromal cells is controlled by dietary vitamin A. J Immunol. 2011 Feb;186(4):1934–1942.

49 Evans RM, Mangelsdorf DJ. Nuclear receptors, RXR, and the Big Bang. Cell. 2014 Mar;157(1):255–266.

50 Takeuchi H, Yokota A, Ohoka Y, Iwata M. Cyp26b1 regulates retinoic acid-dependent signals in T cells and its expression is inhibited by transforming growth factor-beta. PLoS One. 2011;6(1):e16089.

51 Austrup F, Vestweber D, Borges E, Lohning M, Brauer R, Herz U, et al. P- and E-selectin mediate recruitment of T-helper-1 but not T-helper-2 cells into inflammed tissues. Nature. 1997 Jan;385(6611):81–83.

52 Iwata M, Hirakiyama A, Eshima Y, Kagechika H, Kato C, Song SY. Retinoic acid imprints gut-homing specificity on T cells. Immunity. 2004 Oct;21(4):527–538.

53 Schröter M. Regulation der E- und P-selektin-Liganden-Expression auf $CD4^+$ T-Zellen. Humboldt University, Berlin; 2012.

54 Sperandio M, Smith ML, Forlow SB, Olson TS, Xia L, McEver RP, et al. P-selectin glycoprotein ligand-1 mediates L-selectin-dependent leukocyte rolling in venules. J Exp Med. 2003 May;197(10):1355–1363.

55 Baaten BJ, Cooper AM, Swain SL, Bradley LM. Location, location, location: the impact of migratory heterogeneity on T cell function. Frontiers in Immunology. 2013;4(311).

56 Benechet AP, Menon M, Khanna KM. Visualizing T cell migration in-situ. Frontiers in Immunology. 2014;5(363). Available from: `http://www.frontiersin.org/immunological_memory/10.3389/fimmu.2014.00363/abstract`.

57 Kelly M, Hwang JM, Kubes P. Modulating leukocyte recruitment in inflammation. Journal of Allergy and Clinical Immunology. 2007 2015/12/20;120(1):3–10.

58 Hahne M, Jager U, Isenmann S, Hallmann R, Vestweber D. Five tumor necrosis factor-inducible cell adhesion mechanisms on the surface of mouse endothelioma cells mediate the binding of leukocytes. J Cell Biol. 1993 May;121(3):655–664.

59 Panés J, Perry M, Granger DN. Leukocyte-endothelial cell adhesion: avenues for therapeutic intervention. British Journal of Pharmacology. 1999;126(3):537–550.

60 Hirata T, Merrill-Skoloff G, Aab M, Yang J, Furie BC, Furie B. P-Selectin glycoprotein ligand 1 (PSGL-1) is a physiological ligand for E-selectin in mediating T helper 1 lymphocyte migration. J Exp Med. 2000 Dec;192(11):1669–1676.

61 Baumann K, Kowalczyk D, Gutjahr T, Pieczyk M, Jones C, Wild MK, et al. Sulfated and non-sulfated glycopeptide recognition domains of P-selectin glycoprotein ligand 1 and their binding to P- and E-selectin. Angew Chem Int Ed Engl. 2009;48(17):3174–3178.

62 Lowe JB. Glycan-dependent leukocyte adhesion and recruitment in inflammation. Curr Opin Cell Biol. 2003 Oct;15(5):531–538.

63 Buffone AJ, Mondal N, Gupta R, McHugh KP, Lau JTY, Neelamegham S. Silencing alpha1,3-fucosyltransferases in human leukocytes reveals a role for FUT9 enzyme during E-selectin-mediated cell adhesion. J Biol Chem. 2013 Jan;288(3):1620–1633.

64 Mondal N, Buffone AJ, Stolfa G, Antonopoulos A, Lau JTY, Haslam SM, et al. ST3Gal-4 is the primary sialyltransferase regulating the synthesis of E-, P-, and L-selectin ligands on human myeloid leukocytes. Blood. 2015 Jan;125(4):687–696.

65 Prorok-Hamon M, Notel F, Mathieu S, Langlet C, Fukuda M, El-Battari A. N-glycans of core2 beta(1,6)-N-acetylglucosaminyltransferase-I (C2GnT-I) but not those of alpha(1,3)-fucosyltransferase-VII (FucT-VII) are required for the synthesis of functional P-selectin glycoprotein ligand-1 (PSGL-1): effects on P-, L- and E-selectin binding. Biochem J. 2005 Nov;391(Pt 3):491–502.

66 Weninger W, Ulfman LH, Cheng G, Souchkova N, Quackenbush EJ, Lowe JB, et al. Specialized contributions by alpha(1,3)-fucosyltransferase-IV and FucT-VII during leukocyte rolling in dermal microvessels. Immunity. 2000 Jun;12(6):665–676.

67 Snapp KR, Heitzig CE, Ellies LG, Marth JD, Kansas GS. Differential requirements for the O-linked branching enzyme core 2 beta1-6-N-glucosaminyltransferase in biosynthesis of ligands for E-selectin and P-selectin. Blood. 2001 Jun;97(12):3806–3811.

68 Schroeter MF, Ratsch BA, Lehmann J, Baumgrass R, Hamann A, Syrbe U. Differential regulation and impact of fucosyltransferase VII and core 2 beta1,6-N-acetylglycosaminyltransferase for generation of E-selectin and P-selectin ligands in murine CD4+ T cells. Immunology. 2012 Dec;137(4):294–304.

69 Zisoulis DG, Kansas GS. H-Ras and phosphoinositide 3-kinase cooperate to induce alpha(1,3)-fucosyltransferase VII expression in Jurkat T cells. J Biol Chem. 2004 Sep;279(38):39495–39504.

70 Ebel ME, Awe O, Kaplan MH, Kansas GS. Diverse inflammatory cytokines induce selectin ligand expression on murine CD4 T cells via p38alpha MAPK. J Immunol. 2015 Jun;194(12):5781–5788.

71 Lim YC, Xie H, Come CE, Alexander SI, Grusby MJ, Lichtman AH, et al. IL-12, STAT4-dependent up-regulation of CD4(+) T cell core 2 beta-1,6-n-acetylglucosaminyltransferase, an enzyme essential for biosynthesis of P-selectin ligands. J Immunol. 2001 Oct;167(8):4476–4484.

72 White SJ, Underhill GH, Kaplan MH, Kansas GS. Cutting edge: differential requirements for Stat4 in expression of glycosyltransferases responsible for selectin ligand formation in Th1 cells. J Immunol. 2001 Jul;167(2):628–631.

73 Underhill GH, Zisoulis DG, Kolli KP, Ellies LG, Marth JD, Kansas GS. A crucial role for T-bet in selectin ligand expression in T helper 1 (Th1) cells. Blood. 2005 Dec;106(12):3867–3873.

74 Lord GM, Rao RM, Choe H, Sullivan BM, Lichtman AH, Luscinskas FW, et al. T-bet is required for optimal proinflammatory CD4+ T-cell trafficking. Blood. 2005 Nov;106(10):3432–3439.

75 Pink M. Molecular Regulation of the Fucosyltransferase VII in $CD4^+$ T-cells. Humboldt University, Berlin; 2013.

76 Chen GY, Osada H, Santamaria-Babi LF, Kannagi R. Interaction of GATA-3/T-bet transcription factors regulates expression of sialyl Lewis X homing receptors on Th1/Th2 lymphocytes. Proceedings of the National Academy of Sciences. 2006;103(45):16894–16899.

77 Nguyen MLT, Jones SA, Prier JE, Russ BE. Transcriptional Enhancers in the Regulation of T Cell Differentiation. Front Immunol. 2015;6:462.

78 Pal S, Gupta R, Kim H, Wickramasinghe P, Baubet V, Showe LC, et al. Alternative transcription exceeds alternative splicing in generating the transcriptome diversity of cerebellar development. Genome Research. 2011 08;21(8):1260–1272.

79 Alberts B, Bray D, Hopkin K, Johnson AD, Lewis J, Raff M, et al. Essential Cell Biology – Chapter 8. Control of Gene Expression. 4th ed. Garland Science; 2013.

80 Mercer TR, Mattick JS. Structure and function of long noncoding RNAs in epigenetic regulation. Nat Struct Mol Biol. 2013 03;20(3):300–307.

81 Kaikkonen MU, Lam MT, Glass CK. Non-coding RNAs as regulators of gene expression and epigenetics. Cardiovascular Research. 2011 06;90(3):430–440.

82 Bernstein BE, Kamal M, Lindblad-Toh K, Bekiranov S, Bailey DK, Huebert DJ, et al. Genomic maps and comparative analysis of histone modifications in human and mouse. Cell. 2005;120(2):169 – 181.

83 Cloos PAC, Christensen J, Agger K, Helin K. Erasing the methyl mark: histone demethylases at the center of cellular differentiation and disease. Genes & Development. 2008;22(9):1115–1140.

84 Wang Y, Li X, Hu H. {H3K4me2} reliably defines transcription factor binding regions in different cells. Genomics. 2014;103(2–3):222 – 228.

85 Wagner EJ, Carpenter PB. Understanding the language of Lys36 methylation at histone H3. Nature reviews Molecular cell biology. 2012 01;13(2):115–126.

86 Zhou VW, Goren A, Bernstein BE. Charting histone modifications and the functional organization of mammalian genomes. Nat Rev Genet. 2011 01;12(1):7–18.

87 Wei G, Wei L, Zhu J, Zang C, Hu-Li J, Yao Z, et al. Global mapping of H3K4me3 and H3K27me3 reveals specificity and plasticity in lineage fate determination of differentiating CD4+ T cells. Immunity. 2009 Jan;30(1):155–167.

88 Ito S, D'Alessio AC, Taranova OV, Hong K, Sowers LC, Zhang Y. Role of Tet proteins in 5mC to 5hmC conversion, ES-cell self-renewal and inner cell mass specification. Nature. 2010 Aug;466(7310):1129–1133.

89 Cortellino S, Xu J, Sannai M, Moore R, Caretti E, Cigliano A, et al. Thymine DNA glycosylase is essential for active DNA demethylation by linked deamination-base excision repair. Cell. 2011 Jul;146(1):67–79.

90 Bhutani N, Burns DM, Blau HM. DNA demethylation dynamics. Cell. 2011 09;146(6):866–872.

91 Jeffery L, Nakielny S. Components of the DNA Methylation System of Chromatin Control Are RNA-binding Proteins. Journal of Biological Chemistry. 2004;279(47):49479–49487.

92 Tsai MC, Manor O, Wan Y, Mosammaparast N, Wang JK, Lan F, et al. Long noncoding RNA as modular scaffold of histone modification complexes. Science (New York, NY). 2010 08;329(5992):689–693.

93 Jennrich S, Ratsch BA, Hamann A, Syrbe U. Long-term commitment to inflammation-seeking homing in CD4+ effector cells. J Immunol. 2007 Jun;178(12):8073–8080.

94 Ye J, Coulouris G, Zaretskaya I, Cutcutache I, Rozen S, Madden TL. Primer-BLAST: a tool to design target-specific primers for polymerase chain reaction. BMC Bioinformatics. 2012;13:134.

95 Kent WJ, Sugnet CW, Furey TS, Roskin KM, Pringle TH, Zahler AM, et al. The human genome browser at UCSC. Genome Res. 2002 Jun;12(6):996–1006.

96 Ovcharenko I, Nobrega MA, Loots GG, Stubbs L. ECR Browser: a tool for visualizing and accessing data from comparisons of multiple vertebrate genomes. Nucleic Acids Res. 2004 Jul;32(Web Server issue):W280–6.

97 Cartharius K, Frech K, Grote K, Klocke B, Haltmeier M, Klingenhoff A, et al. MatInspector and beyond: promoter analysis based on transcription factor binding sites. Bioinformatics. 2005 Jul;21(13):2933–2942.

98 Messeguer X, Escudero R, Farre D, Nunez O, Martinez J, Alba MM. PROMO: detection of known transcription regulatory elements using species-tailored searches. Bioinformatics. 2002 Feb;18(2):333–334.

99 DeNucci CC, Pagan AJ, Mitchell JS, Shimizu Y. Control of alpha4beta7 integrin expression and CD4 T cell homing by the beta1 integrin subunit. J Immunol. 2010 Mar;184(5):2458–2467.

100 Brenner O, Levanon D, Negreanu V, Golubkov O, Fainaru O, Woolf E, et al. Loss of Runx3 function in leukocytes is associated with spontaneously developed colitis and gastric mucosal hyperplasia. Proc Natl Acad Sci U S A. 2004 Nov;101(45):16016–16021.

101 Heintzman ND, Hon GC, Hawkins RD, Kheradpour P, Stark A, Harp LF, et al. Histone modifications at human enhancers reflect global cell-type-specific gene expression. Nature. 2009 May;459(7243):108–112.

102 Wei L, Vahedi G, Sun HW, Watford WT, Takatori H, Ramos HL, et al. Discrete roles of STAT4 and STAT6 transcription factors in tuning epigenetic modifications and transcription during T helper cell differentiation. Immunity. 2010 Jun;32(6):840–851.

103 Muller CW, Herrmann BG. Crystallographic structure of the T domain-DNA complex of the Brachyury transcription factor. Nature. 1997 10;389(6653):884–888.

104 Gokmen MR, Dong R, Kanhere A, Powell N, Perucha E, Jackson I, et al. Genome-wide regulatory analysis reveals that T-bet controls Th17 lineage differentiation through direct suppression of IRF4. J Immunol. 2013 Dec;191(12):5925–5932.

105 Nakayamada S, Kanno Y, Takahashi H, Jankovic D, Lu KT, Johnson TA, et al. Early Th1 cell differentiation is marked by a Tfh cell-like transition. Immunity. 2011 Dec;35(6):919–931.

106 Kim HP, Kelly J, Leonard WJ. The basis for IL-2-induced IL-2 receptor α chain gene regulation: importance of two widely separated IL-2 response elements. Immunity. 2001;15(1):159 – 172.

107 Brown CC, Esterhazy D, Sarde A, London M, Pullabhatla V, Osma-Garcia I, et al. Retinoic acid is essential for Th1 cell lineage stability and prevents transition to a Th17 cell program. Immunity. 2015 Mar;42(3):499–511.

108 Vahedi G, Takahashi H, Nakayamada S, Sun HW, Sartorelli V, Kanno Y, et al. STATs shape the active enhancer landscape of T cell populations. Cell. 2012 Nov;151(5):981–993.

109 Hiraiwa N, Yabuta T, Yoritomi K, Hiraiwa M, Tanaka Y, Suzuki T, et al. Transactivation of the fucosyltransferase VII gene by human T-cell leukemia virus type 1 Tax through a variant cAMP-responsive element. Blood. 2003 May;101(9):3615–3621.

110 Elgueta R, Sepulveda FE, Vilches F, Vargas L, Mora JR, Bono MR, et al. Imprinting of CCR9 on CD4 T cells requires IL-4 signaling on mesenteric lymph node dendritic cells. J Immunol. 2008 May;180(10):6501–6507.

111 Bode U, Sparmann G, Westermann J. Gut-derived effector T cells circulating in the blood of the rat: preferential re-distribution by TGFβ-1 and IL-4 maintained proliferation. European Journal of Immunology. 2001;31(7):2116–2125.

112 Takeuchi H, Yokota A, Ohoka Y, Kagechika H, Kato C, Song SY, et al. Efficient induction of CCR9 on T cells requires coactivation of retinoic acid receptors and retinoid X receptors (RXRs): exaggerated T Cell homing to the intestine by RXR activation with organotins. J Immunol. 2010 Nov;185(9):5289–5299.

113 Lim YC, Henault L, Wagers AJ, Kansas GS, Luscinskas FW, Lichtman AH. Expression of functional selectin ligands on Th cells is differentially regulated by IL-12 and IL-4. J Immunol. 1999 Mar;162(6):3193–3201.

114 Ohoka Y, Yokota A, Takeuchi H, Maeda N, Iwata M. Retinoic acid-induced CCR9 expression requires transient TCR stimulation and cooperativity between NFATc2 and the retinoic acid receptor/retinoid X receptor complex. J Immunol. 2011 Jan;186(2):733–744.

115 Stemberger C, Huster KM, Koffler M, Anderl F, Schiemann M, Wagner H, et al. A single naive CD8+ T cell precursor can develop into diverse effector and memory subsets. Immunity. 2007;27(6):985 – 997.

116 Helmstetter C, Flossdorf M, Peine M, Kupz A, Zhu J, Hegazy AN, et al. Individual T helper cells have a quantitative cytokine memory. Immunity. 2015 Jan;42(1):108–122.

117 Bucy RP, Karr L, Huang GQ, Li J, Carter D, Honjo K, et al. Single cell analysis of cytokine gene coexpression during CD4+ T-cell phenotype development. Proceedings of the National Academy of Sciences of the United States of America. 1995 08;92(16):7565–7569.

118 Syrbe U, Hoffmann U, Schlawe K, Liesenfeld O, Erb K, Hamann A. Microenvironment-dependent requirement of STAT4 for the induction of P-selectin ligands and effector cytokines on CD4+ T cells in healthy and parasite-infected mice. The Journal of Immunology. 2006;177(11):7673–7679.

119 Harms Pritchard G, Hall AO, Christian DA, Wagage S, Fang Q, Muallem G, et al. Diverse roles for T-bet in the effector responses required for resistance to infection. J Immunol. 2015 Feb;194(3):1131–1140.

120 Pink M, Ratsch BA, Mardahl M, Schroter MF, Engelbert D, Triebus J, et al. Identification of two regulatory elements controlling Fucosyltransferase 7 transcription in murine CD4+ T cells. Mol Immunol. 2014 Nov;62(1):1–9.

121 Kim HP, Leonard WJ. CREB/ATF-dependent T cell receptor–induced FoxP3 gene expression: a role for DNA methylation. The Journal of Experimental Medicine. 2007 07;204(7):1543–1551.

122 Iguchi-Ariga SM, Schaffner W. CpG methylation of the cAMP-responsive enhancer/promoter sequence TGACGTCA abolishes specific factor binding as well as transcriptional activation. Genes Dev. 1989 May;3(5):612–619.

123 Kannagi R. SECTION III Glycotopes Expression, Metabolism, and Functions-III-2 Transcriptional Regulation of Expression of Carbohydrate Ligands for Cell Adhesion Molecules in the Selectin Family. Advances in Experimental Medicine and Biology. 2001;491:267–278.

124 Triebus J. Molecular Regulation of Integrin $\alpha 4$ in $CD4^+$ T cells. Humboldt University; 2015.

125 Ogawa C, Tone Y, Tsuda M, Peter C, Waldmann H, Tone M. TGF-beta-mediated Foxp3 gene expression is cooperatively regulated by Stat5, Creb, and AP-1 through CNS2. J Immunol. 2014 Jan;192(1):475–483.

126 Yang R, Qu C, Zhou Y, Konkel JE, Shi S, Liu Y, et al. Hydrogen sulfide promotes Tet1- and Tet2-mediated Foxp3 demethylation to drive regulatory T cell differentiation and maintain immune homeostasis. Immunity. 2015 Aug;43(2):251–263.

127 Wagers AJ, Waters CM, Stoolman LM, Kansas GS. Interleukin 12 and Interleukin 4 control T cell adhesion to endothelial selectins through opposite effects on α1,3-fucosyltransferase VII gene expression. The Journal of Experimental Medicine. 1998;188(12):2225–2231.

128 Yokota A, Takeuchi H, Maeda N, Ohoka Y, Kato C, Song SY, et al. GM-CSF and IL-4 synergistically trigger dendritic cells to acquire retinoic acid-producing capacity. Int Immunol. 2009 Apr;21(4):361–377.

129 Ruane D, Brane L, Reis BS, Cheong C, Poles J, Do Y, et al. Lung dendritic cells induce migration of protective T cells to the gastrointestinal tract. The Journal of Experimental Medicine. 2013;210(9):1871–1888.

130 Stephensen CB, Rasooly R, Jiang X, Ceddia MA, Weaver CT, Chandraratna RAS, et al. Vitamin A enhances in vitro Th2 development via retinoid X receptor pathway. The Journal of Immunology. 2002;168(9):4495–4503.

131 Umemiya H, Kagechika H, Fukasawa H, Kawachi E, Ebisawa M, Hashimoto Y, et al. Action mechanism of retinoid-synergistic dibenzodiazepines. Biochem Biophys Res Commun. 1997 Apr;233(1):121–125.

132 Mora JR, Cheng G, Picarella D, Briskin M, Buchanan N, von Andrian UH. Reciprocal and dynamic control of CD8 T cell homing by dendritic cells from skin- and gut-associated lymphoid tissues. J Exp Med. 2005 Jan;201(2):303–316.

133 Takeuchi H, Yokota-Nakatsuma A, Ohoka Y, Kagechika H, Kato C, Song SY, et al. Retinoid X receptor agonists modulate Foxp3(+) regulatory T cell and Th17 cell differentiation with differential dependence on retinoic acid receptor activation. J Immunol. 2013 Oct;191(7):3725–3733.

134 Hekimoglu-Balkan B, Aszodi A, Heinen R, Jaritz M, Ringrose L. Intergenic Polycomb target sites are dynamically marked by non-coding transcription during lineage commitment. RNA Biology. 2012 03;9(3):314–325.

135 Yokota-Nakatsuma A, Takeuchi H, Ohoka Y, Kato C, Song SY, Hoshino T, et al. Retinoic acid prevents mesenteric lymph node dendritic cells from inducing IL-13-producing inflammatory Th2 cells. Mucosal Immunol. 2014 Jul;7(4):786–801.